ISTANBUL TECHNICAL UNIVERSITY ★ GRADUATE SCHOOL

THEORETICAL AND OBSERVATIONAL ASPECTS OF INFLATIONARY COSMOLOGY

M.Sc. THESIS

Kemal AKIN

Department of Physics Engineering

Physics Engineering Programme

JUNE 2022

ISTANBUL TECHNICAL UNIVERSITY ★ GRADUATE SCHOOL

THEORETICAL AND OBSERVATIONAL ASPECTS OF INFLATIONARY COSMOLOGY

M.Sc. THESIS

Kemal AKIN
(509181112)

Department of Physics Engineering

Physics Engineering Programme

Thesis Advisor: Prof. Dr. A. Savaş ARAPOĞLU

JUNE 2022

İSTANBUL TEKNİK ÜNİVERSİTESİ ★ LİSANSÜSTÜ EĞİTİM ENSTİTÜSÜ

KOZMİK ENFLASYONA TEORİK VE GÖZLEMSEL BAKIŞ AÇILARI

YüKSEK LİSANS TEZİ

Kemal AKIN
(509181112)

Fizik Mühendisliği Anabilim Dalı

Fizik Mühendisliği Programı

Tez Danışmanı: Prof. Dr. A. Savaş ARAPOĞLU

HAZİRAN 2022

Kemal AKIN, a M.Sc. student of ITU Graduate School student ID 509181112, successfully defended the thesis entitled "THEORETICAL AND OBSERVATIONAL ASPECTS OF INFLATIONARY COSMOLOGY", which he/she prepared after fulfilling the requirements specified in the associated legislations, before the jury whose signatures are below.

Thesis Advisor :	**Prof. Dr. A. Savaş ARAPOĞLU** Istanbul Technical University	.....
Jury Members :	**Prof. Dr. Neşe ÖZDEMİR** Istanbul Technical University	.....
	Assoc. Prof. Nihan KATIRCI Doğuş University	.....

Date of Submission : 30 May 2022
Date of Defense : 22 June 2022

To every young researcher in Turkey,

FOREWORD

I would like to express my sincere gratitude to my advisor Prof. Dr. A. Savaş Arapoğlu for the support of this study, for his patience, motivation, and immense knowledge. His guidance helped me in all the time of research and writing of this thesis.

June 2022

Kemal AKIN
Physics Engineer

TABLE OF CONTENTS

Page

ABBREVIATIONS

GR	**:** General Relativity
CMB	**:** Cosmic Microwave Background
FRW	**:** Friedmann-Robertson-Walker
EoS	**:** Equation of State
WMAP	**:** Wilkinson Microwave Anisotropy Probe
SN Ia	**:** Type Ia Supernovae
SR	**:** Slow–roll
JF	**:** Jordan Frame
EF	**:** Einstein Frame

SYMBOLS

a	: Scale Factor
H	: Hubble Parameter
H_0	: Hubble Constant
Λ	: Cosmological Constant
n	: Number Density
ρ	: Energy Density
Ω	: Dimensionless Density Parameter
p	: Pressure
ω	: Equation of State Parameter
k	: Curvature Constant
z	: Redshift
$g_{\mu\nu}$	: Metric Tensor
$R^{\lambda}{}_{\mu\nu\kappa}$	: Riemann Curvature Tensor
$R_{\mu\nu}$	: Ricci Tensor
R	: Ricci Scalar
$\Gamma^{\lambda}{}_{\mu\nu}$	: Christoffel Symbol
$T_{\mu\nu}$	: Energy-Momentum Tensor
n_s	: Spectral Index
r	: Tensor-to-scalar Ratio

LIST OF TABLES

Page

LIST OF FIGURES

Page

THEORETICAL AND OBSERVATIONAL ASPECTS OF INFLATIONARY COSMOLOGY

SUMMARY

A testable theory of the universe has come up with Einstein's theory of general relativity. Combination of the theory with fundamental physics has provided significant understanding of the universe in the light of modern cosmological observations. On the other hand, the success of the hot Big Bang and Λ-CDM relies on the existence of dark energy and dark matter which are beyond the standard model of particle physics. Another required extension is inflationary mechanism which was suggested as a resolution to shortcomings Big Bang such as horizon and flatness problems. However, the biggest success of the inflationary paradigm is to explain the generation of initial perturbations that are responsible for the structure formation in the universe. A scalar field, called inflaton, leads to a exponential expansion in the early stage of the universe. Although inflation is a very strong theory for the early universe, direct test of the theory is not possible due to extremely-high energy scales. Instead, inflationary models are tested against observations come from imprints of the primordial density perturbations. An important pair of parameters that comes from the observations are spectral index n_s and tensor-to-scalar ratio r. Many inflationary models rely on slow–roll mechanism in which the inflaton slowly rolls through its potential minima so that equation of state parameter satisfies the acceleration condition $\omega < -1/3$. Slow–roll parameters are used to dictate such behaviour to the inflaton field. Besides, perturbations and therefore inflationary observables can be expressed in terms of slow–roll parameters. Despite the fact that various minimally coupled single field models are consistent with current observations, quantum field theory in curved space anticipates a non-minimal coupling of scalar field to curvature scalar R.

In this study, inflationary dynamics within the context of general relativity and scalar–tensor theories of gravitation is investigated. In the minimally coupled case, inflaton with a potential of the form ϕ^n is studied. In the non-minimally coupled case, same model with a coupling $F(\phi) = 1 + \xi\phi^2$ to curvature scalar is examined. In order to study inflation in scalar–tensor theories, usually conformal transformations are used, and for convenience the analysis is performed in Einstein Frame. In addition to standard Einstein frame analysis, we also perform the analysis in the Jordan frame. The predictions of the models are compared with PLANCK dataset using CosmoMC.

KOZMİK ENFLASYONA TEORİK VE GÖZLEMSEL BAKIŞ AÇILARI

ÖZET

Einstein'ın genel görelilik teorisi ile birlikte test edilebilir bir evren teorisi ortaya çıkarılmıştır. Teorinin temel fizikle birleşimi, modern kozmolojik gözlemler ışığında evrenin önemli ölçüde anlaşılmasını sağlamıştır. Öte yandan, Büyük Patlama ve kozmolojinin standard modeli Λ-CDM'in başarısı, standart parçacık fiziği modelinin ötesinde olan karanlık enerji ve karanlık madde gibi çeşitli bileşenlere dayanmaktadır. İhtiyaç duyulan bir diğer uzantı da ufuk ve düzlük sorunlarına çözüm olarak önerilen enflasyon mekanizmasıdır. Ancak, enflasyonist paradigmanın en büyük başarısı, evrendeki yapı oluşumundan sorumlu olan ilkel pertürbasyonların oluşumunu açıklamasıdır. İnflaton adı verilen bir skaler alan, evrenin erken evresinde üstel genişlemeye yol açar. Enflasyon, erken evrenin güçlü bir teori olmasına rağmen, yüksek enerji ölçekleri nedeniyle teorinin doğrudan test edilmesi mümkün değildir. Bunun yerine, enflasyon modelleri, ilkel yoğunluk pertürbasyonlarının izlerinden gelen gözlemlerle test edilir. Gözlemlerden gelen önemli bir parametre çifti, spektral endeks n_s ve tensör-skaler oranı r'dır. Birçok enflasyon modeli, inflaton alanının potansiyel minimumuna doğru yavaşça yuvarlandığı ve böylece hal parametrisinin $\omega < -1/3$ ivmelenme koşulunu karşıladığı yavaş yuvarlanma mekanizmasına dayanır. Bu tür davranışları inflaton alanına dikte etmek için yavaş yuvarlanma parametreleri kullanılır. Ayrıca, pertürbasyonlar ve dolayısıyla enflasyon gözlemlenebilirleri, yavaş yuvarlanma parametreleri cinsinden ifade edilebilir. Tek alandan oluşan çeşitli minimal bağlaşım modelleri mevcut gözlemlerle tutarlı olmasına rağmen, eğri uzaydaki kuantum alan teorisi, skaler alanın eğrilik skaleri R ile minimal olmayan bir bağlaşım içerisinde olmasını öngörür. Enflasyonu skaler-tensör teorilerde incelemeyi kolaylaştırmak için genellikle konformal dönüşümler kullanılır ve analiz Einstein çerçevesinde gerçekleştirilir.

Bu çalışmada, enflasyon dinamikleri hem genel görelilik hem de skaler-tensör kütleçekim teorileri bağlamında araştırılmıştır. Minimal bağlaşım durumunda, ϕ^n biçiminde bir potansiyele sahip enflasyon modeli incelenmiştir. Minimal olmayan bağlaşım durumunda ise, $F(\phi) = 1 + \xi\phi^2$ ile eğrilik skalerine kuple edilmiş model incelenmiştir. Standart Einstein Çerçevesi analizine ek olarak Jordan Çerçevesinde de analizi gerçekleştirilmiştir. Modellerin tahminleri, CosmoMC kullanılarak PLANCK veri seti ile karşılaştırılmıştır.

1. INTRODUCTION

The journey of cosmology started in the early 18th century and the fundamental questions of humanity such as "Where do we come from?", "What are we?", and "Where are we going?" has evolved to understand the universe: Its origin, evolution, and the ultimate fate.

Figure 1.1 : *Where do we come from? What are we? Where are we going?* by Paul Gauguin (1897).

Einstein's Special(1905) and General(1915) Theories of Relativity changed our perspective on the concepts of space and time. As a geometric theory, General Relativity is the framework of cosmology. Although expanding universe was a stable solution of Einstein's equations and some models were suggested, they were not taken seriously at that time [8, 9]. For instance, Lemaitre's "cosmic egg model" [10] was an early prediction of the hot Big Bang. Studies conducted by Edwin Hubble confirmed the expansion of the universe in 1929 by observing that the further away galaxies were receding faster [1].

As the technology advanced, various discoveries achieved in astronomy and cosmology. Pioneering studies for dark matter were conducted in 1930s by Zwicky and Smith [11] with a Newtonian approach, by using Virial theorem in the Coma cluster. In 1948, the existence of cosmic radiation from the hot stage of the universe was predicted by Gamow and Alpher [12] and discovered by Wilson and Penzias [13] in 1965. The

thermal radiation is called Cosmic Microwave Background (CMB). The discovery of CMB was a convincing evidence for the evolution of the universe from hot and dense state.

Although Big Bang was the best theory in the early 80s, there were shortcomings of the theory such as flatness, horizon, and monopole problem. In 1981, Alan Guth suggested "inflation" as a resolution to these problems [14]. Inflationary mechanism takes place at early stages of the universe and it is responsible for the exponential expansion. In 1982 and 1983, Linde's New and Chaotic inflation scenarios have provided more complete resolutions [15, 16]. Inflationary paradigm not only provides solution to these historically important problems but also explains the generation of the primordial density fluctuations which can be considered as the "seeds of structures" in the universe. In addition to single field inflationary models withing the context of GR, various models beyond GR are also suggested in the literature [17].

Over the two decades, accelerated expansion has become a point of interest again. The "late-time acceleration" was discovered in 1998 by two independent teams [18, 19] from Type Ia supernovae observations. According to standard model of cosmology, cosmological constant as dark energy is responsible for the behaviour. Although, the dynamics of inflation and late-time acceleration are similar to each other, it is worth to note that while the current acceleration is an observation, inflation is a "strong" theory of the early universe.

This study is organized as follows: Fundamental concepts and mathematical tools to understand dynamics of the universe are developed in Chapter 2. In Chapter 3, thermal history of the universe is presented and cosmic inventory is developed starting from the microscopic dynamics. The main interest of the study, inflationary paradigm, is investigated within the context of GR in Chapter 4. Then, dynamics of non-minimally coupled scalar field and slow–roll approach are studied in Einstein and Jordan Frame in Chapter 5. The study is finalized with the predictions of non-minimal inflation in the light of recent observations of PLANCK.

2. DYNAMICS OF THE UNIVERSE

A compelling, testable theory of the universe has come up with Theory of General Relativity. Combination of this knowledge with fundamental physics has provided significant understanding of the universe and its possible future(s) with the help of modern cosmological observations [2, 8, 20]. In this section, we will introduce fundamental concepts and mathematical tools to understand dynamics of the universe.

2.1 Homogeneity and Isotropy

On cosmological scales, universe is homogeneous and isotropic. While isotropy implies that there is no preferred *direction*, homogeneity implies that there is no preferred *location* in the universe. These assumptions leads to the cosmological principle that can be stated as there is no special point in the universe. For instance, CMB observations shows that anisotropies is smaller than $\delta T < 10^{-5}$ [7].

Within the context of cosmology, these notions can be stated as spatial distribution of energy sources in the universe is homogeneous and isotropic. Such illustration is shown in Figure 2.1.

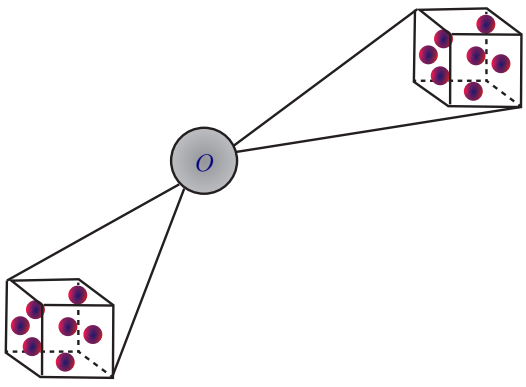

Figure 2.1 : Cosmological principle states that the universe looks the same everywhere on large scales.

As stated above, the universe can not be considered as isotropic until we get to considerably larger scales. For instance, in a 3 Mpc sphere Andromeda and Milk Way

constitutes about the 85% of the total luminosity. Hence, there is a preferred direction. On the contrary, in a sphere with 200 Mpc diameter is considered, then the sphere contains *superclusters* that are usually $\sim$ 100 Mpc in size and separated by $\sim$ 100 Mpc voids . Since there is no overdense region, there is no special region on such scales [8].

2.2 The Expanding Universe and Hubble Law

A fundamental starting point of cosmology is the discovery of expansion of the universe by E. Hubble in 1929 [1]. By comparing the distance and redshift (z) relationship of galaxies, Hubble observed that further away galaxies reeced faster from the observer. Hubble's law is given by

$$v = H_0 d, \tag{2.1}$$

where v is the velocity of retreat, d is the distance to obsersver, and H_0 is the Hubble constant. The original plot of Hubble is given in Figure 2.2.

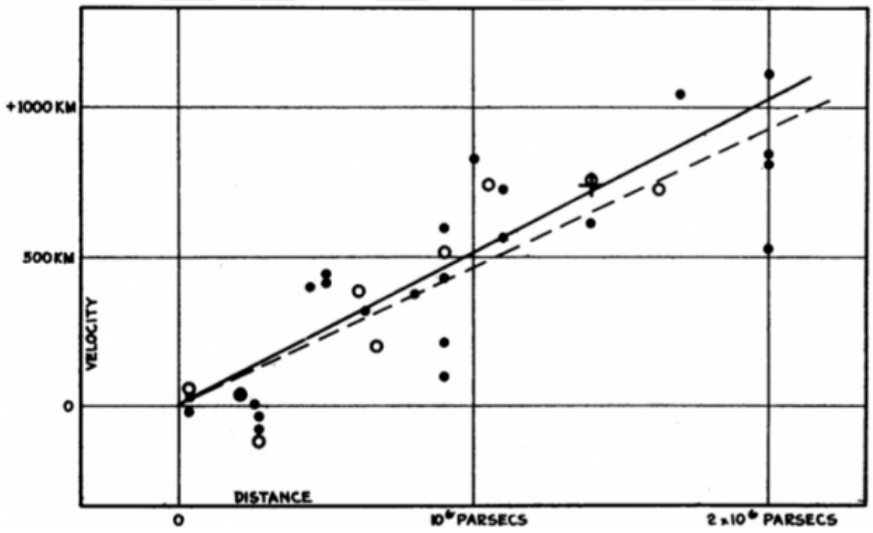

Figure 2.2 : The original velocity-distance relation plot of Edwin Hubble [1].

With a huge error, Hubble found $H_0 = 500\ \mathrm{km\,s^{-1}\,Mpc^{-1}}$. Current observations constrain H_0 as $H_0 \simeq 67\ \mathrm{km\,s^{-1}\,Mpc^{-1}}$ [7, 21] which means a galaxy receeds faster 67 km/s from observer in each Mpc. The dimension of H_0 is $\left[\frac{1}{T}\right]$ and its inverse can be used to approximate the age of the universe. With a simple calculation, if the expansion had been linear, age of the universe would be

$$t_H = \frac{1}{H_0} \approxeq 14.6\ \mathrm{Gyr}, \tag{2.2}$$

which is roughly comparable with current observations. It is also common to express Hubble rate using dimensionless parameter h as

$$H = h\,100\,\text{km/s/Mpc}, \tag{2.3}$$

thus $h \simeq 0.67$ today.

2.3 Elements of General Relativity

2.3.1 Metric and physical distance

Let us start with considering the differential length elements in 3 dimensional space. In Cartesian coordinates,

$$\mathrm{d}l^2 = \mathrm{d}x^2 + \mathrm{d}y^2 + \mathrm{d}z^2 \tag{2.4}$$

and in spherical coordinates, the length element can be expressed as

$$\mathrm{d}l^2 = \mathrm{d}r^2 + r^2\mathrm{d}\theta^2 + r^2\sin^2\theta\mathrm{d}\phi^2. \tag{2.5}$$

Although observers using different coordinate systems do not have to agree on coordinate distances between two points, the physical distance $(\mathrm{d}l)$ is the same for both observers. Thus, coordinate distances are turned into physical distances via metric. In closed form, using the *metric tensor*, the invariant line element can be written as

$$\mathrm{d}l^2 = \sum_{i,j=1}^{3} g_{ij}\,\mathrm{d}x^i\,\mathrm{d}x^j \tag{2.6}$$

where g_{ij} is a 3×3 matrix. Metric tensor in Cartesian and spherical polar coordinates can be written as

$$g_{ij} = \underbrace{\begin{bmatrix}1 & 0 & 0\\ 0 & 1 & 0\\ 0 & 0 & 1\end{bmatrix}}_{\text{Cartesian}}, \quad g_{ij} = \underbrace{\begin{bmatrix}1 & 0 & 0\\ 0 & r^2 & 0\\ 0 & 0 & r^2\sin^2\theta\end{bmatrix}}_{\text{Spherical}}. \tag{2.7}$$

It is important to emphasize the functionality of metric, it turns observer dependent elements into invariants. An illuminative way to illustrate functionality of a metric is to compare a pair of vectors on a topographical map. As can be seen from Figure 2.3, the coordinate distances are the same for both vector. However, the physical distance depends on topography, i.e., background metric.

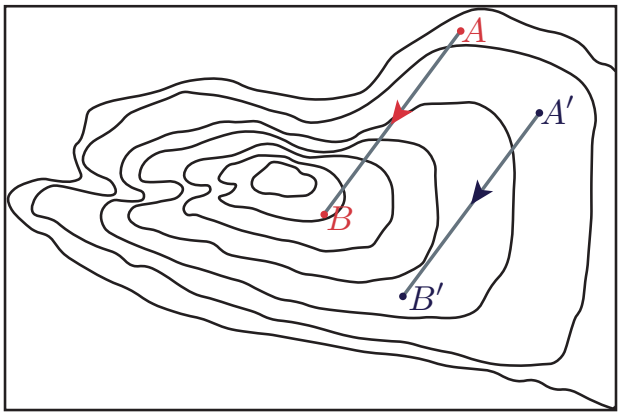

Figure 2.3 : Contour map of a valley.

Within the context of the theory of relativity, metric is the fundamental object. In special relativity, the metric of 4D spacetime is given by Minkowski metric and written as

$$\mathrm{d}s^2 = -\mathrm{d}t^2 + \mathrm{d}x^2 + \mathrm{d}y^2 + \mathrm{d}z^2. \tag{2.8}$$

Therefore metric tensor in Minkowski spacetime $\eta_{\mu\nu}$ is written as

$$\eta_{\mu\nu} = \mathrm{diag}(-1,1,1,1) \tag{2.9}$$

In the Newtonian approach, gravity is considered as external force. In general relativity, however, gravity is directly encoded within the metric and particles move in curved spacetime along the geodesics. The invariant line element in 4D is

$$\mathrm{d}s^2 = \sum_{\mu,\nu=0}^{3} g_{\mu\nu}\,\mathrm{d}x^\mu\,\mathrm{d}x^\nu \equiv g_{\mu\nu}\mathrm{d}x^\mu\mathrm{d}x^\nu \tag{2.10}$$

where $\mu,\nu = 0,1,2,3$. We employed Einstein summation convention where summation is performed over repeated indices. The shorthand notation will be employed for the rest of this study.

Dynamics of the universe is described by Einstein field equations. Although the field equations are complicated, nonlinear partial differential equations, assumption of isotropy that is dictated by Friedmann-Robertson-Walker (FRW) metric, enormously simplifies the equations.

$$\mathrm{d}s^2 = -\mathrm{d}t^2 + a^2(t)\left[\frac{\mathrm{d}r^2}{1-kr^2} + r^2\mathrm{d}\theta^2 + r^2\sin^2\theta\mathrm{d}\phi^2\right]. \tag{2.11}$$

In the metric, scale factor $a(t)$ represents expansion/contraction of the universe, and curvature constant k determines spatial geometry and it can take values -1, 0, or 1. For

convenience, radial component of (2.11), can be expressed through the definition

$$d\chi = \frac{dr}{\sqrt{1-kr^2}} \tag{2.12}$$

which brings the FRW metric into the form

$$ds^2 = -dt^2 + a^2(t)\left[d\chi^2 + S_k^2(\chi)d\Omega^2\right] \tag{2.13}$$

with

$$S_k(\chi) = \begin{cases} \sinh(\chi), & k<0 \\ \chi, & k=0 \\ \sin(\chi), & k>0 \end{cases} \tag{2.14}$$

In the metric, r is the comoving coordinate. However, physical distance depends on the physical coordinate $r_p \equiv a(t)r$ as illustrated in Figure 2.4.

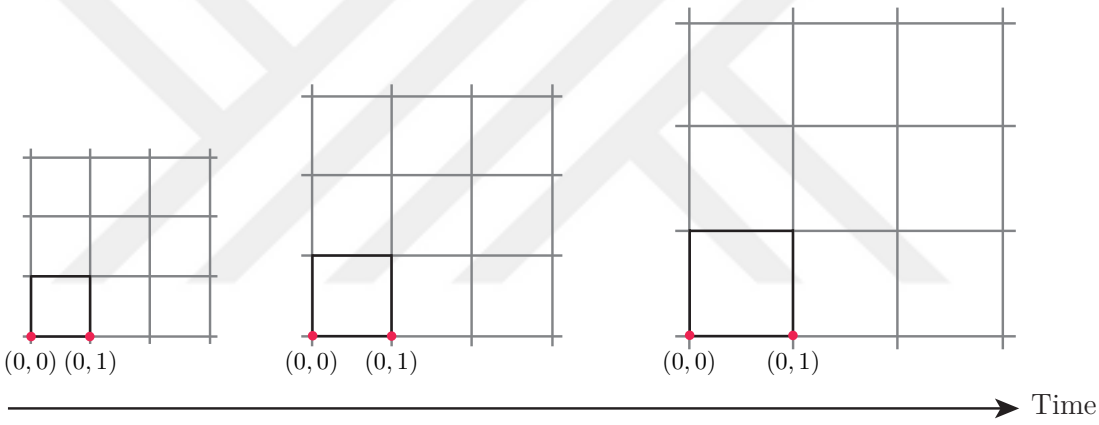

Figure 2.4 : Although the expansion (or contraction) of the physical distance between points on the grid is proportional to scale factor, comoving distance between points, i.e. coordinate distance, remains constant as the universe expands (or contracts). The figure is adapted from [2].

Taking time derivative, physical velocity can be found as

$$v_p \equiv \frac{dr_p}{dt} = \frac{d(ar)}{dt} = \dot{a}(t)r + a(t)\dot{r}. \tag{2.15}$$

where first term is the Hubble flow

$$H(t) \equiv \frac{\dot{a}}{a} \implies \dot{a}r = Hr_p \tag{2.16}$$

and the second terms is the peculiar velocity

$$v_{pec} = a(t)\dot{r}. \tag{2.17}$$

Metric is the most fundamental object in general relativity, namely given a metric one can evaluate Einstein field equations and determine the corresponding dynamics in that background. Before evaluating the field equations to determine dynamics of the universe, let us investigate the field equations more closely. We will directly give the field equations, however detailed derivation from Einstein-Hilbert action is given in Appendix A.

$$G_{\mu\nu} \equiv R_{\mu\nu} - \frac{1}{2} R g_{\mu\nu} = \frac{8\pi G}{c^4} T_{\mu\nu}. \tag{2.18}$$

LHS of the field equations can be identified as Einstein tensor $G_{\mu\nu}$. Its constituents are Ricci tensor $R_{\mu\nu}$ and Ricci scalar R which correspond to geometry of spacetime. RHS corresponds to matter–energy content and it is represented by the energy-momentum tensor $T_{\mu\nu}$. In order to obtain dynamical equations, each of these components should be calculated for the background metric. In our case, it will be FRW metric.

2.3.2 Curvature

2.3.2.1 Christoffel symbols

One can define a unique metric connection which relates vectors in the tangent spaces of nearby points in the manifold and explicit components are called Christoffel symbols [20] that are given by

$$\Gamma^{\lambda}{}_{\mu\nu} = \frac{1}{2} g^{\lambda\sigma} (\partial_\nu g_{\sigma\mu} + \partial_\mu g_{\sigma\nu} - \partial_\sigma g_{\mu\nu}) \tag{2.19}$$

If we evaluate Eq. (2.19) for FRW metric, Christoffel symbols can be obtained as follows

$$\begin{aligned}
&\Gamma^{0}{}_{ij} = \frac{\dot{a}}{a} g_{ij}, \quad \Gamma^{i}{}_{0j} = \Gamma^{i}{}_{j0} = \frac{\dot{a}}{a} \delta^{i}_{j} \\
&\Gamma^{1}{}_{11} = \frac{kr}{1-kr^2}, \quad \Gamma^{1}{}_{22} = -r(1-kr^2), \quad \Gamma^{1}{}_{33} = -r(1-kr^2)\sin^2\theta \\
&\Gamma^{2}{}_{12} = \Gamma^{3}{}_{13} = \frac{1}{r}, \quad \Gamma^{2}{}_{33} = -\sin\theta\cos\theta, \quad \Gamma^{3}{}_{32} = \cot\theta.
\end{aligned} \tag{2.20}$$

Although Christoffel symbols have indices and looks like a tensor, it is important to highlight that they do not transform tensorially and therefore are not tensor. This is why it is called “symbol”. Christoffel symbols do not appear explicitly in the field equations, however it is contained within Riemann tensor as shown in the following

section. The main use of Christoffel symbols are connection coefficients of covariant derivatives and definition of geodesics. Covariant derivative of a vector field A^ν is

$$\nabla_\mu A^\nu = \partial_\mu A^\nu + \Gamma^\nu{}_{\mu\lambda} A^\lambda. \tag{2.21}$$

and the connection is also used to define geodesics,

$$\frac{\mathrm{d}^2 x^\mu}{d\lambda^2} + \Gamma^\mu{}_{\rho\sigma} \frac{\mathrm{d}x^\rho}{\mathrm{d}\lambda} \frac{\mathrm{d}x^\sigma}{\mathrm{d}\lambda} = 0, \tag{2.22}$$

where $x^\mu(\lambda)$ is a geodesic.

2.3.2.2 Riemann curvature tensor

Everything about the curvature of the manifold is embedded to Riemann (curvature) tensor. With a simple definition, it is the technical expression of curvature and defined as

$$R^\lambda{}_{\mu\nu\kappa} \equiv \partial_\nu \Gamma^\lambda{}_{\mu\kappa} - \partial_\kappa \Gamma^\lambda{}_{\mu\nu} - \Gamma^\eta{}_{\mu\nu} \Gamma^\lambda{}_{\kappa\eta} + \Gamma^\eta{}_{\mu\kappa} \Gamma^\lambda{}_{\nu\eta}. \tag{2.23}$$

Riemann tensor vanishes iff the metric is perfectly flat. In fact, what we are trying to achieve is to relate components of Riemann tensor to energy-momentum tensor through Einstein field equations.

2.3.2.3 Ricci tensor

The components of Riemann tensor that are explicitly appear in the field equations are Ricci tensor and scalar. Let us consider $R^\lambda{}_{\mu\lambda\nu}$, Ricci tensor is defined through the contraction

$$R_{\mu\nu} \equiv R^\lambda{}_{\mu\lambda\nu}, \tag{2.24}$$

and Ricci scalar is obtained by the contraction Ricci tensor as

$$R \equiv g^{\mu\nu} R_{\mu\nu}. \tag{2.25}$$

Using Eq. (2.24) components of Ricci tensor for FRW metric can be obtained as follows

$$\begin{aligned} R_{00} &= R^\lambda{}_{0\lambda 0} = R^1{}_{010} + R^2{}_{020} + R^3{}_{030} = -3\frac{\ddot{a}}{a}, \\ R_{ii} &= R^\lambda{}_{i\lambda i} = \frac{g_{ii}}{a^2}(a\ddot{a} + 2\dot{a}^2 + 2k). \end{aligned} \tag{2.26}$$

Finally, Ricci scalar can be obtained as

$$R = g^{\mu\nu}R_{\mu\nu} = 6\left[\frac{\ddot{a}}{ac^2} + \left(\frac{\dot{a}}{ac}\right)^2 + \frac{k}{a^2}\right]. \tag{2.27}$$

All the necessary terms on the LHS of field equations (2.18) are obtained explicitly. In the next section, we will obtain RHS of the field equations.

2.3.3 Energy-momentum tensor

According to GR, the source of the curvature is the energy-momentum content which is captured by energy-momentum tensor $T_{\mu\nu}$. The physical meaning and components of $T_{\mu\nu}$ can be written as

$$T_{\mu\nu} = \left(\begin{array}{c|c} T_{00} & T_{0j} \\ \hline T_{i0} & T_{ij} \end{array}\right) = \left(\begin{array}{c|c} \text{Energy Density} & \text{Momentum Density} \\ \hline \text{Flux} & \text{Stress Tensor} \end{array}\right) \tag{2.28}$$

Energy-momentum tensor in the explicit form is given by

$$T_{\mu\nu} = (\rho + p)\,u_\mu u_\nu + p g_{\mu\nu} \tag{2.29}$$

where ρ is the energy density, p is the pressure and u_μ is the 4-velocity of medium. For FRW metric, one can take the fluid to be in rest frame [20], then 4-velocity components becomes

$$u_\mu = (1,0,0,0). \tag{2.30}$$

In (0-th order) cosmology, the universe is filled with perfect fluid which is isotropic and has no heat conduction or viscosity.

$$T_{\mu\nu} = \begin{bmatrix} \rho & 0 & 0 & 0 \\ 0 & & & \\ 0 & & pg_{ij} & \\ 0 & & & \end{bmatrix}. \tag{2.31}$$

Now, we have obtained all the necessary elements to evaluate Einstein field equations for FRW metric.

2.4 Friedmann Equations

Dynamics of the homogeneous and isotropic universe is described by Friedmann equations. Substitution of Ricci scalar and components of Ricci tensor for FRW metric

in the field equations yields two independent equations. By setting $\mu = \nu = 0$, the first is obtained as

$$\boxed{\left(\frac{\dot{a}}{a}\right)^2 = \frac{8\pi G}{3c^2}\rho - \frac{kc^2}{a^2(t)}}. \tag{2.32}$$

This is the fundamental equation that describes evolution of the scale factor $a(t)$. Here ρ represents sum of the energy density in the universe. By assuming that the constituents are not interact with each other, we will explicitly show each source while solving the Friedmann equation.

Second Friedmann equation is obtained from the spatial part of the field equations,

$$\frac{2\ddot{a}}{a} + \left(\frac{\dot{a}}{a}\right)^2 = -\frac{8\pi G}{c^2}p - \frac{kc^2}{a^2(t)} \tag{2.33}$$

A more common of the second equation is the Raychaudhuri (acceleration) equation which can be obtained by using linear combination of Eqs. (2.33) and (2.32)

$$\boxed{\frac{\ddot{a}(t)}{a(t)} = -\frac{4\pi G}{3c^2}(3p+\rho)}. \tag{2.34}$$

Although acceleration equation is not an independent equation, it directly shows whether the universe accelerates or decelerates for a given energy-matter content. For instance, if $3p+\rho < 0$ one can conclude that universe is accelerating. Such cases will be shown explicitly after defining continuity equation and equation of state.

2.5 Continuity (Fluid) and State Equations

In order to determine evolution of the scale factor $a(t)$, evolution of the energy density have to be specified. At this point, continuity equation and equation of state will be employed.

2.5.1 Continuity equation

In this section, we shall determine the evolution of energy density and pressure in time. In Minkowski spacetime, energy and momentum are conserved quantities. Therefore, as a rule of thumb by promoting partial derivatives to covariant derivatives, general relativistic expressions can be derived:

$$\boxed{\partial_\mu T^\mu{}_\nu = 0 \Rightarrow \nabla_\mu T^\mu{}_\nu = 0}. \tag{2.35}$$

Unpacking the covariant conservation equation,

$$\nabla_\mu T^\mu{}_\nu = \partial_\mu T^\mu{}_\nu + \Gamma^\mu{}_{\mu\lambda} T^\lambda{}_\nu - \Gamma^\lambda{}_{\mu\nu} T^\mu{}_\lambda = 0, \tag{2.36}$$

and by setting $\nu = 0$ for the evolution of the energy density

$$\nabla_\mu T^\mu{}_0 = \partial_\mu T^\mu{}_0 + \Gamma^\mu{}_{\mu\lambda} T^\lambda{}_0 - \Gamma^\lambda{}_{\mu 0} T^\mu{}_\lambda = 0, \tag{2.37}$$

and finally, simply inserting relevant Christoffel symbols, the continuity equation is written as

$$\boxed{\dot{\rho} + 3\frac{\dot{a}}{a}(\rho + p) = 0}. \tag{2.38}$$

Again, here ρ represents total contribution from all components to energy density and, in general, the equation do not have to be satisfied for every single component. For instance, consider a model with only dark matter and dark energy, and let dark matter obeys the equation

$$\dot{\rho}_{\mathrm{DM}} + 3H(\rho_{\mathrm{DM}} + p_{\mathrm{DM}}) = -Q \tag{2.39}$$

then, dark energy component must obey

$$\dot{\rho}_{\mathrm{DE}} + 3H(\rho_{\mathrm{DE}} + p_{\mathrm{DE}}) = +Q. \tag{2.40}$$

Cumulatively, continuity equation is satisfied.

2.5.2 Equation of state

To solve Friedmann equations and determine how scale factor evolves in time, one more equation that relates energy density ρ and pressure p is required. The equation is called equation of state (EoS) and in general it might be a complicated expression. However, in cosmology we usually deal with perfect dilute gas with a simple EoS

$$\boxed{p = \omega\rho}. \tag{2.41}$$

The dimensionless constant ω is called equation of state parameter. In order to analyze evolutionary dynamics for different components, the parameter ω should be known. In Section 3, physical properties of different components of the universe will be developed starting from first principles. However, for now, EoS parameter for matter and radiation will be derived using ideal gas law and basic thermodynamical relations.

$$p = \frac{N}{V} k_B T = n k_B T \tag{2.42}$$

where n is number density. Number density and mass density ρ_m are related by the relation

$$n = \frac{\rho_m}{\mu}, \tag{2.43}$$

where μ is the mean particle mass. Thus, Eq. (2.42) becomes

$$p = \frac{\rho_m}{\mu} k_B T \tag{2.44}$$

Now using the relation between temperature and kinetic energy

$$\frac{3}{2} k_B T = \frac{1}{2} \mu \langle v^2 \rangle, \tag{2.45}$$

equation of state reads

$$p = \frac{\langle v^2 \rangle}{3c^2} \rho = \omega \rho. \tag{2.46}$$

For non-relativistic dust,

$$\omega_{\rm m} \approx \frac{\langle v^2 \rangle}{3c^2} \ll 1 \tag{2.47}$$

Thus, one can obtain $\omega \approx 0$ for matter. We refer baryonic matter and dark matter as matter for simplicity. In the case of relativistic energy source, i.e. radiation,

$$\omega_{\rm r} \approx \frac{\langle v^2 \rangle}{3c^2}. \tag{2.48}$$

EoS parameter can be determined as $\omega_{\rm r} = 1/3$.

We can also determine how the energy density varies with respect to scale factor by integrating continuity equation (2.38),

$$\begin{aligned} \dot{\rho} &= -3 \frac{\dot{a}}{a} (\rho + \omega \rho) \\ \frac{\dot{\rho}}{\rho} &= -3(\omega + 1) \frac{\dot{a}}{a} \end{aligned} \tag{2.49}$$

Thus, energy density as a function of ω and a becomes

$$\rho = \rho_0 \, a^{-3(\omega+1)}. \tag{2.50}$$

While energy density evolves as $\rho_{\rm m} \propto a^{-3}$ for matter, it evolves as $\rho_{\rm r} \propto a^{-4}$ for radiation. As it will be shown in Section 2.6, radiation and matter leads to decelerated

expansion. However, today we know that universe undergoes an accelerating expansion. The condition for acceleration can be obtained from (2.34) as

$$\frac{\ddot{a}(t)}{a(t)} = -\frac{4\pi G}{3c^2}(\rho + 3p)$$
$$\ddot{a} > 0 \implies \rho + 3p < 0 \implies \omega_{\mathrm{DE}} < -\frac{1}{3}. \tag{2.51}$$

Dark energy is referred to explain the current acceleration of the universe [22]. In the standard model, dark energy steps into equations as cosmological constant (Λ) whose EoS is $p = -\rho$ which corresponds to negative pressure. Furthermore,

$$\omega_\Lambda = -1 \implies \rho_\Lambda \propto a^0. \tag{2.52}$$

Thus, it can be inferred the energy density of cosmological constant remains constant as the universe evolves. In Figure 2.5, evolution of the energy densities is plotted against scale factor.

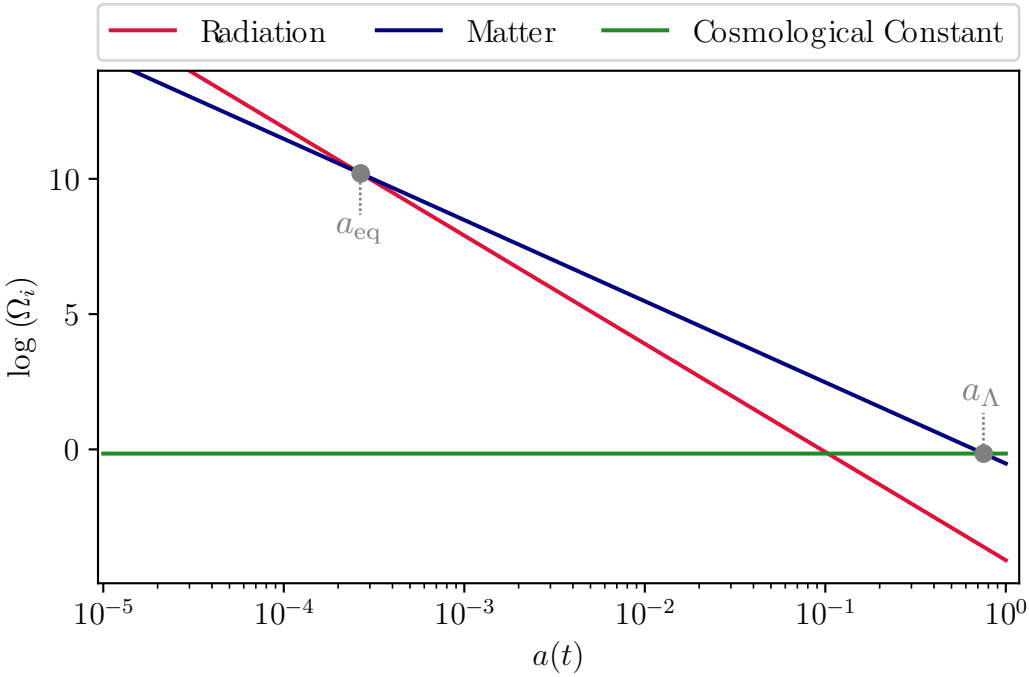

Figure 2.5 : Time evolution of the energy densities of radiation, matter, and cosmological constant as a function scale factor. Although cosmological constant dominates the energy energy density of the universe today, at early times radiation had the largest energy density. Matter-radiation and matter-Λ equalities are shown by a_{eq} and a_Λ, respectively.

2.6 Exact Solutions of Friedmann Equations

In general, evaluation of Friedmann equations requires numerical treatment. However, various exact solutions can be found by assuming one or two of the components dominates the energy budget of the universe. In order to determine evolution of the scale factor for current status of the universe, numerical integration will be employed in Section 2.7.

The Friedmann equation is given by

$$H^2(t) = \frac{8\pi G}{3c^2}\rho(t) - \frac{kc^2}{a^2(t)} \tag{2.53}$$

In the spatially flat ($k = 0$) case, Eq. (2.53) reduces

$$H^2(t) = \frac{8\pi G}{3c^2}\rho(t) \tag{2.54}$$

Note that for a given Hubble parameter, one can define *critical density* as

$$\rho_c(t) = \frac{3c^2}{8\pi G}H^2(t). \tag{2.55}$$

The quantities evaluated today will be indicated using the subscript 0. Thus, the following critical density corresponds to flat universe today,

$$\rho_{c,0} = 1.9 \times 10^{-29} h^2 \,\mathrm{g\,cm^{-3}} \tag{2.56}$$

Furthermore, we can define an another parameter that relates energy density and critical energy density. It is called *energy density parameter* and defined as

$$\Omega_i \equiv \frac{\rho_i}{\rho_c}, \quad i = \mathrm{r}, \mathrm{m}, \Lambda, \phi, \ldots \tag{2.57}$$

Note that energy density parameter directly provides information about the geometry. In terms of energy density parameter Friedmann equation takes the following form

$$\boxed{1 - \Omega(t) = -\frac{kc^2}{a^2(t)H^2(t)}} \tag{2.58}$$

which directly implies

$$\rho > \rho_c \rightarrow \Omega > 1 \implies k = +1$$

$$\rho < \rho_c \rightarrow \Omega < 1 \implies k = -1$$

$$\rho = \rho_c \rightarrow \Omega = 1 \implies k = 0$$

According to current observations, $\rho \simeq \rho_c$ that indicates a spatially flat geometry ($\Omega_0 \simeq 1$) [7]. If we explicitly include all the components within the standard model, Friedmann equation takes the form

$$\frac{H^2}{H_0^2} = \frac{\Omega_{\mathrm{r},0}}{a^4} + \frac{\Omega_{\mathrm{m},0}}{a^3} + \Omega_{\Lambda,0} + \frac{\Omega_{k,0}}{a^2} \tag{2.59}$$

where we have defined energy density for curvature as $\Omega_{k,0} \equiv -kc^2/H_0^2$. At present time $t = t_0$, the equation yields the constraint

$$1 = \Omega_{\mathrm{r},0} + \Omega_{\mathrm{m},0} + \Omega_{\Lambda,0} + \Omega_{k,0}. \tag{2.60}$$

Furthermore, if we denote energy density contribution from radiation, matter, and dark energy as Ω_0, then curvature parameter can be written as

$$\Omega_{k,0} = 1 - \Omega_0. \tag{2.61}$$

2.6.1 Evolution of the scale factor in single-component universe models

By assuming a single component(radiation, matter, or dark energy) dominates the total energy, exact solutions for $a(t)$ can be obtained. As we will see later, single-component treatment remains incapable, however, evolution during the various epochs can be approximated using such treatment.

In the most general form, we have obtained Friedmann equation as

$$\frac{H^2}{H_0^2} = \frac{\Omega_{\mathrm{r},0}}{a^4} + \frac{\Omega_{\mathrm{m},0}}{a^3} + \Omega_{\Lambda,0} + \frac{\Omega_{k,0}}{a^2}. \tag{2.62}$$

Multiplying Eq. (2.62) by a^2 and taking the square root

$$\frac{\mathrm{d}a}{\mathrm{d}t} = H_0 \left(\frac{\Omega_{\mathrm{r},0}}{a^2} + \frac{\Omega_{\mathrm{m},0}}{a} + a^2 \Omega_{\Lambda,0} + \Omega_{k,0} \right)^{\frac{1}{2}}, \tag{2.63}$$

which can be rearranged to find the cosmic time as

$$H_0 t = \int_0^a \frac{da'}{\left(\Omega_{\mathrm{r},0}/a'^2 + \Omega_{\mathrm{m},0}/a' + a'^2 \Omega_{\Lambda,0} + \Omega_{k,0} \right)^{1/2}}. \tag{2.64}$$

While in general this expression requires numerical integration, in this section we will assume just a one component dominates the total energy density. If we consider the radiation dominated era ($\Omega_{\mathrm{r}} \approx 1$), Eq. (2.64) is then reduced to

$$\begin{aligned} H_0 t &\approx \int_0^a a' \, \mathrm{d}a' \\ H_0 t &= \frac{a_{\mathrm{r}}^2}{2} \end{aligned} \tag{2.65}$$

and scale factor evolves as

$$a_{\mathrm{r}}(t) = (2H_0 t)^{1/2} \propto t^{1/2}. \tag{2.66}$$

Similarly, if we consider matter domination ($\Omega_{\mathrm{m}} \approx 1$),

$$\begin{aligned} H_0 t &\approx \int_0^a \sqrt{a'}\,\mathrm{d}a' \\ H_0 t &= \frac{2}{3} a_{\mathrm{m}}^{3/2} \end{aligned} \tag{2.67}$$

and scale factor evolves as

$$a_{\mathrm{m}}(t) = \left(\frac{3}{2} H_0 t\right)^{2/3} \propto t^{2/3}. \tag{2.68}$$

Finally, let us consider cosmological constant domination ($\Omega_\Lambda \approx 1$),

$$\begin{aligned} H_0 t &\approx \int_0^a \frac{\mathrm{d}a'}{a'} \\ H_0 t &= \ln a \implies a_\Lambda \propto e^{H_0 t} \end{aligned} \tag{2.69}$$

While radiation and matter domination corresponds to decelerated expansion, cosmological constant (dark energy) domination corresponds to accelerated expansion. Evolution of the scale factor for single-component models is shown Figure 2.6.

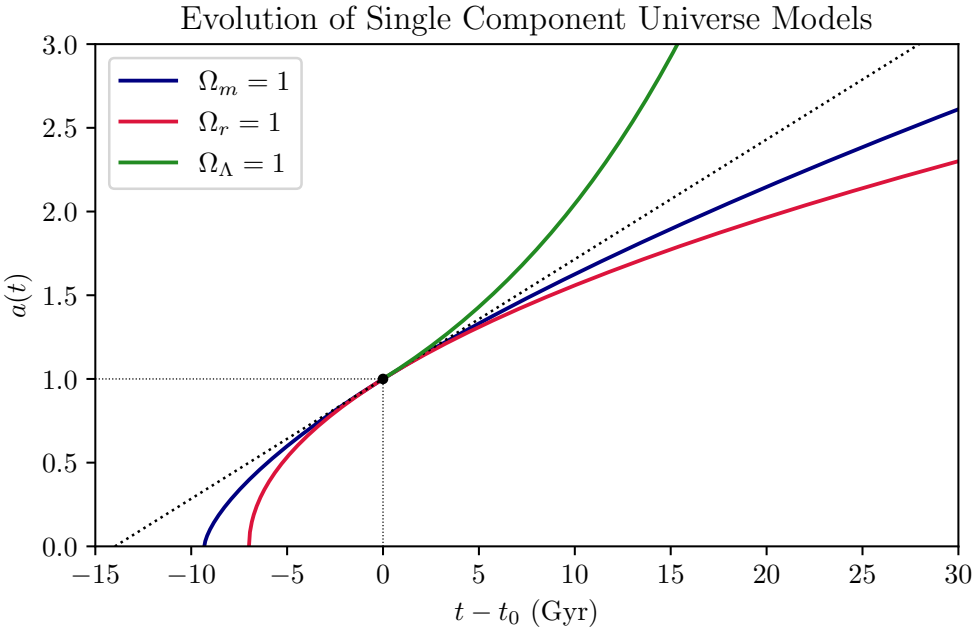

Figure 2.6 : Time evolution of the scale factor for each component in the Standard Big Bang Cosmology. The $x-$axis is chosen as $t - t_0$ to point out age of the relevant universe model.

As a summary, behaviour of the universe for different ingredients of the standard model is shown in Table 2.1.

Table 2.1 : Evolution of Λ-CDM Components.

Matter	Radiation	Cosmological Constant
$\omega_{\mathrm{m}} = 0$	$\omega_{\mathrm{r}} = 1/3$	$\omega_{\Lambda} = -1$
$\rho_{\mathrm{m}} = \rho_{\mathrm{m},0}\, a^{-3}$	$\rho_{\mathrm{r}} = \rho_{\mathrm{r},0}\, a^{-4}$	$\rho_{\Lambda} = \rho_{\Lambda,0}$
$a \propto t^{2/3}$	$a \propto t^{1/2}$	$a \propto e^{Ht}$

2.6.2 Evolution of the scale factor in multi-component universe models

In this section, time evolution of the scale factor in a universe with multiple components will be discussed with the assumption that components do not interact with each other.

A close approximated model that is compatible with current observations is flat universe model dominated by cosmological constant and matter. For these two components, Friedmann equation (2.62) reduces

$$\frac{H^2}{H_0^2} = \frac{\Omega_{\mathrm{m},0}}{a^3} + \Omega_{\Lambda,0}. \tag{2.70}$$

By using the flat geometry constraint $\Omega_{\mathrm{m},0} + \Omega_{\Lambda,0} = 1$,

$$\frac{H^2}{H_0^2} = \frac{\Omega_{\mathrm{m},0}}{a^3} + 1 - \Omega_{\mathrm{m},0} \tag{2.71}$$

The equation can be rearranged as

$$\begin{aligned} \frac{1}{H_0}\frac{\mathrm{d}a}{\mathrm{d}t} &= \sqrt{\frac{\Omega_{\mathrm{m},0}}{a} + (1-\Omega_{\mathrm{m},0})\, a^2} \\ t &= \frac{1}{H_0}\int_0^a \frac{\sqrt{a'}\mathrm{d}a'}{\sqrt{\Omega_{\mathrm{m},0} + (1-\Omega_{\mathrm{m},0})\, a'^3}} \end{aligned} \tag{2.72}$$

Evaluation of the last expression yields,

$$H_0 t = \frac{2}{3\sqrt{1-\Omega_{\mathrm{m},0}}} \ln\left\{ \left(\frac{a}{a_{\mathrm{m}\Lambda}}\right)^{3/2} + \sqrt{1 + \left(\frac{a}{a_{\mathrm{m}\Lambda}}\right)^3} \right\} \tag{2.73}$$

where $a_{\mathrm{m}\Lambda}$ denotes the scale factor at which the density contributions of matter and Λ are equal, i.e

$$a_{\mathrm{m}\Lambda} = \left(\frac{\Omega_{\mathrm{m},0}}{\Omega_{\Lambda,0}}\right)^{1/3} = \left(\frac{\Omega_{\mathrm{m},0}}{1-\Omega_{\mathrm{m},0}}\right)^{1/3} \tag{2.74}$$

Scale factor as function of time is then

$$\boxed{a(t) = \left(\frac{\Omega_{\mathrm{m},0}}{\Omega_{\Lambda,0}}\right) \sinh^{2/3}\left(\frac{3}{2}\sqrt{\Omega_{\Lambda,0}} H_0 t\right)} \tag{2.75}$$

In the literature various models are suggested. Some of these and energy densities of corresponding models are given in Table 2.2.

Table 2.2 : Various Universe Models.

Model	$\Omega_{\mathrm{m},0}$	$\Omega_{\mathrm{r},0}$	$\Omega_{\Lambda,0}$
Loitering	0.3	0	1.70
Λ Collapse	1	0	-0.3
Big Bounce	0.3	0	1.8
Λ-CDM	0.301	8.99×10^{-5}	0.691

If all components are included, without any approximation, the age integral

$$H_0 t = \int_0^a \frac{\mathrm{d}a'}{\left(\Omega_{\mathrm{r},0}/a'^2 + \Omega_{\mathrm{m},0}/a' + a'^2\,\Omega_{\Lambda,0} + \Omega_{k,0}\right)^{1/2}}. \tag{2.76}$$

should be solved numerically. Evolution of the scale factor for various suggested models is shown in Figure 2.11.

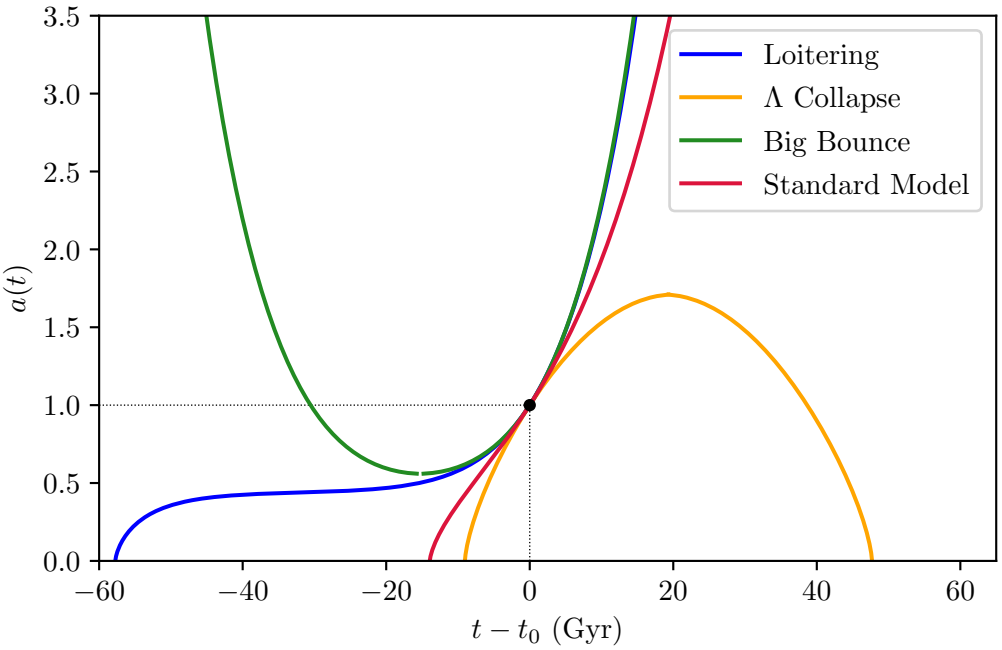

Figure 2.7 : Time evolution of scale factor for various scenarios given in Table 2.2.

2.7 Current Status of the Universe

By the mid-90s, distances larger than 1000 Mpc were started to measure by the help of supernovae. Redshift - luminosity distance measurements of Type Ia supernovae by High-Z Supernova Search and Supernova Cosmology Project teams have revealed the accelerated expansion of the universe [18, 19]. While this was a milestone for our understanding of the universe, as we have shown in Section 2.5 accelerated expansion requires universe to be dominated by a fluid whose equation of state parameter $\omega < -1/3$. Thus, matter and radiation are failed to describe the late time acceleration. This "mysterious" form of energy is called dark energy. Although there are numerous models to satisfy such behaviour, CMB observations assessed by COBE(1989), WMAP(2001) and currently by PLANCK tightly constraints models. For instance, observations indiate that geometry of the universe is close to be flat, which constraints total energy density as $\Omega_0 \simeq 1$. Supernovae observations from various sky surveys and the best fits for flat-geometry is shown in Figure 2.8.

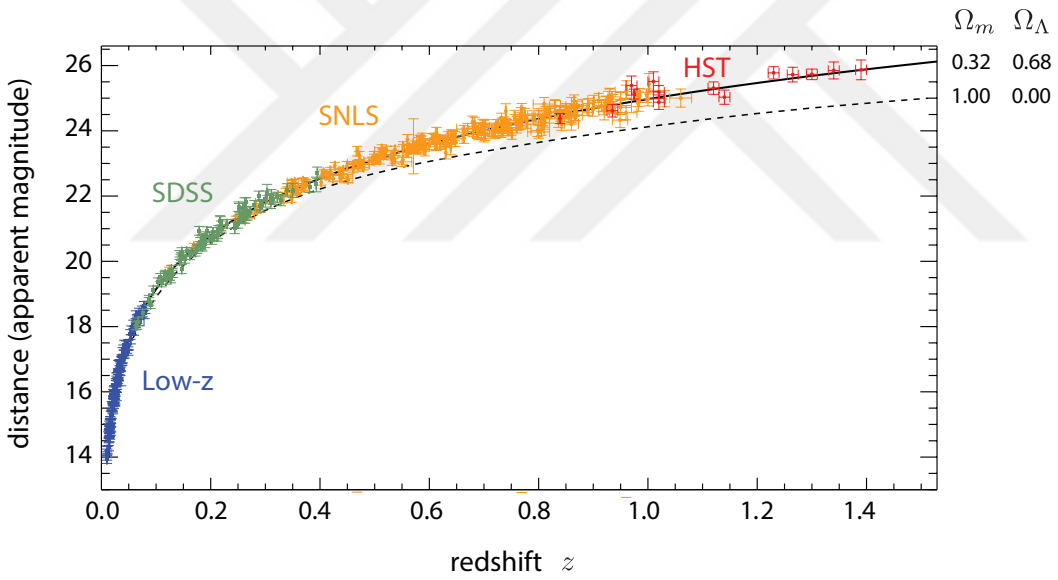

Figure 2.8 : Cumulative data and best fits from low and high-redshift supernovae observations.

The power spectrum of CMB anisotropies is shown in Figure 2.9. While the position of the first peak ($l \approx 200$) depends on the curvature, the height of the peak is a measure of matter density. Angular separation $\approx 1^\circ$ corresponds to spatially flat geometry.

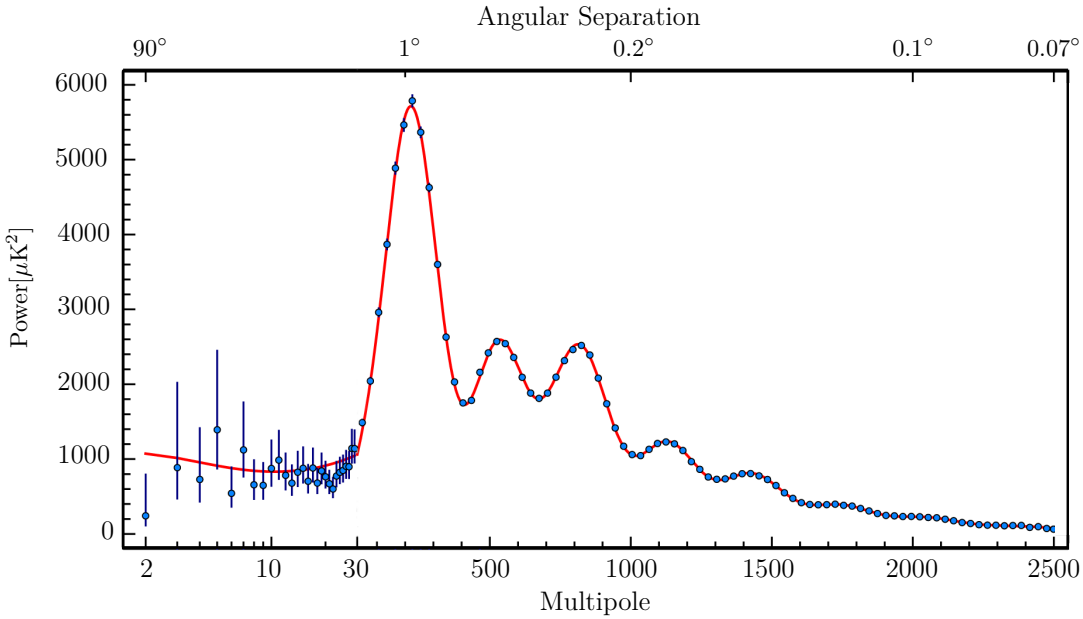

Figure 2.9 : CMB temperature power spectrum assessed by Planck mission.

According to latest PLANCK data [7], while radiation density is $\Omega_{r,0} = 8.99 \times 10^{-5}$, matter density is $\Omega_{m,0} = 0.3089 \pm 0.001$. Contribution by cosmological constant is constrained as $\Omega_{\Lambda,0} = 0.6911 \pm 0.0062$.

Currently, Λ-CDM is the simplest model that is compatible with the latest observations. CMB, evolution of LSS, abundance of elements, and the late-time acceleration can be explained by Λ-CDM model. Key parameters and their values from PLANCK are given in Table 2.3.

Table 2.3 : Key parameters to describe the universe and current observed values

Parameter	Symbol	Value
Photon Density	$\Omega_{\gamma,0}$	5.35×10^{-5}
Radiation Density	$\Omega_{r,0}$	8.99×10^{-5}
Baryon Density	$\Omega_{b,0}$	0.0486 ± 0.0010
Matter Density	$\Omega_{m,0}$	0.3089 ± 0.0010
Dark Energy Density	$\Omega_{\Lambda,0}$	0.6911 ± 0.0062
Critical Density	ρ_c	$(8.62 \pm 0.12) \times 10^{-27}$ kg/m^3
Spatial Curvature	$\lvert\Omega_{k,0}\rvert$	< 0.01
Expansion Rate	H_0	67.74 ± 0.46 km/s/Mpc
Age of the Universe	t_0	13.799 ± 0.021 Gyr

68% and 95% confidence intervals for the cosmological parameters $H_0, \Omega_{\rm m}$, and Ω_Λ are shown in Figure 2.10. Evolution of the scale factor with best-fit parameters are shown by green solid line in Figure 2.11.

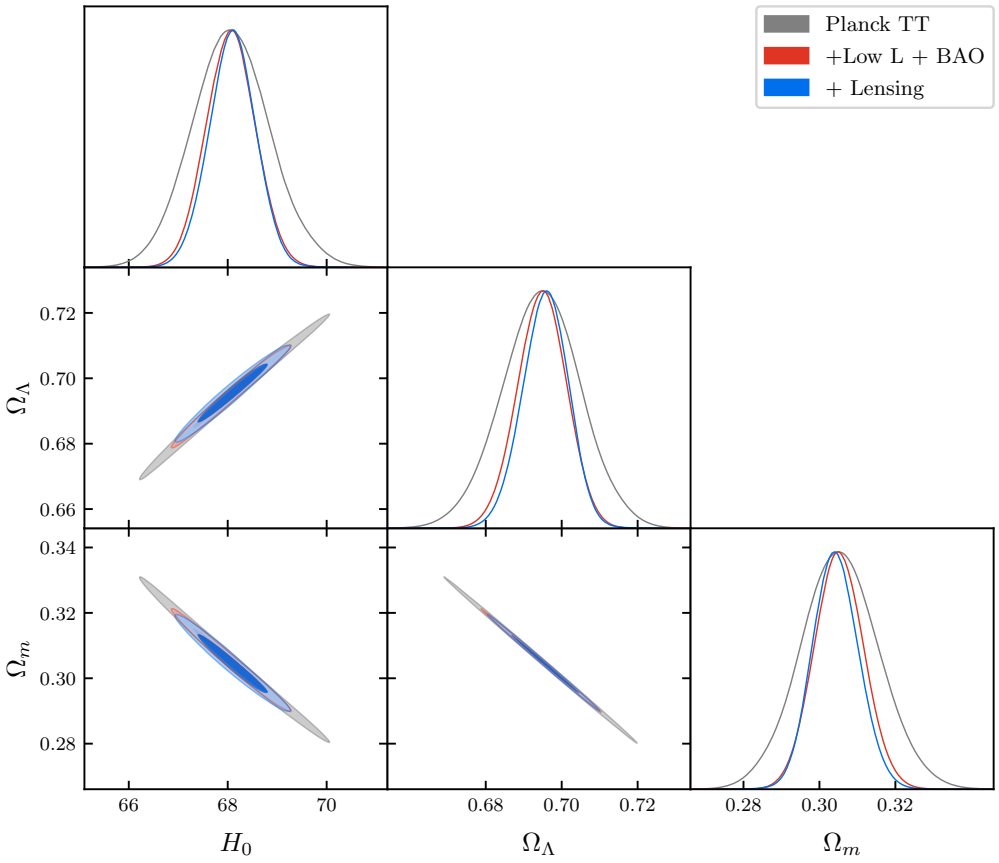

Figure 2.10 : PLANCK constraints for $\Omega_{\Lambda,0}, \Omega_{\rm m,0}$, and H_0.

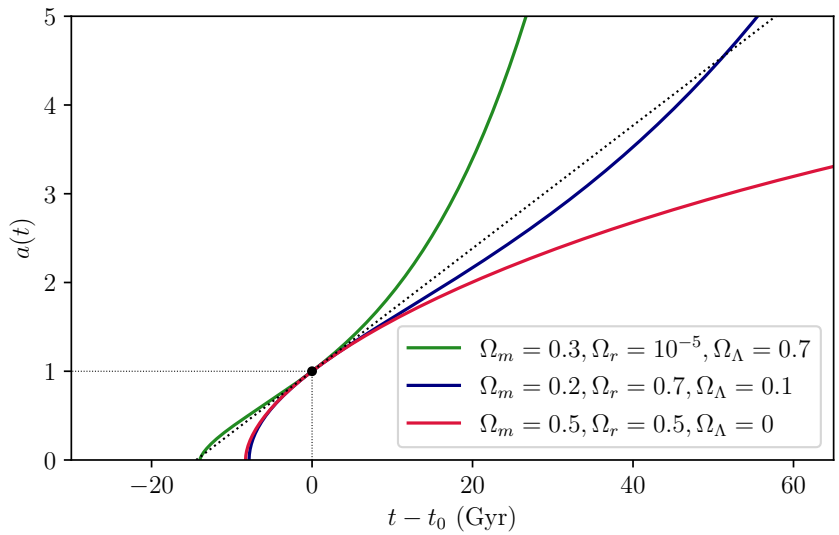

Figure 2.11 : Evolution of the scale factor in multiple component models. Since the energy density of cosmological constant is constant in time, eventually Λ becomes dominant component and universe starts to accelerate.

3. THERMAL HISTORY OF THE UNIVERSE

In this section, a part of thermal history of the universe, the "first 3 minutes" following inflation, is presented in detail. The thermodynamics of the universe is described by local equilibrium at early times, however non-equilibrium thermodynamics explains "why there is something rather than nothing". Non-equilibrium thermodynamics is important for the formation of light elements and origin of CMB.

3.1 Equilibrium Thermodynamics

A key point for the discussion of the thermal history of universe is the relation between the rate of interactions and expansion. If the interaction rate Γ is larger than the expansion rate H, then the reactions are fast enough to keep different species in equilibrium. In fact, this holds true and different species shares common temperature T through most of the early universe. On the other hand, the answer of "why there is something rather than nothing?" lies in dynamics of out-of-equilibrium.

In order to establish thermal equilibrium $\Gamma \gg H$, and in terms of time scales this condition can be expressed as

$$t_c \equiv \frac{1}{\Gamma} \ll t_H \equiv \frac{1}{H}. \tag{3.1}$$

As the universe expands, it becomes cooler and Γ starts to decrease faster than H. As a result, time scales of interactions and the expansion become comparable $t_c \sim t_H$. This is where particles start to decouple from the thermal bath. Decoupling time depends on the interaction rate of specific particle. In general, rate of particle interactions can be expressed in terms of number density n, cross-section σ and average velocity v as

$$\Gamma \equiv n\sigma v \tag{3.2}$$

The equilibrium condition given by Eq. (3.1) is satisfied within the interval

$$100\,\mathrm{GeV} < T < 10^{16}\,\mathrm{GeV}$$

3.1.1 From microscopic to macroscopic

In equilibrium, different species share same the temperature with thermal bath. In this section, we will start from microscopic dynamics and examine how this common temperature affects the energy density and pressure of species.

In the phase space, the smallest region for the localization of a particle is

$$\Delta x.\Delta p \sim h = 2\pi\hbar. \tag{3.3}$$

Hence, the density of the states can be simply expressed as

$$\frac{1}{h^3} = \frac{1}{(2\pi\hbar)^3}. \tag{3.4}$$

For g internal DoF, the density of states reads

$$\frac{g}{(2\pi\hbar)^3} \equiv \frac{g}{(2\pi)^3} \tag{3.5}$$

where we switched to natural units in the second equality. If the density of states is known, number and energy density of particles can be derived by using distribution functions $f_i(\boldsymbol{x},\boldsymbol{p},t)$. In 0–th order smooth universe, distribution functions can be simplified thanks to homogeneity and isotropy,

$$f(\boldsymbol{x},\boldsymbol{p},t) \xrightarrow[\text{homogeneity}]{} f(\boldsymbol{p},t) \xrightarrow[\text{isotropy}]{} f(p,t) \tag{3.6}$$

Note that time dependence of distribution function manifests itself in temperature, therefore it can be left implicit. The particle density can simply be expressed as

$$\frac{g}{(2\pi)^3} \times f(p). \tag{3.7}$$

and by integrating particle density over momentum, the number density of particles (n_i) can be found as

$$n = \frac{g}{(2\pi)^3} \int \mathrm{d}^3p\, f(p), \tag{3.8}$$

In the same manner, the energy density can be written as

$$\rho = \frac{g}{(2\pi)^3} \int \mathrm{d}^3p\, f(p)\, E(p) \tag{3.9}$$

and the pressure becomes

$$p = \frac{g}{(2\pi)^3} \int \mathrm{d}^3p\, f(p) \frac{p^2}{3E} \tag{3.10}$$

A critical point is to determine energy of a particle. By considering weak interactions, energy of a particle is

$$E(p) = \sqrt{m^2 + p^2}. \tag{3.11}$$

We are done with the fundamental expressions, starting from next section we will evaluate energy density and pressure for different species.

3.1.2 Local thermal equilibrium

Thermal equilibrium is achieved when the species are in both kinetic and chemical equilibrium. The species share a common temperature $T_i = T$ that can be identified as photon temperature T_γ.

In the kinetic equilibrium, energy and momentum is exchanged efficiently between the the particles. Fermions and bosons can be described with Fermi–Dirac and Bose–Einstein distribution function, respectively.

$$f(p) = \frac{1}{e^{[E(p)-\mu]/T} \pm 1}, \begin{cases} +1 \text{ for fermions like electron} \\ -1 \text{ for bosons like photon} \end{cases} \tag{3.12}$$

If the sum of chemical potentials of the reacting particles and the products are equal to each other, then the particles is said to be in chemical equilibrium. This also implies that forward and reverse reactions rates are equal. From the fundamental thermodynamic relation, chemical potential can be obtained as

$$\begin{gathered} \mathrm{d}E = T\mathrm{d}S - P\mathrm{d}V + \mu\mathrm{d}N \quad \text{OR} \quad \mathrm{d}S = \frac{\mathrm{d}E}{T} + \frac{P}{T}\mathrm{d}V - \frac{\mu}{T}\mathrm{d}N \\ \mu = -T\left(\frac{\partial S}{\partial N}\right)_{E,V} \end{gathered} \tag{3.13}$$

3.1.3 Energy density and pressure

The aim of the section is to relate the energy density and pressure of weakly interacting particles to temperature of the universe. The chemical potential μ can be neglected at early times [2, 23]. Then Eqs. (3.8) and (3.9) becomes

$$n = \frac{g}{2\pi^2}\int_0^\infty \mathrm{d}p \frac{p^2}{\exp\left[\sqrt{p^2+m^2}/T\right] \pm 1} \tag{3.14}$$

and

$$\rho = \frac{g}{2\pi^2}\int_0^\infty \mathrm{d}p \frac{p^2\sqrt{p^2+m^2}}{\exp\left[\sqrt{p^2+m^2}/T\right] \pm 1} \tag{3.15}$$

where we have reduced the dimension via

$$\int \mathrm{d}^3p = \int_0^\infty p^2\mathrm{d}p \underbrace{\int_0^\pi \sin\theta\,\mathrm{d}\theta \int_0^{2\pi} \mathrm{d}\phi}_{=4\pi}. \tag{3.16}$$

For convenience, let us define $x \equiv m/T$ and $\xi \equiv p/T$, then the density expressions takes the form

$$\begin{aligned} n &= \frac{g}{2\pi^2}T^3 \int_0^\infty \mathrm{d}\xi\, \frac{\xi^2}{\exp\left[\sqrt{\xi^2+x^2}\right]\pm 1} \\ \rho &= \frac{g}{2\pi^2}T^4 \int_0^\infty \mathrm{d}\xi\, \frac{\xi^2+\sqrt{\xi^2+x^2}}{\exp\left[\sqrt{\xi^2+x^2}\right]\pm 1} \end{aligned} \tag{3.17}$$

In general, evaluation of equation set (3.17) may require numerical integration, however in relativistic and non-relativistic limits analytical results can be obtained using Riemann-Zeta functions.

$$\begin{aligned} \text{B - E:} \int_0^\infty \mathrm{d}\xi\, \frac{\xi^n}{e^\xi - 1} &= \zeta(n+1)\Gamma(n+1) \\ \text{F - D:} \int_0^\infty \mathrm{d}\xi\, \frac{\xi^n}{e^\xi + 1} &= \left(1-\frac{1}{2^n}\right)\Gamma(n+1)\zeta(n+1) \\ \int_0^\infty \mathrm{d}\xi\, \xi^n e^{-\xi^2} &= \frac{1}{2}\Gamma\left(\frac{n+1}{2}\right) \end{aligned} \tag{3.18}$$

Number and energy densities for bosons and fermions will be evaluated at relativistic and non-relativistic limits.

3.1.3.1 Relativistic limit

When the temperature is much higher than the mass of a particle, i.e., in the limit $T \gg m \implies x \to 0$, number and energy density integrals reduce to

$$\begin{aligned} n &= \frac{g}{2\pi^2}T^3 \int_0^\infty \mathrm{d}\xi\, \frac{\xi^2}{e^\xi \pm 1} \\ \rho &= \frac{g}{2\pi^2}T^4 \int_0^\infty \mathrm{d}\xi\, \frac{\xi^3}{e^\xi \pm 1} \end{aligned} \tag{3.19}$$

Now, in order to proceed systematically let us consider bosons and fermions seperately.

Bosons

For bosons, Eq. (3.19) can be evaluated as

$$n_b = \frac{g}{2\pi^2} T^3 \int_0^\infty \mathrm{d}\xi \, \frac{\xi^2}{e^\xi - 1} = \frac{g}{2\pi^2} T^3 \zeta(3)\Gamma(3) = \frac{\zeta(3)}{\pi^2} g T^3 \tag{3.20}$$

and

$$\rho_b = \frac{g}{2\pi^2} T^4 \int_0^\infty \mathrm{d}\xi \, \frac{\xi^3}{e^\xi - 1} = \frac{g}{2\pi^2} T^4 \zeta(4)\Gamma(4) = \frac{\pi^2}{30} g T^4 \tag{3.21}$$

where we have defined number density and energy density of bosons as n_b and ρ_b, respectively.

Fermions

For fermions, Eq. (3.19) can be evaluated as

$$\begin{aligned} n_f &= \frac{g}{2\pi^2} T^3 \int_0^\infty d\xi \, \frac{\xi^2}{e^\xi + 1} \frac{g}{2\pi^2} T^3 \left(1 - \frac{1}{2^2}\right) \cdot 2 \cdot \zeta(3) = \frac{3}{4} \frac{\zeta(3)}{\pi^2} g T^3 \\ \rho_f &= \frac{g}{2\pi^2} T^4 \int_0^\infty d\xi \, \frac{\xi^3}{e^\xi + 1} = \frac{g}{2\pi^2} T^4 \left(1 - \frac{1}{2^3}\right) \cdot 3! \cdot \zeta(4) = \frac{7}{8} \frac{\pi^2}{30} g T^4 \end{aligned} \tag{3.22}$$

where we have defined number density and energy density of fermions as n_f and ρ_f, respectively. When we compare equations obtained for bosons and fermions, it can be seen that number / energy density expressions for fermions differ by just numerical factor. Therefore, it is more convenient to express them as

$$\boxed{n = \frac{\zeta(3)}{\pi^2} g T^3 \begin{cases} 1 & : \text{bosons} \\ \frac{3}{4} & : \text{fermions} \end{cases}} \tag{3.23}$$

and

$$\boxed{\rho = \frac{\pi^2}{30} g T^4 \begin{cases} 1 & : \text{bosons} \\ \frac{7}{8} & : \text{fermions} \end{cases}} \tag{3.24}$$

3.1.3.2 Non - relativistic limit

In the case of temperature drops below the mass, i.e. $m \gg T \implies x \gg 1$, number density becomes

$$n \approx \frac{g}{2\pi^2} T^3 \int_0^\infty \mathrm{d}\xi \, \frac{\xi^2}{\exp\left(\sqrt{\xi^2 + x^2}\right)}. \tag{3.25}$$

In the above equation, the larger contribution comes from x, therefore

$$\begin{aligned} f(\xi) &\equiv \left(\xi^2 + x^2\right)^{1/2} \text{ near } \xi = 0 \\ f(\xi) &\approx x + \frac{\xi^2}{2x}. \end{aligned} \tag{3.26}$$

The number density becomes

$$\begin{aligned} n &= \frac{g}{2\pi^2} T^3 \int_0^\infty \mathrm{d}\xi \, \frac{\xi^2}{e^x \cdot e^{\xi^2/2x}} \\ &= \frac{g}{2\pi^2} T^3 e^{-x} \underbrace{\int_0^\infty \mathrm{d}\xi \, \xi^2 e^{-\xi^2/2x}}_{\frac{1}{4}\sqrt{8\pi x^3}} \\ &= \frac{g}{2\pi^2} T^3 e^{-x} \cdot (2x)^{3/2} \cdot \frac{\sqrt{\pi}}{4} \end{aligned} \tag{3.27}$$

If we substitute $x \equiv m/T$ back, then n in non-relativistic limit can be obtained as

$$\boxed{n = g \left(\frac{mT}{2\pi}\right)^{3/2} e^{-m/T}} \tag{3.28}$$

Simce $E(p) = \sqrt{p^2 + m^2} \approx m$ in this limit, energy density then equals to $\rho \approx mn$. Eq. (3.28) has an important result: Energy density of a species is "Boltzmann suppressed" when the temperature drops below the mass of that species. This can also be interpreted as the annihilation of particles and anti-particles [4].

3.2 Cosmic Inventory

In this section, the developed formalism for the bosons and fermions is applied explicitly to components of the universe. Also, current observations and surveys for each gradient are briefly summarized.

3.2.1 Photons

The major contribution to Ω_r comes from the photons. Temperature of CMB as measured by FIRAS is $T_0 = 2.726 \pm 0.001\,\mathrm{K}$ [24]. For photons, energy density equation for bosons, Eq. (3.21), reduces to

$$\rho_\gamma = \frac{\pi^2}{15} T^4 \tag{3.29}$$

where we used $g = 2$ for the two spin-states. As we have shown in the previous sections, energy density of radiation scales a^{-4}, therefore $T_{\text{CMB}} \propto a^{-1}$.

$$\Omega_{\gamma,0} = \frac{\rho_{\gamma,0}}{\rho_{c,0}} = \frac{\pi^2 (k_B T_0)^4}{15\hbar c^3} \cdot \underbrace{\frac{8\pi G}{3H_0^2 c^2}}_{\rho_{c,0}} \Longrightarrow \boxed{\Omega_{\gamma,0} h^2 = 2.47 \times 10^{-5}} \tag{3.30}$$

If we explicitly show the dependence on scale factor, energy density for photons becomes

$$\Omega_{\gamma} h^2 = \frac{2.47 \times 10^{-5}}{a^4}. \tag{3.31}$$

Since we have used 0-th order distribution functions and neglect the perturbations, photon energy density only depends on time via the scale factor. The perturbations with spatial dependence correspond to CMB anisotropies [2].

3.2.2 Baryons

Although it is technically wrong[1], we refer to all ordinary matter as baryons by using the standard convention. Baryons can not be simply described as a gas and they must be measured directly unlike the photons. On the other hand, direct measuring methods also relies on matter - radiation interaction. Various measurement methods and constraints for baryons from the surveys are given below:

1. Direct Measurement

   (a) Counting the amount in stars and galaxies: Since the detection of hot ionized gas is difficult, there is uncertainty in estimations [25].

   (b) Spectra of quasars: The amount of absorbed the light is a measure of hydrogen which can be related to baryon density. However, since the absorption spectrum relies on the thermal state of inter-galactic medium, there is also uncertainty in the estimations [26].

2. Measurements from the Early Universe

   (a) Big Bang Nucleosynthesis: As we will shown in the following sections, total baryon density plays important role on the abundance of light elements.

[1] Since electrons are leptons

Measurements come from fractional amount of Deuterium indicates $\Omega_b h^2 = 0.0222 \pm 0.005 \implies \Omega_b \approx 0.045$ [27].

(b) Cosmic Microwave Background: Plasma oscillations that we see their imprints as CMB anisotropies implies $\Omega_b h^2 = 0.0225 \pm 0.0003 \implies \Omega_b \approx 0.046$ [7].

These techniques estimates $\sim 5\%$ of the critical density takes contribution from baryons.

3.2.3 Dark matter

Methods based on the gravitational effects are used to determine dark matter density.

1. Cosmic Microwave Background Anisotropies: Using the effect of matter on the expansion history and on gravitational potential, one can infer matter density from CMB anisotropies. According to Planck, $\Omega_m h^2 = 0.1431 \pm 0.0025 \implies \Omega_m \approx 0.29$ [7].

2. Supernovae Observations: Combination of CMB data with Type Ia Supernovae observations indicates that $\Omega_m = 0.311 \pm 0.006$.

3. Large Scale Structure: Observations of galaxy velocities and gravitational lensing by Dark Energy Survey constrained matter density as $\Omega_m = 0.27^{+0.03}_{-0.02}$ [28].

4. Thermal X-Ray Emission: Most of the baryonic matter is located in a galaxy clusters as hot gas. Therefore, they are observable through thermal X-ray emission. The ratio Ω_b/Ω_m is determined through these observations and since baryon density is known by observations, matter density can be determined $\Omega_b/\Omega_m = (0.089 \pm 0.012)h^{-3/2} \implies \Omega_b/\Omega_m \approx 1/6$ [29].

These observations are all in agreement with $\Omega_b \sim 0.05$ and $\Omega_m \sim 0.3$

3.2.4 Neutrinos

Although neutrinos have not been directly observed, their theoretical foundation is quite strong. Besides, various surveys such as PLANCK constrain not only the photon density, but also the total contribution of relativistic particles Ω_{r}. Theoretical

expectation of contribution from neutrinos is consistent with current observations [2]. A convenient way to study neutrinos is to relate them with a very well-known quantity. The best candidates are photons for this purpose. The main goal in this part is to relate neutrino temperature to photon temperature, i.e. obtaining the famous ratio $\frac{T_\nu}{T_\gamma} = \left(\frac{4}{11}\right)^{1/3}$ and evaluate energy density for neutrinos through this ratio.

Neutrinos are decoupled ($T \sim 0.8\,\mathrm{MeV}$) before the electron-positron annihilation ($T \sim 0.5\,\mathrm{MeV}$)

$$e^+ + e^- \leftrightarrow \gamma + \gamma, \tag{3.32}$$

and therefore energy density are transferred to only photons. As a result, photons become hotter than neutrinos [2, 4]. A quantity that we can relate them is the total entropy density s:

$$\begin{aligned} s &= \sum_i \frac{\rho_i + P_i}{T_i} = \frac{\rho_r + P_r}{T} = \frac{4}{3T}\rho_r \\ &= \frac{2\pi^2}{45} T^3 \left(g_b + \frac{7}{8} g_f \right). \end{aligned} \tag{3.33}$$

Before annihilation at (a_1, T_1) we have

$$s(a_1) = \frac{2\pi^2}{45} T_1^3 \left[2 + \frac{7}{8}(2+2+3+3) \right] = \frac{43\pi^2}{90} T_1^3 \tag{3.34}$$

where T_1 is the common temperature for photons and neutrinos. However, after annihilation at (a_2), temperature of neutrinos(T_ν) and photons(T_γ) must be distinguished:

$$s(a_2) = \frac{2\pi^2}{45} \left[2T_\gamma^3 + \frac{7}{8} \cdot 6T_\nu^3 \right] \tag{3.35}$$

Since the entropy density scales as

$$s \propto a^{-3} \implies s(a_1) a_1^3 = s(a_2) a_2^3 \tag{3.36}$$

one can evaluate entropy density at a_1 and a_2 as

$$\begin{aligned} \frac{43\pi^2}{90} (T_1 a_1)^3 &= \frac{2\pi^2}{45} \left[2T_\gamma^3 + \frac{7}{8} \cdot 6T_\nu^3 \right] a_2^3 \\ \frac{43}{2} (T_1 a_1)^3 &= 4 \left[\left(\frac{T_\gamma}{T_\nu} \right)^3 + \frac{21}{8} \right] (T_\nu a_2)^3 \end{aligned} \tag{3.37}$$

Neutrino temperature scales as $T_\nu \propto 1/a$, therefore $a_1 T_1 = a_2 T_\nu(a_2)$. Putting all together, the ratio of temperature of neutrinos to photons can be obtained as

$$\frac{43}{8} = \frac{21}{8} + \left(\frac{T_\gamma}{T_\nu}\right)^3 \implies \boxed{\frac{T_\nu}{T_\gamma} = \left(\frac{4}{11}\right)^{1/3}}. \tag{3.38}$$

Since the energy density of photons is known, using temperature ratio given by Eq. (3.38) neutrino energy density can be determined. Using the energy density expression for fermions and boson, the energy density ratio of neutrinos to photons can be obtained as

$$\frac{\rho_\nu}{\rho_\gamma} = \frac{\frac{7}{8} g_\nu T_\nu^4}{g_\gamma T_\gamma^4} = \frac{21}{8}\left(\frac{4}{11}\right)^{4/3}. \tag{3.39}$$

Since Ω_γ is known, Ω_ν can also be determined as

$$\Omega_{\nu,0} = \left(2.47 \times 10^{-5} h^{-2}\right) \times \frac{21}{8}\left(\frac{4}{11}\right)^{4/3} = \frac{1.68 \times 10^{-5}}{h^2}. \tag{3.40}$$

Following similar manner, the ratio of number densities can be found as

$$\frac{n_\nu}{n_\gamma} = \frac{\frac{3}{4} g_\nu T_\nu^3}{g_\gamma T_\gamma^3} = \frac{9}{11} \tag{3.41}$$

where n_γ is equal to

$$n_\gamma = \frac{2\zeta(3)}{\pi^2 \hbar^3 c^3}(k_B T)^3 \implies n_{\gamma,0} = 410.48\,\mathrm{cm}^{-3} \tag{3.42}$$

Therefore, number density of one generation neutrino is obtained as

$$n_{\nu(1),0} = n_{\gamma,0}\frac{3}{11} = 410.48 \times \frac{3}{11} = 111.95\,\mathrm{cm}^{-3} \tag{3.43}$$

3.3 Origin of Species

In this section, we shall investigate the non-equilibrium thermodynamics and formation/abundance of light elements in Big Bang Nucleosynthesis by the help of Boltzmann equation. Non-equilibrium physics is also responsible for recombination and dark matter production.

3.3.1 The Boltzmann equation

In the simplest form Boltzmann equation is given by

$$\frac{\mathrm{d}f}{\mathrm{d}t} = C[f] \tag{3.44}$$

where f is the distribution function of the tracked species and $C[f]$ is the collision term. Notice that collisional term is a functional of distribution function and it represents interactions of the particles in a system. Without any interaction, the number density evolves as

$$\frac{dn_i}{dt} + 3\frac{\dot{a}}{a}n_i = 0 \tag{3.45}$$

When we include effects of interactions

$$\frac{dn_i}{dt} + 3\frac{\dot{a}}{a}n_i = C_i\left[\{n_j\}\right] \tag{3.46}$$

where the collision term on the RHS depends on the specific interactions under consideration. In order to express more rigorously, let us keep track of number density n_1 of species 1 in the following reaction

$$1 + 2 \leftrightarrow 3 + 4, \tag{3.47}$$

where particles 1 and 2 annihilate to produce 3 and 4, or the inverse process may occur. For this system, Boltzmann equation is written as

$$\begin{aligned} a^{-3}\frac{\mathrm{d}\left(n_1 a^3\right)}{\mathrm{d}t} = &\int \frac{\mathrm{d}^3 p_1}{(2\pi)^3 2E_1}\int \frac{\mathrm{d}^3 p_2}{(2\pi)^3 2E_2}\int \frac{\mathrm{d}^3 p_3}{(2\pi)^3 2E_3}\int \frac{\mathrm{d}^3 p_4}{(2\pi)^3 2E_4} \\ &\times (2\pi)^4 \delta_{\mathrm{D}}^{(3)}\left(\boldsymbol{p}_1 + \boldsymbol{p}_2 - \boldsymbol{p}_3 - \boldsymbol{p}_4\right)\delta_{\mathrm{D}}^{(1)}\left(E_1 + E_2 - E_3 - E_4\right)|\mathscr{M}|^2 \\ &\times \{f_3 f_4\left[1 \pm f_1\right]\left[1 \pm f_2\right] - f_1 f_2\left[1 \pm f_3\right]\left[1 \pm f_4\right]\} \end{aligned} \tag{3.48}$$

Notice that, in the case of no interaction the expression reduces to Eq. (3.45). Here the 2nd line is the basically energy-momentum conservation for interactions, and the nature of interactions is represented by the amplitude $|\mathscr{M}|^2$. The last tine corresponds to proportionality of the rate of change for particle 1, and $[1 + f_i]$ and $[1 - f_i]$ contributions are called "Bose enhancement" and "Pauli blocking", respectively [30].

Although this form of Eq.(3.48) is complicated for practical applications, it can be simplified. The temperature scales we are dealing with $T \ll E - \mu$, thus

$$f(E) = \frac{1}{e^{[E-\mu]/T} \pm 1} \xrightarrow{T \ll E-\mu} e^{\mu/T} e^{-E/T}. \tag{3.49}$$

In order to justify our approximation, let us plot the distribution functions in the limit $T \ll E - \mu$ in Figure 3.1.

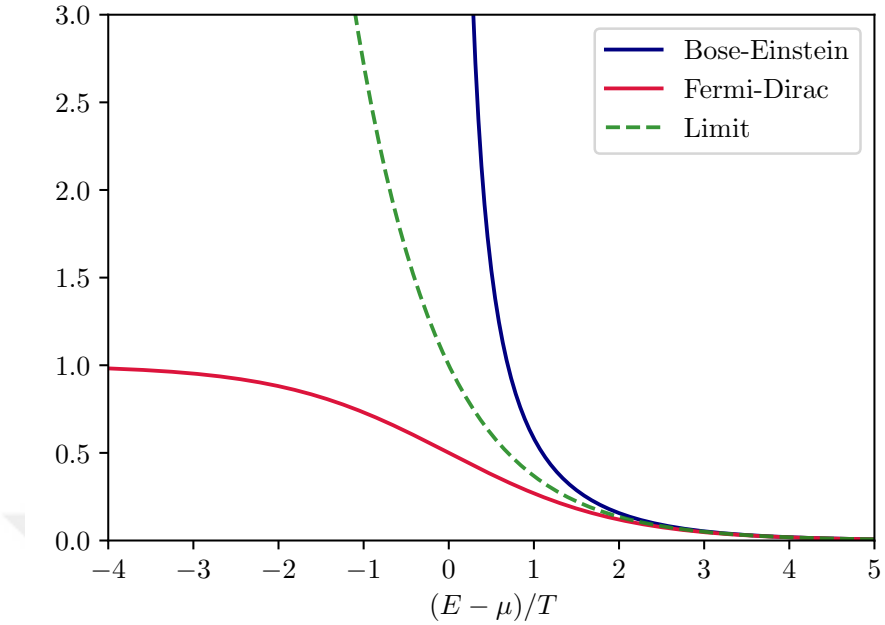

Figure 3.1 : Bose - Einstein, Fermi - Dirac distributions and low T limits given by Eq. (3.49).

Similarly, contributions from Bose enhancement and Pauli blocking can be neglected,

$$f_3 f_4 \left[1 \pm f_1\right]\left[1 \pm f_2\right] - f_1 f_2 \left[1 \pm f_3\right]\left[1 \pm f_4\right] \to f_3 f_4 - f_1 f_2. \tag{3.50}$$

Inserting Eq. (3.49) and using energy conservation $E_1 + E_2 = E_3 + E_4$ in the last line

$$e^{-(E_1+E_2)/T}\left\{e^{(\mu_3+\mu_4)/T} - e^{(\mu_1+\mu_2)/T}\right\} \tag{3.51}$$

Employing these approximations the number density given by Eq. (3.8) for species s is written as

$$n_s = g_s e^{\mu_s/T} \int \frac{\mathrm{d}^3 p}{(2\pi)^3} e^{-E_s(p)/T}. \tag{3.52}$$

As we have shown separately for relativistic and non-relativistic cases, number density for $\mu_s = 0$ becomes

$$n_s^{(0)} \equiv g_s \int \frac{\mathrm{d}^3 p}{(2\pi)^3} e^{-E_s(p)/T} = \begin{cases} g_s \left(\dfrac{m_s T}{2\pi}\right)^{3/2} e^{-m_s/T} & m_s \gg T \\ g_s \dfrac{T^3}{\pi^2} & m_s \ll T \end{cases} \tag{3.53}$$

Using this definition,

$$e^{(\mu_3+\mu_4)/T} - e^{(\mu_1+\mu_2)/T} = \frac{n_3 n_4}{n_3^{(0)} n_4^{(0)}} - \frac{n_1 n_2}{n_1^{(0)} n_2^{(0)}}.$$

Now, by defining thermally averaged cross section $\langle \sigma v \rangle$ as

$$\begin{aligned}\langle \sigma v \rangle \equiv & \frac{1}{n_1^{(0)} n_2^{(0)}} \int \frac{\mathrm{d}^3 p_1}{(2\pi)^3 2E_1} \int \frac{\mathrm{d}^3 p_2}{(2\pi)^3 2E_2} \int \frac{\mathrm{d}^3 p_3}{(2\pi)^3 2E_3} \int \frac{\mathrm{d}^3 p_4}{(2\pi)^3 2E_4} e^{-(E_1+E_2)/T} \\ & \times (2\pi)^4 \delta_{\mathrm{D}}^{(3)} (\boldsymbol{p}_1 + \boldsymbol{p}_2 - \boldsymbol{p}_3 - \boldsymbol{p}_4) \, \delta_{\mathrm{D}}^{(1)} (E_1 + E_2 - E_3 - E_4) \, |\mathscr{M}|^2 \end{aligned} \tag{3.54}$$

Boltzmann equation given by Eq. (3.48) becomes

$$\boxed{a^{-3} \frac{\mathrm{d}\left(n_1 a^3\right)}{\mathrm{d}t} = n_1^{(0)} n_2^{(0)} \langle \sigma v \rangle \left\{ \frac{n_3 n_4}{n_3^{(0)} n_4^{(0)}} - \frac{n_1 n_2}{n_1^{(0)} n_2^{(0)}} \right\}} \tag{3.55}$$

With these approximations and definitions, we obtained a simple differential equation to track the number density of each species. When the interaction rates are large, Eq. (3.55) approaches to

$$\boxed{\frac{n_3 n_4}{n_3^{(0)} n_4^{(0)}} = \frac{n_1 n_2}{n_1^{(0)} n_2^{(0)}}} \tag{3.56}$$

The relation corresponds to *nuclear statistical equilibrium* and also known as *Saha equation*. When $\Gamma \gg H$, Saha equation (3.56) must be satisfied.

3.3.2 Big Bang Nucleosynthesis

Big Bang Nucleosynthesis is the formation of the primordial light elements, it corresponds to $t \sim 3\,\mathrm{m}$ when the temperature was about $T \sim 0.1$ MeV. At this time, relativistic particles in equilibrium(photons, electrons, positrons), decoupled relativistic particles(neutrinos), and non-relativistic particles(baryons) consist the cosmic plasma. The main goal of the section is to determine evolution of the baryons. In principle we will evaluate the coupled differential equations

$$a^{-3} \frac{\mathrm{d}\left(n_1 a^3\right)}{\mathrm{d}t} = n_1^{(0)} n_2^{(0)} \langle \sigma v \rangle \left\{ \frac{n_3 n_4}{n_3^{(0)} n_4^{(0)}} - \frac{n_1 n_2}{n_1^{(0)} n_2^{(0)}} \right\} \tag{3.57}$$

for all nuclei. For simplification, we will assume that elements heavier than He are not produced. Thus, only hydrogen and helium, and their isotopes: deuterium, tritium, and ^{3}He will be tracked. Another simplification is that no other light nuclei has formed

except neutrons and protons above $T \sim 0.1$ MeV. These assumptions based on the fact that when the temperatures higher than the binding energies, every produced nuclei is destroyed by photons with high energy [2]. Also the smallness of baryon-to-photon ratio η_b supports the assumptions.

$$\begin{aligned}\frac{n_b}{n_\gamma} &= \frac{\frac{\rho_b}{m_p}}{n_\gamma} \times \frac{\rho_c}{\rho_c} \\ &= \Omega_b \frac{1.87\,h^2 \times 10^{-29}\ \mathrm{g\ cm^{-3}}}{1.673 \times 10^{-24}\ \mathrm{g} \cdot 411\ \mathrm{cm^{-3}}} \\ &= 2.725 \times 10^{-8}\,\Omega_b h^2 \\ &= 6.0 \times 10^{-10} \left(\frac{\Omega_b h^2}{0.022}\right)\end{aligned} \tag{3.58}$$

3.3.2.1 Deuterium production and Deuterium bottleneck

As mentioned in the previous section, formed deuterium nuclei are destroyed by high-energy photons and without deuterium BBN can not occur. This is called deuterium bottleneck. In order to express quantitatively, consider the reaction

$$n + p \leftrightarrow D + \gamma, \tag{3.59}$$

and the equilibrium condition for the reaction can be written using Saha equation (3.56) as

$$\frac{n_D n_\gamma}{n_D^{(0)} n_\gamma^{(0)}} = \frac{n_n n_p}{n_n^{(0)} n_p^{(0)}} \xrightarrow[n_\gamma = n_\gamma^0]{\mu_\gamma \ll 1} \frac{n_D}{n_D^{(0)}} = \frac{n_n n_p}{n_n^{(0)} n_p^{(0)}}, \tag{3.60}$$

and by rearranging it becomes

$$\boxed{\frac{n_D}{n_n n_p} = \frac{n_D^{(0)}}{n_n^{(0)} n_p^{(0)}}} \tag{3.61}$$

From Eq. (3.53), we can obtain species dependent number density for $\mu_s = 0$ as

$$\begin{aligned} n_D^{(0)} &= g_D \left(\frac{m_D T}{2\pi}\right)^{3/2} e^{-m_D/T} \\ n_n^{(0)} &= g_n \left(\frac{m_n T}{2\pi}\right)^{3/2} e^{-m_n/T} \\ n_p^{(0)} &= g_p \left(\frac{m_p T}{2\pi}\right)^{3/2} e^{-m_p/T} \end{aligned} \tag{3.62}$$

Then, Eq. (3.61) becomes

$$\begin{aligned}\frac{n_D}{n_n n_p} &= \frac{g_D}{g_n g_p}\left(\frac{2\pi m_D}{m_n m_p T}\right)^{3/2} e^{(m_n+m_p-m_D)}/T \\ \frac{n_D}{n_n n_p} &= \frac{3}{4}\left(\frac{4\pi}{m_p T}\right)^{3/2} e^{B_D/T}\end{aligned} \tag{3.63}$$

where we have defined B_D as deuterium binding energy:

$$B_D \equiv m_n + m_p - m_D = 2.22 \text{ MeV}. \tag{3.64}$$

The prefactor $\frac{3}{4}$ comes from the evaluation of DoFs (3 for D, 2 each for p and n) and the term inside the parenthesis is simplified using $m_D = 2m_n = 2m_p$. Further, both protons and neutron density are proportional to the baryon density:

$$n_n \simeq n_p \simeq n_b = \eta_b n_\gamma^{(0)} \tag{3.65}$$

where the photon number density is given by

$$n_\gamma^{(0)} = \frac{2T^3}{\pi^2} \tag{3.66}$$

Therefore, Eq. (3.63) becomes

$$\boxed{\frac{n_{\rm D}}{n_{\rm b}} \sim \eta_{\rm b}\left(\frac{T}{m_p}\right)^{3/2} e^{B_{\rm D}/T}} \tag{3.67}$$

In the above expression for deuterium-to-baryon ratio, the small prefactor η_b dominates this expression. Thus the small η_b thus prevents nuclei production, until the exponential term $e^{B_{\rm D}/T}$ dominates Eq. (3.67). After deuterium bottleneck, the following chain reactions occurs in BBN

$$\begin{aligned} p + n &\to {\rm D} + \gamma \\ D + D &\to D + {}^3{\rm He} + n \\ D + {}^3{\rm He} &\to D + {}^4{\rm He} + p \end{aligned} \tag{3.68}$$

3.3.2.2 Neutron abundance

Protons are converted into neutrons with

$$p + e^- \to n + \nu_e \tag{3.69}$$

and they were in equilibrium until the temperature $T \sim$ MeV. To keep track of neutrons, we will evaluate the Boltzmann equation

$$a^{-3}\frac{\mathrm{d}\left(n_1 a^3\right)}{\mathrm{d}t} = n_1^{(0)} n_2^{(0)} \langle \sigma v \rangle \left\{ \frac{n_3 n_4}{n_3^{(0)} n_4^{(0)}} - \frac{n_1 n_2}{n_1^{(0)} n_2^{(0)}} \right\} \tag{3.70}$$

by the help of neutron-proton ratio. Starting from the number densities for $\mu_s = 0$,

$$n_s^{(0)} \equiv g_s \int \frac{\mathrm{d}^3 p}{(2\pi)^3} e^{-E_s(p)/T} = g_s \left(\frac{m_s T}{2\pi}\right)^{3/2} e^{-m_s/T}, \tag{3.71}$$

the number densities for neutron and proton can be separately written as

$$\begin{aligned} n_n^{(0)} &= g_n \left(\frac{m_n T}{2\pi}\right)^{3/2} e^{-m_n/T} \\ n_p^{(0)} &= g_p \left(\frac{m_p T}{2\pi}\right)^{3/2} e^{-m_p/T}. \end{aligned} \tag{3.72}$$

Now, neutron-to-proton ratio can be formed, but since the mass proportionally $(m_p/m_n)^{3/2}$ is at the order of unity it can be neglected. However, this mass difference in exponential is important, we will keep it. Then the ratio can be written as

$$\frac{n_p^{(0)}}{n_n^{(0)}} = e^{\mathscr{Q}/T}, \tag{3.73}$$

where we defined the mass difference as $\mathscr{Q} \equiv m_n - m_p = 1.293\,\mathrm{MeV}$. Therefore, at high temperatures ($T \gg \mathscr{Q}$) abundance of p and n are roughly equal. For convenience, we define the ratio of neutrons to total nuclei and track it via Boltzmann equation. It is defined as

$$\boxed{X_n \equiv \frac{n_n}{n_n + n_p}}. \tag{3.74}$$

and in equilibrium,

$$X_{n,eq} \equiv \frac{1}{1 + n_p^{(0)}/n_n^{(0)}}. \tag{3.75}$$

In order to track X_n, we will start from Boltzmann equation again

$$\begin{aligned} a^{-3}\frac{\mathrm{d}(n_n a^3)}{\mathrm{d}t} &= n_n^{(0)} n_l^{(0)} \langle \sigma v \rangle \left\{ \frac{n_p n_l}{n_p^{(0)} n_l^{(0)}} - \frac{n_n n_l}{n_n^{(0)} n_l^{(0)}} \right\} \\ &= \underbrace{n_l^{(0)} \langle \sigma v \rangle}_{\equiv \lambda_{np}} \left\{ \frac{n_p n_n^{(0)}}{n_p^{(0)}} - n_n \right\} \end{aligned} \tag{3.76}$$

where the index l for particles 2 and 4 corresponds to leptons. Furthermore, λ_{np} is identified as the rate for neutron to proton conversion [31] and it is given by

$$\lambda_{np} = \frac{255}{\tau_n x^5}\left(12+6x+x^2\right) \tag{3.77}$$

where neutron life-time $\tau_n = 886.7$ s. The equation can be simplified even more. Remember, in Eq. (3.76), we defined neutron-to-proton ratio as $\frac{n_n^{(0)}}{n_p^{(0)}} = e^{-\mathcal{Q}}/T$. Now, let us rewrite n_n on the LHS using this definition as $(n_n+n_p)X_n$,

$$\begin{aligned} a^{-3}\frac{\mathrm{d}\left[(n_n+n_p)X_n a^3\right]}{\mathrm{d}t} &= \lambda_{np}\left\{n_p e^{-\mathcal{Q}/T} - n_n\right\} \\ a^{-3}\cdot(n_n+n_p)a^3\cdot\frac{\mathrm{d}X_n}{\mathrm{d}t} &= \lambda_{np}\left\{n_p e^{-\mathcal{Q}/T} - n_n\right\} \\ \frac{\mathrm{d}X_n}{\mathrm{d}t} &= \lambda_{np}\left\{\frac{n_p}{n_n+n_p}e^{-\mathcal{Q}/T} - \frac{n_n}{n_n+n_p}\right\} \\ \boxed{\frac{\mathrm{d}X_n}{\mathrm{d}t} &= \lambda_{np}\left\{(1-X_n)e^{-\mathcal{Q}/T} - X_n\right\}}. \end{aligned} \tag{3.78}$$

Using a new variable x defined as

$$x \equiv \frac{\mathcal{Q}}{T} \implies \mathrm{d}x = -\mathcal{Q}\frac{\mathrm{d}T}{T^2} = -\frac{\mathcal{Q}}{T}\frac{\mathrm{d}T}{T} = -x\frac{\mathrm{d}T}{T}, \tag{3.79}$$

the LHS of Eq. (3.78) becomes

$$\frac{\mathrm{d}X_n}{\mathrm{d}t} = \frac{\mathrm{d}X_n}{\mathrm{d}x}\frac{\mathrm{d}x}{\mathrm{d}t} = \dot{x}\frac{\mathrm{d}X_n}{\mathrm{d}x}. \tag{3.80}$$

To go further,

$$T \propto 1/a \to \dot{T} \propto -\dot{a}/a^2 \implies \frac{\dot{T}}{T} = -H = -\sqrt{\frac{8\pi G}{3}\rho} \tag{3.81}$$

BBN takes place in the radiation dominated epoch, thus energy density mostly comes from relativistic particles

$$\rho_r = \frac{\pi^2}{30}T^4\underbrace{\left\{\sum_{s=\text{bosons}} g_s + \frac{7}{8}\sum_{s=\text{fermions}} g_s\right\}}_{\equiv g_*:\,\text{effective relativistic DoF}} = g_*\frac{\pi^2}{30}T^4 \tag{3.82}$$

At $T \sim 1$ MeV we have photons ($g_\gamma = 2$), neutrinos ($g_\nu = 6$), electrons ($g_{e^-} = 2$), positrons ($g_{e^+} = 2$), therefore effective relativistic DoF is $g_* = 10.75$. Using these, Eq. (3.78) becomes

$$\boxed{\frac{\mathrm{d}X_n}{\mathrm{d}x} = \frac{x\,\lambda_{np}}{H(x=1)}\left\{e^{-x} - X_n(1+e^{-x})\right\}} \tag{3.83}$$

where $H(x)$ is defined as

$$H(x) = \sqrt{\frac{8\pi G}{3}\frac{g_*\pi^2 T^4}{30}} = \sqrt{\frac{4\pi^3 G}{45} g_* \frac{\mathscr{Q}^4}{x^4}} = x^{-2}\sqrt{\frac{4\pi^3 G}{45} g_* \mathscr{Q}^4}. \tag{3.84}$$

therefore $H(x=1) = 1.13\ \mathrm{s}^{-1}$. Numerical solution of the differential equation (3.83) is shown in Figure 3.2.

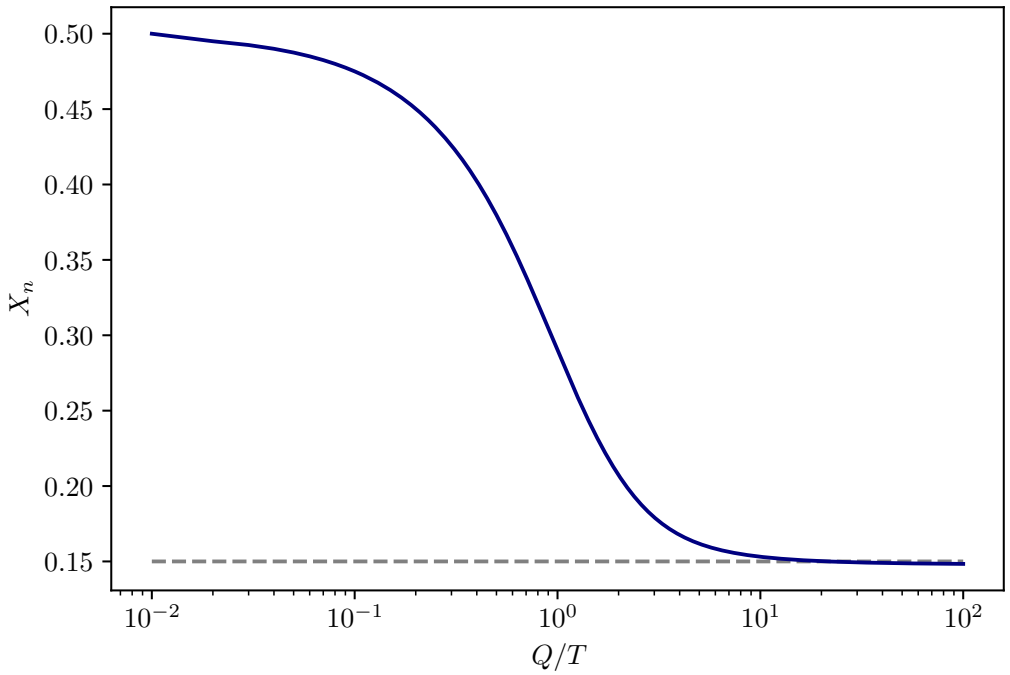

Figure 3.2 : Numerical solution of neutron-to-nuclei ratio.

As marked on the Figure 3.2, neutron-to-nuclei ratio $X_n \to 0.15$ in the limit $x \to \infty$. In fact, this is not a good approximation. Since there are other processes related to neutrons, the coupled Boltzmann equations must be numerically solved for them. We will take into account β-decay correction to bring $X_n = 0.15$ into an acceptable level. Neutron decay is given by the reaction

$$n \to p + e^- + \bar{\nu} \tag{3.85}$$

and the reaction shows itself as a correction to X_n by the factor $\exp(-t/\tau_n)$. Now, we shall calculate t_{BBN}. As we have shown before, in the radiation-dominated epoch

$$H^2 = \frac{8\pi G}{3}\rho_r = g_* T^4 \frac{4\pi^3 G}{45} \tag{3.86}$$

and since $a \propto \sqrt{t}$ in epoch of radiation,

$$\frac{1}{4t^2} = H^2 = g_* T^4 \frac{4\pi^3 G}{45} \tag{3.87}$$

Electron-positron annihilation has already occurred at the temperature $T_{\rm BBN} \approx 0.07$ MeV, and we only have photons and neutrinos. Thus effective relativistic DoF can be found as

$$\begin{aligned} g_* &= \sum_{i=bos} g_i \left(\frac{T_i}{T}\right)^4 + \frac{7}{8} \sum_{i=fer} g_i \left(\frac{T_i}{T}\right)^4 \\ &= 2 + \frac{7}{8} \cdot 6 \cdot \left(\frac{4}{11}\right)^{4/3} \approx 3.36. \end{aligned} \tag{3.88}$$

In the last step, the temperature ratio of neutrinos and photons as given by Eq. (3.38) is used. Thus, from Eq. (3.87)

$$t = 271 \left(\frac{0.07 \text{ MeV}}{T}\right)^2 \text{ s} = 132 \left(\frac{0.01 \text{ MeV}}{T}\right)^2 \text{ s} \tag{3.89}$$

Evaluating X_n at temperature $T_{\rm BBN}$ we find

$$\boxed{X_n(T_{\rm BBN}) = 0.15 \cdot e^{-271/886.7} \approx 0.11}. \tag{3.90}$$

3.3.2.3 Abundance of light elements

We have shown in Eq. (3.67) that deuterium abundance is negligible in the case of $T \gg B_D$,

$$\frac{n_{\rm D}}{n_{\rm b}} \sim \eta_{\rm b} \left(\frac{T}{m_p}\right)^{3/2} e^{B_{\rm D}/T} \tag{3.91}$$

Even if $T \sim B_D$, deuterium abundance is still very small due to small η_b. Taking the logarithm of above expression at $T_{\rm BBN}$ in which $n_D \sim n_b$ yields,

$$\ln\left(\frac{12}{\sqrt{\pi}}\eta_b\right) + \frac{3}{2}\ln\left(\frac{T_{\rm BBN}}{m_p}\right) = -\frac{B_D}{T_{\rm BBN}} \tag{3.92}$$

and solving for $T_{\rm BBN}$, one can find $T_{\rm BBN} \approx 0.07$ MeV. We have used this temperature in the previous section. Two neutrons form ^{4}He, thus we can infer that at $T_{\rm BBN}$, ^{4}He abundance can be found as

$$Y_p \equiv 4X_{^4\text{He}} \equiv \frac{4\,n(^4\text{He})}{n_b} = \frac{4 \times 0.5 n_n}{n_b} = 2X_n\,(T_{\rm BBN}) = 0.22 \tag{3.93}$$

where Y_p is the ratio of helium to protons and neutrons in mass density. It is a approximated solution, however, it is in agreement with numerical results in the literature [23]:

$$Y_P = 0.2262 + 0.0135 \ln\left(\eta_b / 10^{-10}\right) = 0.2505. \tag{3.94}$$

Thus , the final expression for helium abundance has dependence on baryon density.

4. INFLATION

Inflation is the accelerated expansion of the universe during the early stages and it was introduced in order to explain homogeneity of the universe on large scales [14–16, 32, 33]. More specifically, the problem arises from how patches on CMB that have never been in causal contact, share the same temperature. Thus, historically, motivation for inflation was largely based on more philosophical grounds concerning "*whether the initials conditions required for the hot Big Bang seem likely or not*". However, the major success of inflation was realized after: inflationary mechanism as a solution to horizon and flatness problems can also be the answer for the generation of initial perturbations in the universe. Although it is the most widely accepted scenario of the early universe, direct test of inflation is difficult due to energy scales that are far beyond the current accelerators. On the other hand, generic predictions of inflationary stage provides constraints on initial conditions that can be verified experimentally with current and upcoming surveys. Observations indicate that initial conditions for the structure formation is adiabatic, Gaussian and has a scale invariant spectrum, i.e. spectral index $n_s < 1$.

We will start with the discussion of the problems of Big Bang and how the inflating universe resolves these problems, then examine the dynamics of inflaton and slow–roll mechanism. The section will be finalized with the analysis of single field inflation models with a potential of the form $V(\phi) \propto \phi^n$.

4.1 Shortcomings of Standard Big Bang Scenario

4.1.1 Flatness problem

Current observations indicate that geometry of the universe is very close to be flat, i.e. $\Omega_0 \simeq 1$. On the other hand, if we simply look at the energy density expression, flatness of the universe requires extremely fine-tuned initial conditions. As shown in Section

2,

$$1-\Omega(t) = -\frac{kc^2}{a^2(t)H^2(t)}, \tag{4.1}$$

and using present moment convention at $t = t_0$, $a(t = t_0) = 1$

$$1-\Omega_0 = -\frac{kc^2}{H_0^2} \implies -kc^2 = (1-\Omega_0)H_0^2 \tag{4.2}$$

Plugging $-kc^2$ term into Eq. (4.1) yields

$$1-\Omega(t) = \frac{(1-\Omega_0)H_0^2}{a^2(t)H^2(t)}, \tag{4.3}$$

and by neglecting dark energy, Friedmann equation for radiation and matter reads

$$\frac{H^2}{H_0^2} = \frac{\Omega_{r,0}}{a^4} + \frac{\Omega_{m,0}}{a^3}$$

and deviation term becomes

$$1-\Omega(t) = \frac{1-\Omega_0}{a^2}\left[\frac{a^4}{\Omega_{\mathrm{r},0} + a\Omega_{\mathrm{m},0}}\right] = \frac{(1-\Omega_0)a^2}{\Omega_{\mathrm{r},0} + a\Omega_{\mathrm{m},0}} \tag{4.4}$$

Final expression of the deviation of energy density from one can be expressed as,

$$\boxed{1-\Omega(t) = a^2\,\frac{1-\Omega_0}{\Omega_{r,0} + a\,\Omega_{m,0}}} \tag{4.5}$$

Notice that the deviation term is different in different epochs and can be summarized as

$$\begin{cases} \text{Radiation Dominated Era:} & |1-\Omega(t)| \propto a_{(r)}^2 = (t^{1/2})^2 = t \\ \text{Matter Dominated Era:} & |1-\Omega(t)| \propto a_{(m)} = t^{2/3} \end{cases} \tag{4.6}$$

Thus, one can conclude that since $|1-\Omega(t)|$ increases in radiation and matter dominated eras, universe had to be much more flatter in the past. More specifically, if we extrapolate the divergence from $\Omega = 1$ to matter-radiation equality, BBN, and Planck time:

$$\begin{aligned} |1-\Omega_{\mathrm{eq}}| &\leq 10^{-6}, \\ |1-\Omega_{\mathrm{BBN}}| &\leq 10^{-16}, \\ |1-\Omega_{\mathrm{pl}}| &\leq 10^{-62}. \end{aligned} \tag{4.7}$$

We can extrapolate classical theory farthest to Planck time and it requires such an extreme fine-tuning to agree with current observations. Conversely, accelerated

expansion leads $|1-\Omega(t)|$ to decrease in time, and therefore enables Big Bang to start with more generic conditions. Schematic illustration of how inflation drives Ω to 1 is shown in Figure 4.1.

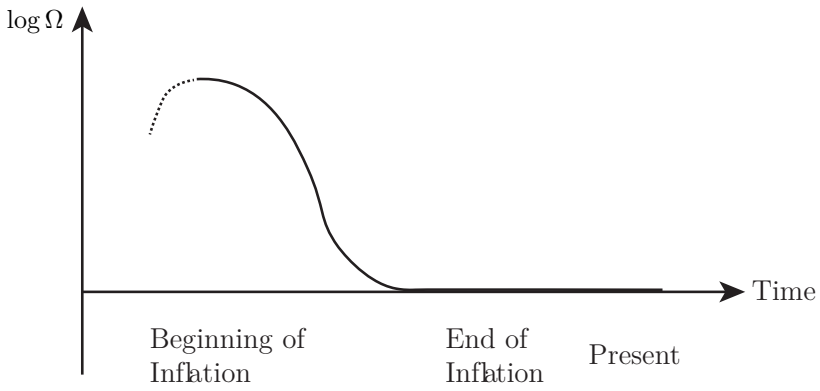

Figure 4.1 : Schematic illustration of inflationary solution to flatness problem. Energy density Ω is driven towards to unity. The figure is adapted from [3].

4.1.2 Horizon problem

Big Bang cosmology does not explain homogeneity and isotropy on large scales. On the contrary, it predicts many causally disconnected regions of space in the early universe. If we start with a inhomogeneous universe, these disjoint patches did not have time to causal contact at the time of recombination, i.e., when CMB was started to release. Before proceeding with the horizon problem, we will define horizons to understand the concept of causality.

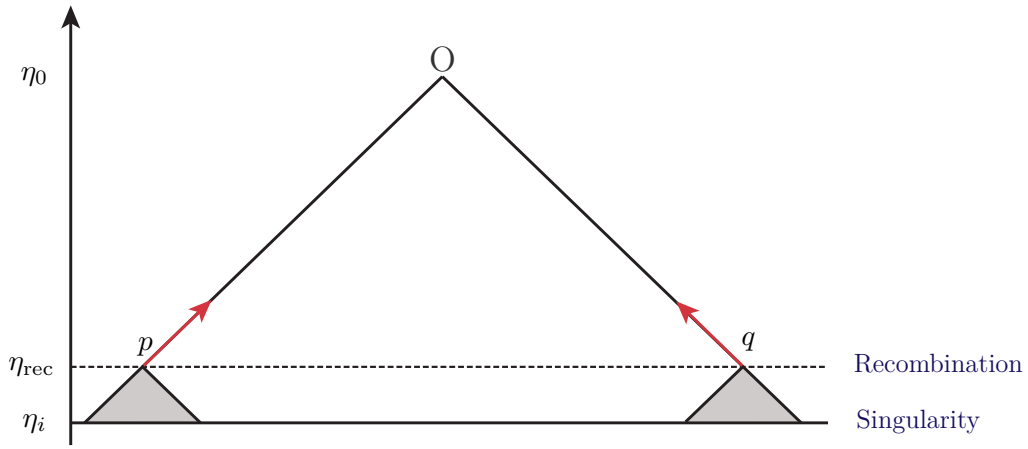

Figure 4.2 : Illustration of horizon problem. The figure is adapted from [4].

4.1.2.1 Particle horizon

In order to determine the size of a causally connected region of space, we should find how far photon can travel in a particular time interval. The propagation of photons

in an expanding space can be easily studied using conformal time. For simplicity, consider a light ray in the radial direction. Then the line element in conformal time is

$$\mathrm{d}s^2 = a^2(\eta)\left[\mathrm{d}\eta^2 - \mathrm{d}\chi^2\right], \tag{4.8}$$

and since photons follow null geodesics, then their path is

$$\mathrm{d}s = 0 \implies \Delta\chi(\eta) = \pm\Delta\eta. \tag{4.9}$$

Conformal time allows us to describe light cone with straight lines in $\chi - \eta$ coordinates. We can define (comoving) particle horizon as "the greatest comoving distance from which an observer at time t would receive the signals" as

$$d_h(\eta) = \int_{t_i}^{t} \frac{\mathrm{d}t}{a(t)} = \eta - \eta_i. \tag{4.10}$$

The concept of particle horizon is illustrated in Figure 4.3.

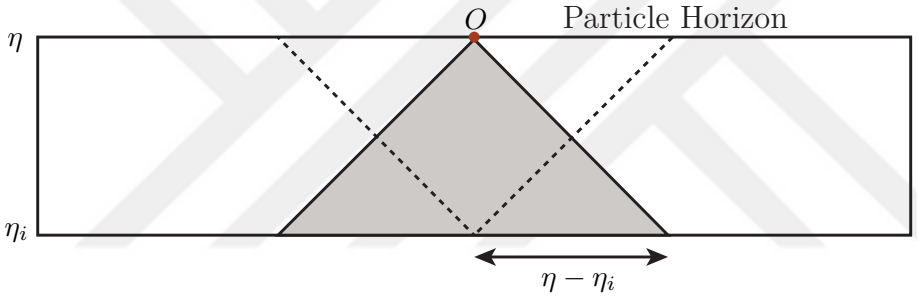

Figure 4.3 : Schematic illustration of particle horizon. The figure is adapted from [4].

4.1.2.2 Hubble radius

We can rewrite the conformal interval given by Eq. (4.10) in terms of Hubble radius as

$$d_h(\eta) = \int_{t_i}^{t} \frac{\mathrm{d}t}{a(t)} = \int_{a_i}^{a} \frac{\mathrm{d}t}{\mathrm{d}a}\frac{\mathrm{d}a}{a} = \int_{a_i}^{a} \frac{\mathrm{d}a}{a\dot{a}} = \int_{\ln_{a_i}}^{\ln_a} \frac{1}{aH}\mathrm{d}\ln a \tag{4.11}$$

By the help of this expression, causal structure and comoving Hubble radius can be related. More explicitly, for a perfect fluid with constant EoS

$$(aH)^{-1} = \frac{1}{H_0} a^{\frac{1}{2}(1+3\omega)}. \tag{4.12}$$

During matter and radiation dominated epochs, Hubble radius expands as the universe expands. If we evaluate the integral using Eq. (4.12) in Eq. (4.11),

$$d_h(a) = \eta - \eta_i = \frac{2}{H_0(1+3\omega)}\left\{a^{\frac{1}{2}(1+3\omega)} - a_i^{\frac{1}{2}(1+3\omega)}\right\} \tag{4.13}$$

and using the fact that the largest contribution come from late times

$$\eta_i = \frac{2}{H_0(1+3\omega)} a_i^{\frac{1}{2}(1+3\omega)} \xrightarrow{\omega>-\frac{1}{3},\, a_i\to 0} 0, \tag{4.14}$$

then finite comoving horizon is obtained as

$$d_h(t) = \frac{2}{H_0(1+3\omega)} a(t)^{\frac{1}{2}(1+3\omega)} = \frac{2}{1+3\omega}(aH)^{-1}. \tag{4.15}$$

Thus, for a universe dominated by fluid with $(1+3\omega) > 0$ leads to a growing Hubble sphere. Now let us examine a shrinking Hubble sphere as a resolution to horizon problem:

$$\frac{\mathrm{d}}{\mathrm{d}t}(aH)^{-1} < 0. \tag{4.16}$$

Then η_i can be written as

$$\eta_i = \frac{2}{H_0(1+3\omega)} a_i^{\frac{1}{2}(1+3\omega)} \xrightarrow{\omega<-\frac{1}{3},\, a_i\to 0} -\infty. \tag{4.17}$$

It can be inferred that all the spots that we observe in the CMB, in fact originated from a causally connected region. The resolution illustrated in Figure 4.4. However, such resolution comes with a price: shrinking sphere requires a fluid with $\omega < -\frac{1}{3}$. With this regard, late time acceleration and inflation corresponds to similar phenomena.

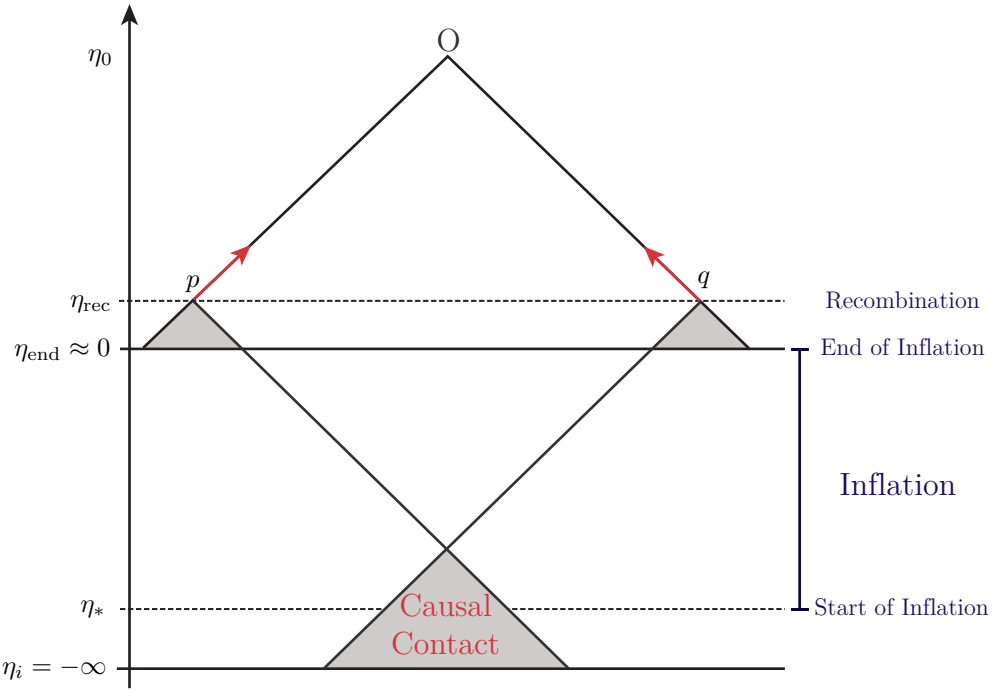

Figure 4.4 : Inflationary solution to horizon problem: All spots in the CMB have originated from a causally connected region. The figure is adapted from [4].

An illuminating way to understand resolution of the horizon problem is illustrate dynamical behaviour of comoving Hubble radius and physical evolution of the observable universe. These two schematics are shown in Figures 4.5 and 4.6.

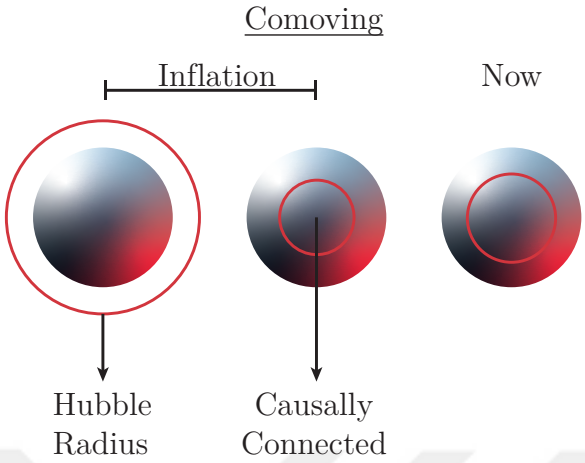

Figure 4.5 : Illustration of the inflationary solution to horizon problem via shrinking comoving Hubble sphere. The figure is adapted from [5].

Physical evolution of the observable universe during the inflationary period:

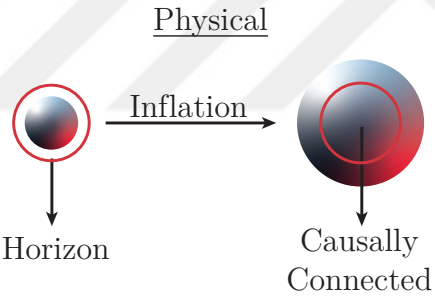

Figure 4.6 : Illustration of the inflationary solution to horizon problem via considering physical evolution of the observable universe. The figure is adapted from [5].

4.2 Inflationary Dynamics

In the single field inflationary scenario, a homogeneous scalar field called inflaton that is minimally coupled gravity is responsible for the accelerated expansion of the universe. The Lagrangian density of the field is given by

$$\mathscr{L}_\phi = \frac{1}{2} g^{\mu\nu} \left(\partial_\mu \phi\right) \left(\partial_\nu \phi\right) - V(\phi) \tag{4.18}$$

and with the gravity part, total action is

$$\begin{aligned} S &= \int \mathrm{d}^4x\sqrt{-g}\left\{\mathscr{L}_{(g)}+\mathscr{L}_{(\phi)}\right\} \\ &= \int \mathrm{d}^4x\sqrt{-g}\left\{\frac{R}{2\kappa^2}+\frac{1}{2}g^{\mu\nu}\left(\partial_\mu\phi\right)\left(\partial_\nu\phi\right)-V(\phi)\right\} \end{aligned} \tag{4.19}$$

where $\kappa^2 = 8\pi G = \frac{8\pi}{m_{\mathrm{pl}}^2} = \frac{1}{M_{\mathrm{pl}}^2}$. While the variation of the action (4.19) with respect to the inverse metric yields the field equations, variation with respect to the field yields equation of motion for the scalar field. The detailed derivations of the system of equations are given in Appendices A and B. Einstein field equations for the action (4.19) can be found as

$$R_{\mu\nu}-\frac{1}{2}Rg_{\mu\nu} = \kappa^2\left\{-g_{\mu\nu}\left[\frac{1}{2}(\partial\phi)^2+V(\phi)\right]+\left(\partial_\mu\phi\right)\left(\partial_\nu\phi\right)\right\}. \tag{4.20}$$

In the flat FRW background, field equations become

$$\begin{aligned} H^2 &= \frac{\kappa^2}{3}\left[\frac{1}{2}\dot{\phi}^2+V(\phi)\right] \\ 2\dot{H}+3H^2 &= -\kappa^2\left[\frac{1}{2}\dot{\phi}^2-V(\phi)\right]. \end{aligned} \tag{4.21}$$

Using the above set, acceleration equation can be expressed as

$$\dot{H} = -\kappa^2\frac{\dot{\phi}^2}{2}. \tag{4.22}$$

Equation of motion for inflaton field for the action (4.19) can be found as

$$\Box\phi-\frac{\partial V}{\partial\phi} = 0 \tag{4.23}$$

Again, in flat FRW background, Eq. (4.23) becomes

$$\ddot{\phi}+3H\dot{\phi}+\frac{\mathrm{d}V(\phi)}{\mathrm{d}\phi} = 0. \tag{4.24}$$

The above equation of motion describes how the inflaton field evolves in time. In Eq. (4.24), while the derivative of the potential behaves like a force, the expansion of the universe acts like damping term/friction.

Another important quantities are energy density ρ and pressure p which can be extracted from energy-momentum tensor $T_{\mu\nu}$,

$$T_{\mu\nu} = \left(\partial_\mu\phi\right)\left(\partial_\nu\phi\right)-g_{\mu\nu}\left[\frac{1}{2}g^{\alpha\beta}\left(\partial_\alpha\phi\right)\left(\partial_\beta\phi\right)-V(\phi)\right] \tag{4.25}$$

Then, energy density and pressure of the field can be written as

$$\begin{aligned} \rho_\phi &= \frac{1}{2}\dot{\phi}^2 + V(\phi) \\ p_\phi &= \frac{1}{2}\dot{\phi}^2 - V(\phi) \end{aligned} \tag{4.26}$$

EoS parameter reads

$$\omega_\phi = \frac{p}{\rho} = \frac{\dot{\phi}^2 - 2V(\phi)}{\dot{\phi}^2 + 2V(\phi)} \tag{4.27}$$

Most of the inflationary models relies on so-called slow–roll(SR) mechanism [34, 35], in which the field and the Hubble rate vary slowly. Schematic representation of SR mechanism for small and large-field models is shown in Figure 4.7. Quantitatively, the conditions can be written as

$$\dot{\phi}^2 \ll V(\phi), \quad \ddot{\phi} \ll H\dot{\phi} \tag{4.28}$$

Note that under SR conditions, Eq. (4.27) becomes

$$\omega_\phi = \frac{\dot{\phi}^2 - 2V(\phi)}{\dot{\phi}^2 + 2V(\phi)} \xrightarrow{V(\phi) \gg \dot{\phi}^2} \omega_\phi \simeq -1 \tag{4.29}$$

As we have shown in Section 2, a fluid with $\omega < -1/3$ leads to accelerated expansion of the universe. Although, inflaton field and cosmological constant lead universe to exhibits similar behaviours, an important difference between them is that ω_ϕ is not constant through the evolution of the field. It is a time-dependent quantity and its evolution is determined by the field itself through Eq. (4.24). Inflationary period during the slow–roll of the inflaton field does not last forever. After inflationary period, the field behaves like a damped oscillator near the potential minima [36].

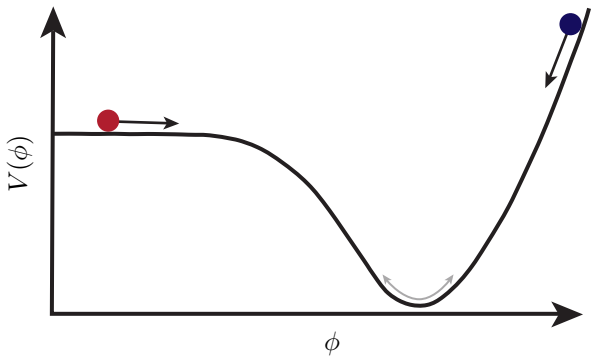

Figure 4.7 : Schematic representation of slowly rolling field through potential $V(\phi)$. While red circle represents small-field models, blue circle corresponds to large-field models. The inflationary epoch ends when the field reaches to potential minima.

Under SR conditions (4.28), Friedmann equation and equation of motion reduce to

$$\begin{aligned} H^2 &\simeq \frac{\kappa^2}{3} V(\phi) \\ 3H\dot{\phi} + V' &\simeq 0. \end{aligned} \tag{4.30}$$

Since the typical solution of the scale factor has the form $a(t) \propto e^{Ht}$, e-folding number is useful quantity for the discussion of inflationary dynamics. Number of e-folding is defined as

$$N \equiv \ln \frac{a_f}{a_i} = \int_{t_*}^{t_e} H \mathrm{d}t. \tag{4.31}$$

Here, t_* and t_e corresponds to cosmic time at the beginning and end of inflation, respectively.

The dynamics of SR inflation can be described by slow–roll parameters. We will define the parameters through evolution of comoving Hubble radius as following.

$$\frac{\mathrm{d}}{\mathrm{d}t} (aH)^{-1} = -\frac{\dot{a}H + a\dot{H}}{(aH)^2} = -\frac{1}{a}\left(1 + \frac{\dot{H}}{H^2}\right) \tag{4.32}$$

Therefore, shrinking Hubble sphere corresponds to

$$\frac{\mathrm{d}}{\mathrm{d}t} (aH)^{-1} < 0 \implies -\frac{\dot{H}}{H^2} < 1. \tag{4.33}$$

First Hubble slow-roll parameter ε_H defined as

$$\varepsilon_H \equiv -\frac{\dot{H}}{H^2} \tag{4.34}$$

as long as $\varepsilon_H < 1$, the universe continues to accelerate. Second Hubble slow-roll parameters η_H is defined through the duration of inflation, $\varepsilon_H < 1$ should be satisfied for sufficient time, i.e, 50-60 e-folds.

$$\eta_H \equiv \frac{\mathrm{d} \ln \varepsilon_H}{\mathrm{d}N} = \frac{\dot{\varepsilon}}{\varepsilon H} \tag{4.35}$$

Notice that as long as $|\eta_H| < 1$, fractional change per e-fold for ε_H remains small. SR parameters can be expressed in terms of potential as

$$\varepsilon_V \equiv \frac{1}{2\kappa^2}\left(\frac{V'}{V}\right)^2 \qquad \eta_V \equiv \frac{1}{\kappa^2}\left(\frac{V''}{V}\right). \tag{4.36}$$

Hubble and potential SR parameters are equivalent to each other. However, potential dependent compact form of enables one to calculate inflationary parameters directly using potential.

Direct test of inflation is not possible since the inflationary energy scale is far beyond the current accelerators. However, imprints of the initial density fluctuations enable one to test the model. In the era of precision cosmology, temperature anisotropies on CMB are measured with a high-accuracy by Planck satellite. Statistical properties of CMB can be expressed through primordial power spectrum which is commonly parametrized as a power-law spectrum with two free parameters [37–39]

$$P_R(k) = A_s \left(\frac{k}{k_{\text{pivot}}} \right)^{n_s - 1} \tag{4.37}$$

where n_s is the scalar spectral index and $n_s = 1$ corresponds to scale-invariant spectrum, i.e., P_R is independent from characteristic scale k. The amplitude of the spectrum $A_s \simeq 10^{-9}$ determines variance of the fluctuations. Signatures on CMB enables us to compare models with observables such as spectral index n_s and tensor-to-scalar ratio r. Spectral index and tensor-to-scalar ratio are defined through

$$\begin{aligned} n_s - 1 \equiv \left. \frac{\mathrm{d} \ln P_R}{\mathrm{d}k} \right|_{k=aH} &= -6\varepsilon_V(\phi_*) + 2\eta_V(\phi_*) \\ r \equiv \left. \frac{P_T}{P_R} \right|_{k=aH} &= 16\varepsilon_V(\phi_*) \end{aligned} \tag{4.38}$$

where ϕ_* is the value of inflaton at horizon crossing. The latest PLANCK constraints on $n_s - r$ are [7]

$$\begin{aligned} r &< 0.11 && \text{(95\% CL, Planck TT,TE,EE + lensing)} \\ n_s &= 0.9659 \pm 0.0041 && \text{(95\% CL, Planck TT,TE,EE + lensing)} \end{aligned} \tag{4.39}$$

4.3 Worked Example: Monomial Potentials

In this section, we shall employ inflaton with a potential of the form $V(\phi) \propto \phi^n$ to demonstrate slow–roll analysis and obtain inflationary observables. Slow–roll equations and parameters have already been obtained in Section 4.2. Keeping the general form, potential and its derivatives are

$$V(\phi) \propto \phi^n \implies V'(\phi) = n\phi^{n-1}, \quad V''(\phi) = n(n-1)\phi^{n-2} \tag{4.40}$$

Therefore, potential SR parameters can be written as

$$\begin{aligned} \varepsilon_V &= \frac{1}{2\kappa^2} \left(\frac{V'}{V} \right)^2 = \frac{1}{2\kappa^2} \left(\frac{n\phi^{n-1}}{\phi^n} \right)^2 = \frac{1}{2\kappa^2} \frac{n^2}{\phi^2}, \\ \eta_V &= \frac{1}{\kappa^2} \left(\frac{V''}{V} \right) = \frac{1}{\kappa^2} \left(\frac{n(n-1)\phi^{n-2}}{\phi^n} \right) = \frac{1}{\kappa^2} \frac{n(n-1)}{\phi^2}. \end{aligned} \tag{4.41}$$

For a minimally coupled inflaton field, e-folding number can also be expressed in terms of potential only.

$$N \equiv \ln \frac{a_e}{a_*} = \int_{t_*}^{t_e} H \mathrm{d}t = \int_{\phi_*}^{\phi_e} \frac{H}{\dot{\phi}} \mathrm{d}\phi = \int_{\phi_*}^{\phi_e} \frac{3H^2}{V'} \mathrm{d}\phi = -\kappa^2 \int_{\phi_*}^{\phi_e} \frac{V}{V'} \mathrm{d}\phi, \tag{4.42}$$

where we employed SR equations given by the set (4.30). The number of e-folding also can be written in terms of potential SR parameters as

$$\boxed{N = -\kappa \int_{\phi_*}^{\phi_e} \frac{\mathrm{d}\phi}{\sqrt{2\varepsilon_V(\phi)}}}. \tag{4.43}$$

The value of inflaton at the end of inflation can be found as

$$\varepsilon_V(\phi_e) = 1 \implies \phi_e^2 = \frac{n^2}{2\kappa^2}. \tag{4.44}$$

In order to determine the initial value of inflaton, we shall integrate Eq. (4.43) for required number of e-folding.

$$N = -\kappa^2 \int_{\phi_*}^{\phi_e} \frac{\phi}{n} \mathrm{d}\phi = -\frac{\kappa^2}{2n} \left(\phi_e^2 - \phi_*^2\right) \implies \phi_*^2(N) = \frac{n(4N+n)}{2\kappa^2} \tag{4.45}$$

Therefore, universe expands N e-foldings while the field evolves from ϕ_* to ϕ_e. The evolution of the field is in the case of $V(\phi) = \frac{1}{2}m^2\phi^2$ inflation is shown in Figure 4.8.

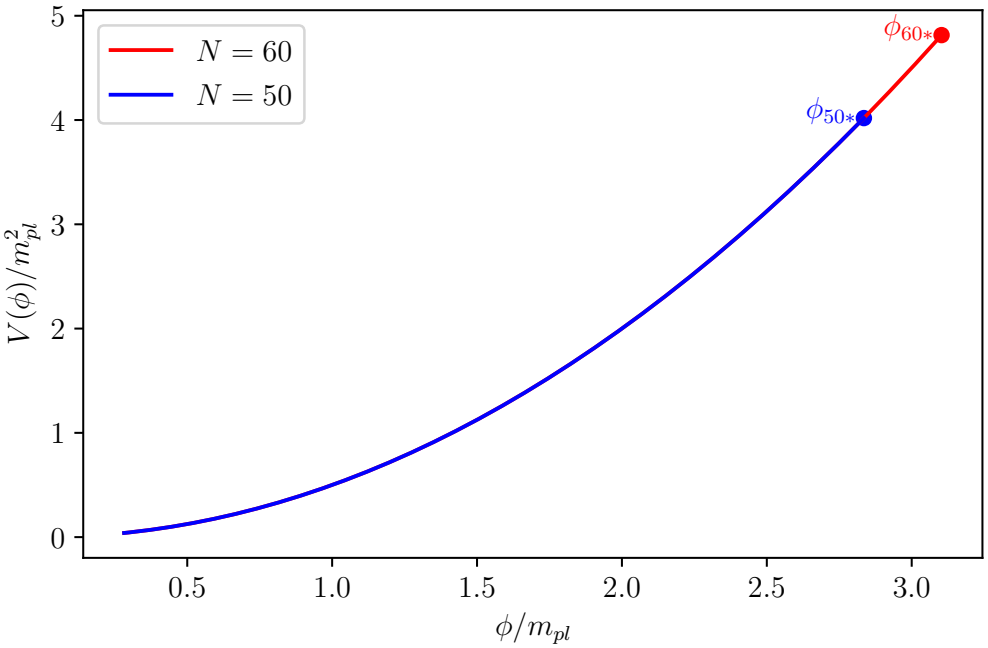

Figure 4.8 : Plot of the field and potential during the evolution of field from ϕ_* to ϕ_e.

An another way to understand the behaviour of the system is to consider equation of motion. In order to solve EoM numerically, one should reduce the equation to 2 coupled first order DE. Defining a new variable $\psi \equiv \dot{\phi}$, we obtain the following set

$$\begin{aligned} \dot{\phi} &= \psi \\ \ddot{\phi} &= \dot{\psi} = -3H\psi - V' \end{aligned} \tag{4.46}$$

From the first Friedmann equation, H can be written as

$$H = \left\{ \frac{\kappa^2}{3} \left[\frac{1}{2}\dot{\phi}^2 + V(\phi) \right] \right\}^{1/2} \tag{4.47}$$

Then the set (4.46) becomes

$$\begin{aligned} \dot{\phi} &= \psi \\ \ddot{\phi} &= \dot{\psi} = -3\psi \left\{ \frac{\kappa^2}{3} \left[\frac{1}{2}\psi^2 + V(\phi) \right] \right\}^{1/2} - V' \end{aligned} \tag{4.48}$$

To evaluate Eq. (4.48) any ODE solver can be used providing initial conditions ϕ_0 and $\dot{\phi}_0 \equiv \psi_0$. Phase space and the attractor behaviour of the field is shown in Figure 4.9.

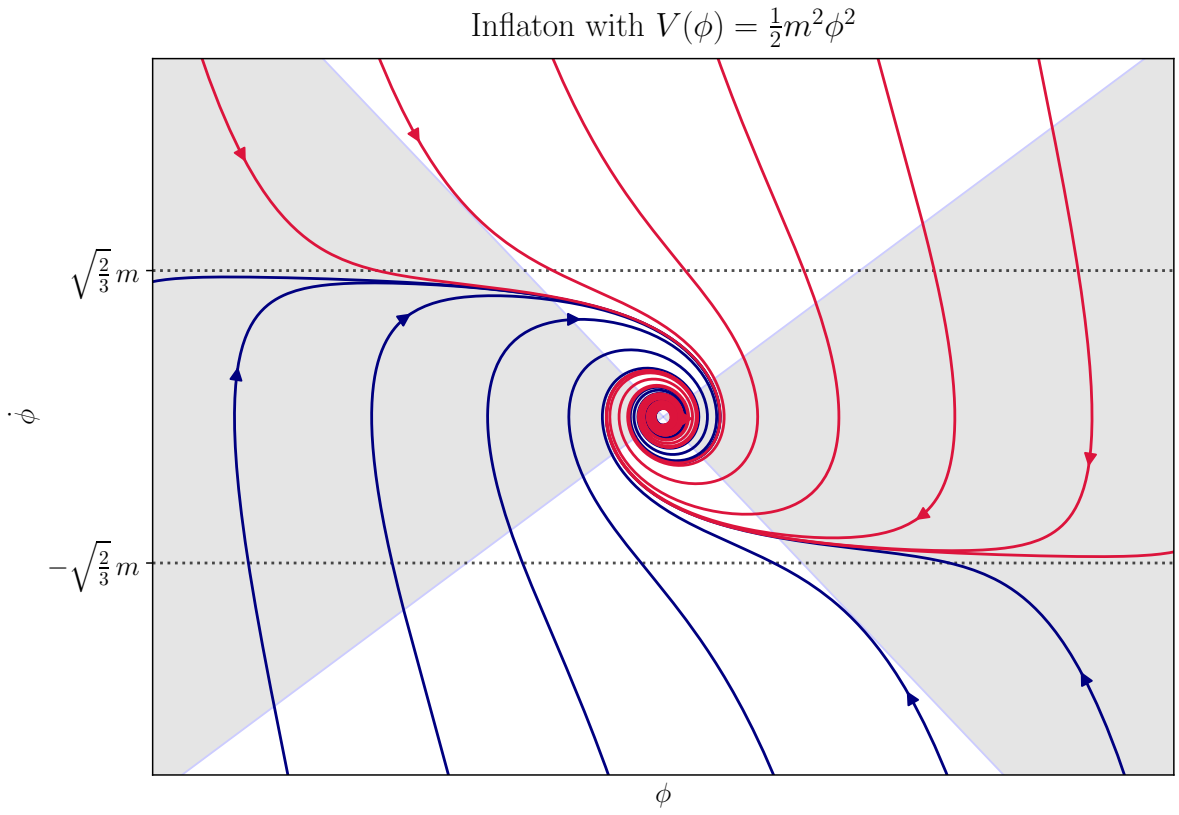

Figure 4.9 : Phase space of inflaton field with potential $V(\phi) = \frac{1}{2}m^2\phi^2$. Gray-shaded area corresponds to inflationary solutions. Analytical solution of SR approximation are shown by horizontal dashed lines.

We will finalize this section by obtaining $n_s - r$ pair for models with monomial potential. Evaluating the set (4.41) for the model $V(\phi) \propto \phi^n$ yields

$$\begin{aligned} n_s &= 1 - 6\varepsilon_V(\phi_*) + 2\eta_V(\phi_*) = 1 - \frac{2(n+2)}{4N+n} \\ r &= 16\varepsilon_V(\phi_*) = \frac{16n}{4N+n}. \end{aligned} \tag{4.49}$$

We have obtained the pair (n_s, r) as a function of number of e-folding and the exponent of the potential. Predictions of the models in the light of PLANCK data is shown in Figure 4.10.

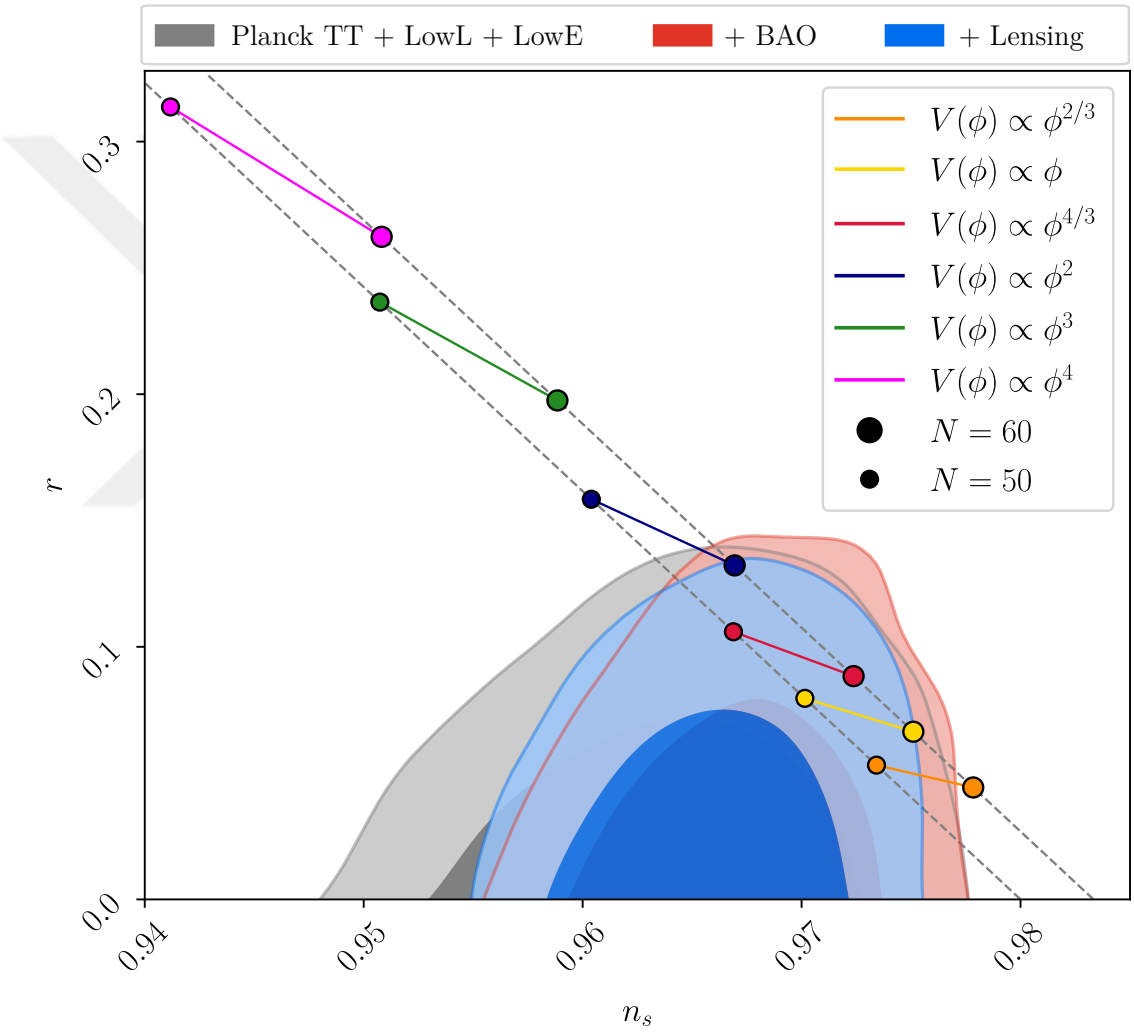

Figure 4.10 : 68% and 95% CL regions of (n_s, r) with the predictions of the models $V(\phi) \propto \phi^n$. The figure is generated using CosmoMC [6] and PLANCK 2018 Data [7].

As can be seen from the above figure, common models such as $V(\phi) \propto \phi^2$ and $V(\phi) \propto \phi^4$ are barely compatible or completely ruled-out by the recent data.

5. INFLATION IN SCALAR–TENSOR THEORIES OF GRAVITATION

Various single-field inflationary models predict anticipates scale-invariant density perturbations that is consistent with the current CMB observations. Nevertheless, QFT in curved spacetime predicts non-minimal coupling between the scalar field and the curvature. Even such a coupling is absent in the classical action, first loop corrections generate non-zero ξ [40–43]. Such coupling may alter the dynamics of the field and since non-minimal coupling is important for the success or failure of inflation, it is better to take it into account and examine its effects. In general, the coupling of the form $\xi\phi^2$ with a constant ξ is expected.

The dynamics of a non-minimally coupled scalar field is governed by the action

$$S_J = \int \mathrm{d}^4x\sqrt{-g}\left\{F(\phi)R - \frac{1}{2}g^{\mu\nu}\left(\partial_\mu\phi\right)\left(\partial_\nu\phi\right) - V(\phi)\right\}, \tag{5.1}$$

where ϕ is the scalar field that is non-minimally coupled to curvature. A convenient way to study inflation in scalar–tensor theories is to map model in Jordan Frame(JF) to Einstein Frame(EF) via conformal transformations. We shall perform the SR analysis in both EF and JF, in a similar way to the one performed in Section 4. Just like in the minimally coupled case, first, we find the value inflaton at the end of inflation, i.e. $\varepsilon(\phi_e) = 1$. The next step is to determine horizon crossing value of inflaton($\phi_\star$) for a specific coupling constant ξ. In order to do this, e-folding integration should be performed for the given ξ and e-folding. After determining the $\phi_\star$, SR parameters are evaluated to determine observational parameters n_s and r. A slightly different nuance in this situation is that, since the e-folding expression becomes complicated due to non-minimal coupling, in general, numerical methods should be employed to perform complete analysis. Finally, spectral index and tensor-to-scalar ratio for various coupling constants will be compared against PLANCK 2018 data.

5.1 Slow–Roll Inflation in Einstein Frame

Performing the following canonical transformation [42],

$$\tilde{g}_{\mu\nu} \equiv \Omega(\phi) g_{\mu\nu}, \quad \Omega(\phi) = \kappa^2 F(\phi), \tag{5.2}$$

action in EF takes the form

$$S_E = \int \mathrm{d}^4x\sqrt{-\tilde{g}}\left\{\frac{\tilde{R}}{2\kappa^2} - \frac{1}{2}\tilde{g}^{\mu\nu}\left(\partial_\mu\varphi\right)\left(\partial_\nu\varphi\right) - U(\varphi[\phi])\right\}, \tag{5.3}$$

where φ is the canonically normalized scalar field, and it is related to the original field by the relation

$$\left(\frac{\mathrm{d}\varphi}{\mathrm{d}\phi}\right)^2 = \frac{1}{\Omega} + \frac{3}{2}\kappa^2\left(\frac{\Omega'}{\Omega}\right)^2. \tag{5.4}$$

In terms of the non-minimally coupled inflaton ϕ, potential takes the form

$$U[\varphi(\phi)] = \frac{V(\phi)}{\Omega^2(\phi)}. \tag{5.5}$$

In flat FRW background, Friedmann equations and equation of motion can be written in the similar way to minimally coupled case as

$$3\tilde{H}^2 = \kappa^2\left[\frac{1}{2}\dot{\varphi}^2 + U(\varphi)\right] \tag{5.6a}$$

$$\ddot{\varphi} + 3\tilde{H}\dot{\phi} + U'(\varphi) = 0 \tag{5.6b}$$

Slow–Roll Equations in EF

Under the generic SR conditions [34]

$$\dot{\varphi}^2 \ll U(\varphi), \quad \ddot{\varphi} \ll \tilde{H}\dot{\phi},$$

slow-roll equations in EF can be obtained as

$$\begin{aligned} \tilde{H}^2 &\simeq \frac{\kappa^2}{3}U(\varphi) \\ 3\tilde{H}\dot{\phi} + U' &\simeq 0 \end{aligned} \tag{5.7}$$

which are in the same form with the ones in minimally coupled case. Analysis in EF has a great advantage by means of mathematical convenience. Besides, SR parameters are also defined in the same way as

$$\varepsilon_V = \frac{1}{2\kappa^2}\left(\frac{U'}{U}\right)^2, \eta_V = \frac{1}{\kappa^2}\left(\frac{U''}{U}\right). \tag{5.8}$$

The number of e-folding is then written as

$$N = -\kappa \int_{\varphi_*}^{\varphi_e} \frac{\mathrm{d}\varphi}{\sqrt{2\varepsilon_V(\varphi)}} = -\kappa \int_{\phi_*}^{\phi_e} \frac{\mathrm{d}\phi}{\sqrt{2\varepsilon_V(\phi)}} \left(\frac{\mathrm{d}\varphi}{\mathrm{d}\phi}\right) \tag{5.9}$$

Using the relation between EF and JF fields as given by Eq. (5.4), and using

$$\frac{\mathrm{d}U}{\mathrm{d}\varphi} = \frac{\mathrm{d}V}{\mathrm{d}\phi}\frac{\mathrm{d}\phi}{\mathrm{d}\varphi}, \tag{5.10}$$

every necessary expression can be obtained in terms of JF scalar field ϕ. Moreover, inflationary observables, n_s and r are

$$n_s = 1 - 6\varepsilon_V(\phi_*) + 2\eta_V(\phi_*)$$

$$r = 16\varepsilon_V(\phi_*).$$

We will exemplify rest of the analysis by considering the potentials $V(\phi) \propto \phi^2$ and $V(\phi) \propto \phi^4$ with the coupling $F(\phi) = \frac{1}{2}\left(\frac{1}{\kappa^2} + \xi\phi^2\right)$ to gravity.

As illustrated in the minimally coupled case, we start with determining the inflaton at the end of inflation

$$\varepsilon_V(\phi_e) = 1 \implies \phi_e = \begin{cases} \dfrac{M_p}{\sqrt{2}}\sqrt{\dfrac{-4\xi + \sqrt{48\xi^2+16\xi+1}-1}{\xi\,(4\xi+1)}} & ,n=2 \\ \dfrac{M_p}{\sqrt{2}}\sqrt{\dfrac{\sqrt{192\xi^2+32\xi+1}-1}{\xi\,(6\xi+1)}} & ,n=4 \end{cases} \tag{5.11}$$

The next step is to calculate ϕ_* using e-folding integral given by Eq. (5.9) and evaluate (n_s, r) for the ϕ_*. We consider the following ξ range that consists of 1000 points.

$$V(\phi) \propto \phi^2 \ : \ \xi \in [-1\times10^{-3}, 5\times10^{-3}] \tag{5.12}$$

$$V(\phi) \propto \phi^4 \ : \ \xi \in [-1\times10^{-1}, 2\times10^{-1}] \tag{5.13}$$

The rest of the analysis is numerically performed and the predicted spectral index and tensor-to-scalar ratio for ϕ^2 and ϕ^4 models are shown in Figures 5.1 and 5.2, respectively. While these models are ruled-out in the minimally coupled case, they can be considered within %95 CL through the coupling constant ξ.

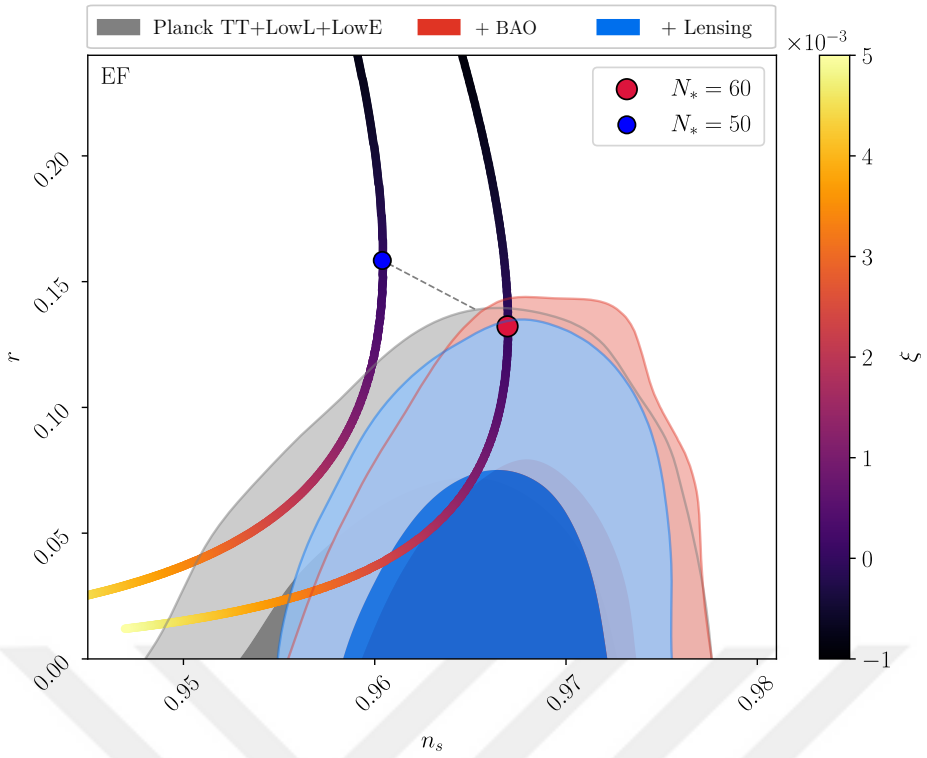

Figure 5.1 : Spectral index and tensor-to-scalar ratio for non-minimally coupled inflaton with potential $V(\phi) \propto \phi^2$ in EF. Blue and red dots corresponds to minimally coupled case for 50 and 60 e-folding.

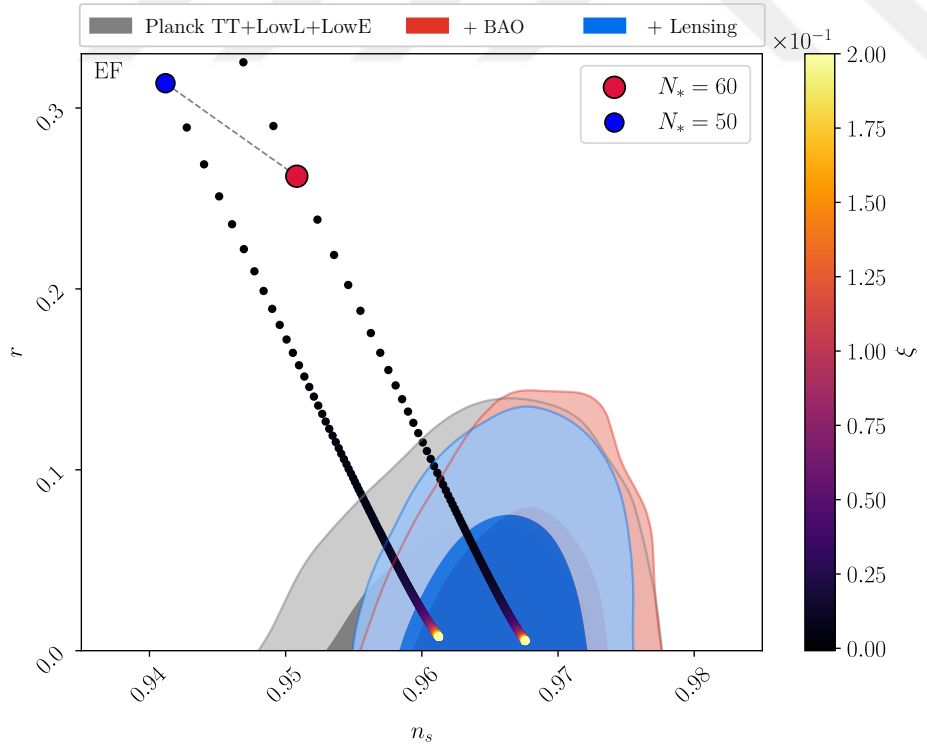

Figure 5.2 : Spectral index and tensor-to-scalar ratio for non-minimally coupled inflaton with potential $V(\phi) \propto \phi^4$ in EF. Blue and red dots corresponds to minimally coupled case for 50 and 60 e-folding.

5.2 Slow–Roll Inflation in Jordan Frame

As stated, inflationary models relies on the slow–roll mechanism, in which the existence of inflationary attractor is assumed. In the non-minimally coupled case, ξ directly affects the inflationary dynamics. In order to establish how ξ affects the dynamics, we also perform the analysis in the JF with the discussion of phase space of the inflaton field.

We start with the action

$$S_J = \int \mathrm{d}^4x\sqrt{-g}\left\{F(\phi)R - \frac{1}{2}g^{\mu\nu}\left(\partial_\mu\phi\right)\left(\partial_\nu\phi\right) - V(\phi)\right\}, \tag{5.14}$$

and the variation with respect to the inverse metric yields the field equations as

$$R_{\mu\nu} - \frac{1}{2}Rg_{\mu\nu} = \frac{1}{2F}\left\{-\frac{1}{2}g_{\mu\nu}\left(\partial\phi\right)^2 - g_{\mu\nu}V(\phi) + 2\nabla_\mu\nabla_\nu F(\phi) - 2g_{\mu\nu}\Box F(\phi) + \left(\partial_\mu\phi\right)\left(\partial_\nu\phi\right)\right\} \tag{5.15}$$

where $\Box$ is the D'Alembertian operator and explicitly, it is written as

$$\Box F(\phi) \equiv \frac{1}{\sqrt{-g}}\partial_\mu\left[\sqrt{-g}g^{\mu\nu}\partial_\nu F(\phi)\right]. \tag{5.16}$$

In flat FRW background, the equation set (5.15) becomes

$$\begin{aligned} 6H^2F &= \frac{1}{2}\dot{\phi}^2 + V(\phi) - 6H\dot{F} \\ 4\dot{H}F &= -\dot{\phi}^2 + 2H\dot{F} - 2\ddot{F} \end{aligned} \tag{5.17}$$

where overdot denotes derivative with respect to cosmic time t. Since the non-minimal coupling to gravity is a function of the scalar field, i.e. $F = F(\phi)$, sometimes it is convenient to express derivative with respect to field as given below

$$\dot{F} = \frac{\mathrm{d}\phi}{\mathrm{d}t}\frac{\partial F}{\partial\phi} = \dot{\phi}F'. \tag{5.18}$$

Variation with respect to the field yields equation of motion for the scalar field as

$$\frac{\partial F}{\partial\phi}R + \Box\phi - \frac{\partial V}{\partial\phi} = 0. \tag{5.19}$$

Again, in flat FRW background, equation of motion becomes

$$\ddot{\phi} + 3H\dot{\phi} - 6F'(\dot{H} + 2H^2) + \frac{\partial V}{\partial\phi} = 0. \tag{5.20}$$

As we have performed in Section 4.3, EoM can be reduced to two coupled first order differential equation by defining $\dot{\phi} \equiv \psi$

$$\begin{aligned} \dot{\phi} &= \psi \\ \dot{\psi} &= -3H\psi + 6\left(2H^2 + \dot{H}\right)F'(\phi) - V'(\phi) \end{aligned} \tag{5.21}$$

As can be seen from Figure 5.3, in the case of strong coupling $\xi \gg 1$, phase space structure is not conserved and inflationary attractor does not exist. Therefore, it is not valid to impose SR conditions in such cases and the phase space structure of the given model should be examined.

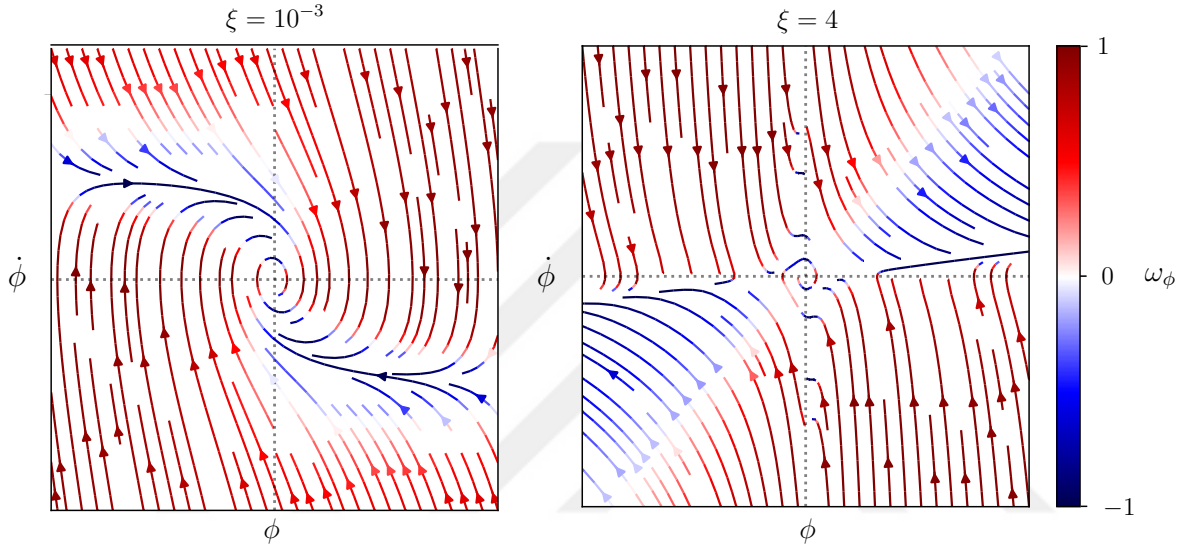

Figure 5.3 : Numerical evolution of the equation of motion of non-minimally coupled inflaton field with potential $V(\phi) \propto \phi^2$ for $\xi = 10^{-3}$ and $\xi = 4$.

Generalized and Higher Order Slow–Roll Equations in JF

The generalization of slow–roll conditions (GSR) to scalar-tensor theories with a coupling of the form $F(\phi)$ was first studied in [44] as

$$|\ddot{F}| \ll H|\dot{F}| \ll H^2|F| \tag{5.22}$$

Direct application of GSR conditions to the field equations (5.17) reads

$$H^2 \simeq \frac{V(\phi)}{6F(\phi)}\,, \tag{5.23a}$$

$$3H\dot{\phi} \simeq 2V(\phi)\frac{F'(\phi)}{F(\phi)} - V'(\phi) \tag{5.23b}$$

On the other hand, as we have illustrated as Figure 5.3, non-minimal coupling ξ can drastically change the dynamics. Thus, the SR approximation has to be applied

carefully. Direct employment of the GSR approach [44–46] may lead to deviations from the inflationary trajectory and therefore the initial conditions. As an alternative method, we will keep a higher order term ($\dot{H}$) in the equation of motion and call this to higher-order SR approximation (HSR) [47]. Under HSR conditions, field and motion equations become

$$H^2 \simeq \frac{V(\phi)}{6F(\phi)} \tag{5.24a}$$

$$3H\dot{\phi} \simeq 2V(\phi)\frac{F'(\phi)}{F(\phi)} + 3\dot{H}F' - V' \tag{5.24b}$$

where $\dot{H}$ is obtained from Eq. (5.24a) as

$$\dot{H} = \frac{\dot{\phi}}{6HF^2}(V'F - VF') = \frac{\dot{\phi}}{6H}\left(\frac{V}{F}\right)' \tag{5.25}$$

and $\dot{\phi}/H$ is

$$\frac{\dot{\phi}}{H} = \frac{F(4V'F' - V'F)}{3V(F')^2 + 2F} = \left[2 + 3\frac{(F')^2}{F}\right]^{-1} FV'\left(4\frac{F'}{F} - 1\right) . \tag{5.26}$$

The difference in the EoM between GSR and HSR approach is the existence of term $3\dot{H}F'$. Numerical solutions of the full, GSR, and HSR approximated EoMs are shown in Figure 5.4 for potential $V(\phi) \propto \phi^4$ with coupling $\xi = 1 \times 10^{-1}$.

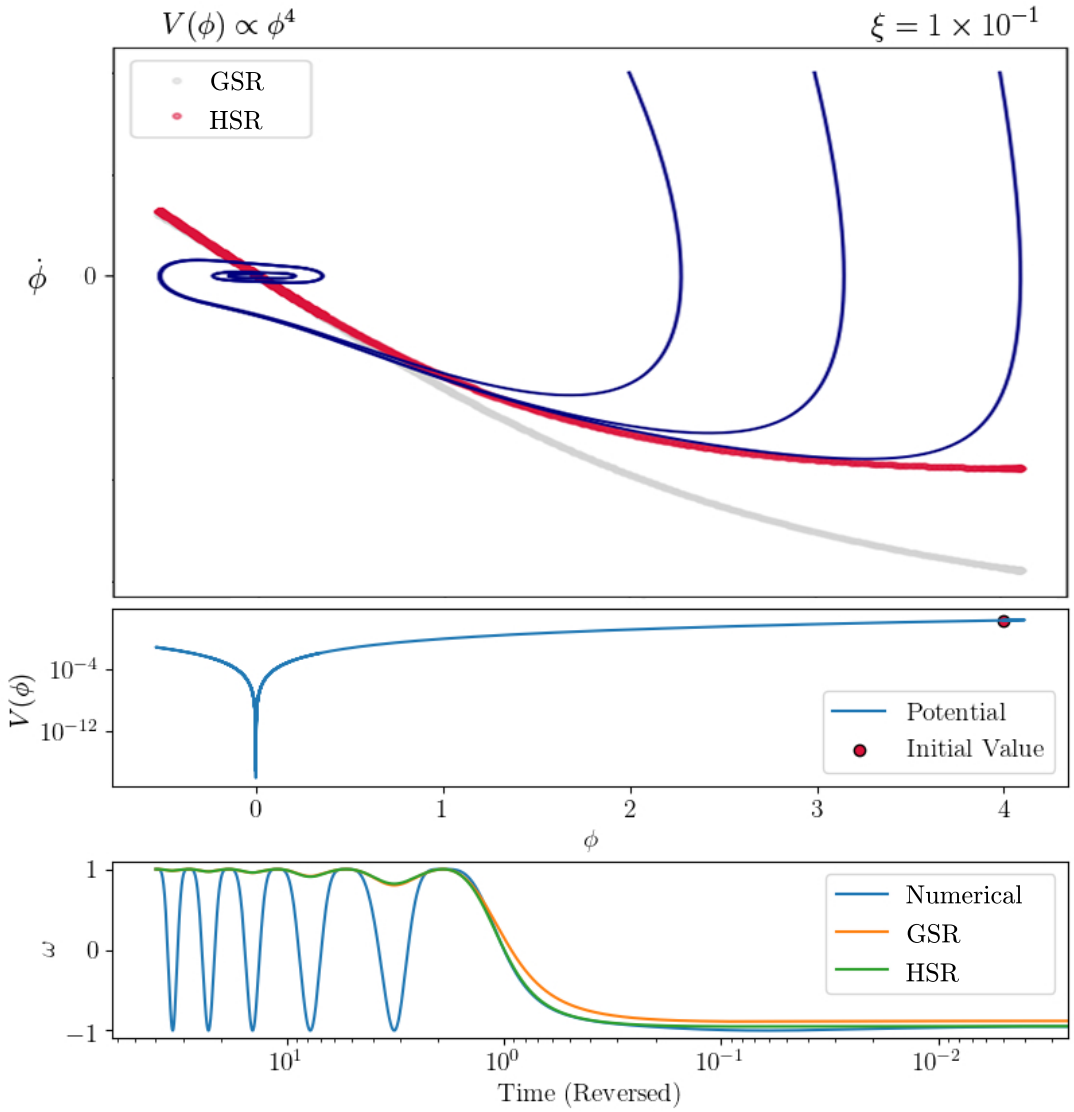

Figure 5.4 : Numerical solutions of full the and approximated equations of motions for potential $V(\phi) \propto \phi^4$ with coupling $\xi = 1 \times 10^{-1}$.

As can be seen from the above figure, GSR leads deviations from the inflationary trajectory. Due to this reason we will continue the analysis with HSR approximations.

In order to perform slow–roll analysis, first we define SR parameters as

$$\varepsilon_H \equiv -\frac{\dot{H}}{H^2}, \qquad \eta_H \equiv \frac{\dot{\varepsilon}_H}{H\varepsilon_H}; \qquad \varepsilon_F \equiv \frac{\dot{F}}{HF}, \qquad \eta_F \equiv \frac{\dot{\varepsilon}_F}{H\varepsilon_F}, \tag{5.27}$$

and the observables, spectral index and tensor-to-scalar ratio in terms of these SR parameters are defined as [46]

$$\begin{aligned} n_s &= 1 - 2\varepsilon_H - \varepsilon_F - \frac{2\varepsilon_H \eta_H + \varepsilon_F \eta_F}{2\varepsilon_H + \varepsilon_F} \\ r &= 8\,(2\varepsilon_H + \varepsilon_F). \end{aligned} \tag{5.28}$$

Using HSR equations (5.24), the parameters can be written as

$$\begin{aligned} \varepsilon_H &= \left[2+3\frac{(F')^2}{F}\right]^{-1} F\left(\frac{F'}{F}-\frac{V'}{V}\right)\left(2\frac{F'}{F}-\frac{V'}{V}\right) \quad , \quad \eta_H = \frac{\dot\phi}{H}\frac{\varepsilon_H'}{\varepsilon_H} \\ \varepsilon_F &= \left[2+3\frac{(F')^2}{F}\right]^{-1} 2F'\left(2\frac{F'}{F}-\frac{V'}{V}\right) \quad , \quad \eta_F = \frac{\dot\phi}{H}\frac{\varepsilon_F'}{\varepsilon_F} \end{aligned} \tag{5.29}$$

where we denote η_H and η_F in terms of the first SR parameters. Further, $\dot\phi/H$ is given by Eq. (5.26), and the final required expression for the analysis, number of e-folding, can be obtained as

$$N = \int H\mathrm{d}t = \int_{\phi_*}^{\phi_e} \frac{H}{\dot\phi}\,\mathrm{d}\phi = \int_{\phi_*}^{\phi_e} \frac{3VF'^2+2F}{F(4V'F'-V'F)}\,\mathrm{d}\phi\ . \tag{5.30}$$

The rest of the analysis mostly relies on numerical methods. After obtaining the value of inflaton at the end of inflation for each ξ, we numerically evaluate e-folding integral (5.30) to determine corresponding ϕ_*. Inflationary observables given by Eq. (5.28) are evaluated, and then plotted as shown in Figures 5.5 and 5.6. We consider the same coupling range as considered in EF:

$$V(\phi)\propto\phi^2\ :\ \xi\in[-1\times10^{-3},5\times10^{-3}] \tag{5.31}$$

$$V(\phi)\propto\phi^4\ :\ \xi\in[-1\times10^{-1},2\times10^{-1}] \tag{5.32}$$

The same results are obtained in EF and JF: In the case of non-minimal coupling to curvature, it is still possible consider excluded models within the 95% CL limits. Thus, in general, it is worth to consider various models with all generality before completely rule out them from the range of theoretical possibilities.

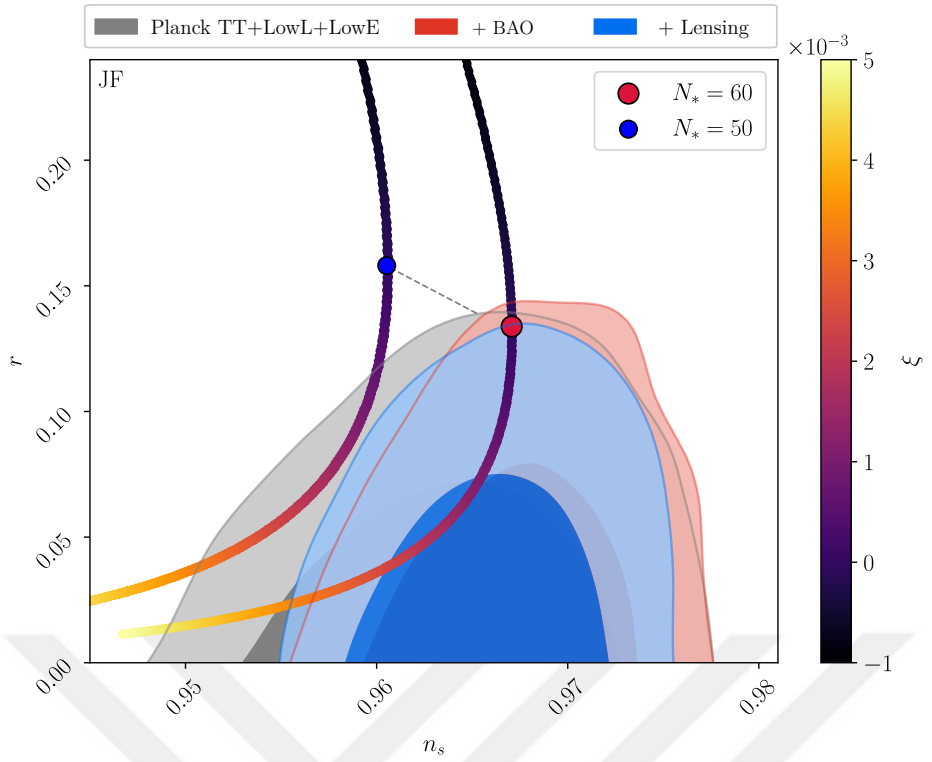

Figure 5.5 : Spectral index and tensor-to-scalar ratio for non-minimally coupled inflaton with potential $V(\phi) \propto \phi^2$ in JF. Blue and red dots corresponds to minimally coupled case for 50 and 60 e-folding.

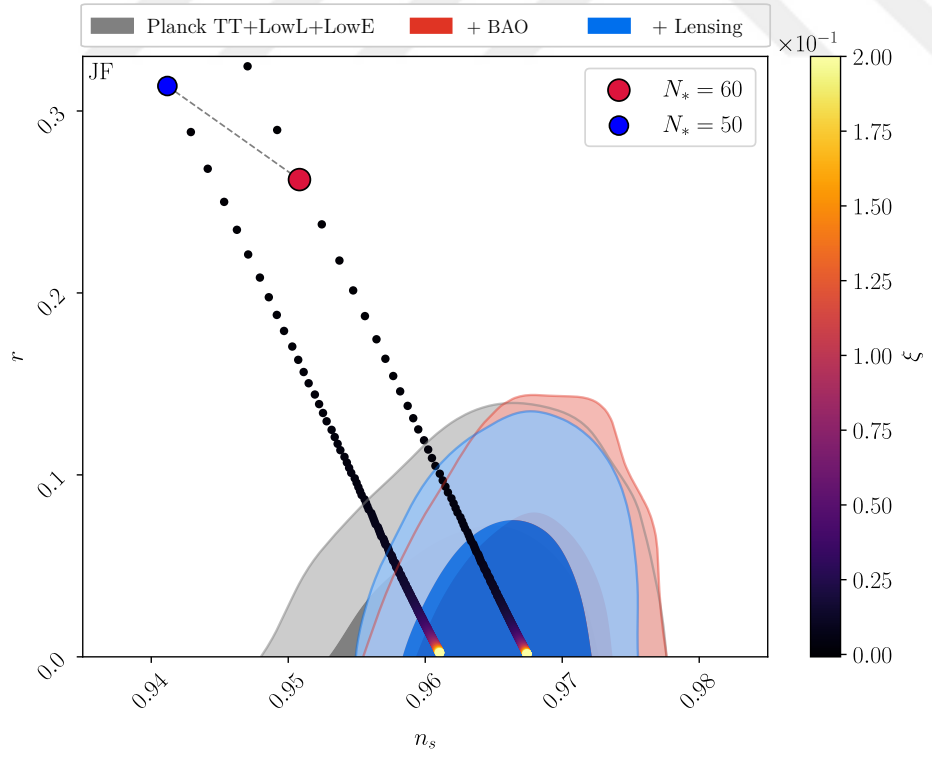

Figure 5.6 : Spectral index and tensor-to-scalar ratio for non-minimally coupled inflaton with potential $V(\phi) \propto \phi^4$ in JF. Blue and red dots corresponds to minimally coupled case for 50 and 60 e-folding.

6. CONCLUSION

Λ-CDM as the standard model of cosmology is the simplest model broadly consistent with the latest observations. However, its success relies not only on the "dark sector" but also on the inflationary paradigm. Homogeneity of the universe on large scales and generations of initial density perturbations can be explained with inflation. Similar to late-time acceleration, the universe undergoes exponential expansion during the early stages via inflationary mechanism. A homogeneous scalar field is responsible for the acceleration. Many inflationary models relies on slow–roll mechanism in which the inflaton field slowly rolls through its potential minima so that acceleration condition $\omega < -1/3$ is satisfied. Since inflation occurs in high energy scales beyond the current accelerator, its direct test is not possible. Instead, inflationary models are tested against observations come from imprints of the primordial density perturbations. We are in the era of "precision cosmology", and the information from early universe can be accurately extracted from the observations such as CMB anisotropies as probed by PLANCK satellite. An important pair of parameters that comes from the observations are spectral index n_s and tensor-to-scalar ratio r.

$$r < 0.11 \qquad \text{(95\% CL, Planck TT,TE,EE + lensing)}$$

$$n_s = 0.9659 \pm 0.0041 \qquad \text{(95\% CL, Planck TT,TE,EE + lensing)}$$

Minimally coupled models are accurately constrained by the high-precision observations. On the other hand, it is worth to consider various models with all generality before completely rule out them from the range of theoretical possibilities. For instance, QFT in curved spacetime anticipates a non-minimal coupling ξ between the scalar field and curvature scalar. This coupling may alter the inflationary dynamics drastically. As we shown in Chapter 5, although models with potential $V(\phi) \propto \phi^n$ are ruled in minimally coupled case, a small ξ can put these models into the acceptable range again. Therefore it is comprehensible to consider the models with all generality. As shown in Section 4.2, inflationary models relies on the slow–roll mechanism, where we a priori assume the existence of inflationary attractor and apply GSR conditions to

perform the analysis. Since ξ has an important effect on the inflationary dynamics, we also examine the phase space structure in JF without any transformation through the EoM of inflaton. As shown in Figure 5.3, strong coupling $\xi \gg \mathcal{O}(1)$ to gravity inhibits formation of inflationary attractors in the phase plane. Independent from this context, data-compatible ϕ^2 and ϕ^4 models favor $\xi \ll \mathcal{O}(1)$. Coupling at this order also enables inflationary attractor to form. To go deeper, we utilize the HSR conditions and show how the GSR conditions results in deviations from the inflationary trajectory. This difference shows itself in the $n_s - r$ predictions for $\xi \ll \mathcal{O}(1)$ at the order of 10^{-4} which is in fact in the precision range of the data. Moreover, a large portion of the analysis is based on the numerical methods, and thus the are also contributions to this difference come from the numerical precision and computation capacity.

REFERENCES

[1] **Hubble, E.** (1929). A relation between distance and radial velocity among extra-galactic nebulae, *Proceedings of the National Academy of Sciences*, *15*(3), 168–173.

[2] **Dodelson, S. and Schmidt, F.** (2020). *Modern Cosmology*, Academic Press, 2nd edition.

[3] **Liddle, A.R. and Lyth, D.H.** (2000). *Cosmological inflation and large-scale structure*, Cambridge University Press.

[4] **Baumann, D.** (2017). *Lecture Notes on Cosmology*.

[5] **Vázquez, J.A.**, **Padilla, L.E. and Matos, T.** (2018). Inflationary Cosmology: From Theory to Observations, `arXiv:astro-ph/1810.09934`.

[6] **Lewis, A.** (2019). GetDist: a Python package for analysing Monte Carlo samples, `arXiv:1910.13970`.

[7] **Aghanim, N.** *et al.* (2020). Planck 2018 results. VI. Cosmological parameters, *Astron. Astrophys.*, *641*, A6, `arXiv:1807.06209`.

[8] **Barbara, R.** (2017). *Introduction to Cosmology*, Cambridge University Press, 2nd edition.

[9] **M, R.** (2003). *Introduction to Cosmology*, Wiley Scientific, 3rd edition.

[10] **Lemaître, G.** (1927). Un Univers homogène de masse constante et de rayon croissant rendant compte de la vitesse radiale des nébuleuses extra-galactiques, *Annales de la Société Scientifique de Bruxelles*, *47*, 49–59.

[11] **Zwicky, F.** (1933). Die Rotverschiebung von extragalaktischen Nebeln, *Helvetica Physica Acta*, *6*, 110–127.

[12] **Alpher, R.A.**, **Bethe, H. and Gamow, G.** (1948). The Origin of Chemical Elements, *Physical Review*, *73*(7), 803–804.

[13] **Penzias, A.A. and Wilson, R.W.** (1965). A Measurement of Excess Antenna Temperature at 4080 Mc/s., *Astrophysical Journal*, *142*, 419–421.

[14] **Guth, A.H.** (1981). Inflationary universe: A possible solution to the horizon and flatness problems, *Physical Review D*, *23*(2), 347–356.

[15] **Linde, A.D.** (1982). Coleman-Weinberg theory and the new inflationary universe scenario, *Physics Letters B*, *114*(6), 431–435.

[16] **Linde, A.D.** (1983). Chaotic Inflation, *Phys. Lett. B*, *129*, 177–181.

[17] **Martin, J.** (2005). Inflationary Cosmological Perturbations of Quantum-Mechanical Origin, *Planck Scale Effects in Astrophysics and Cosmology*, 199–244, 0406011.

[18] **Riess, A.G.** *et al.* (1998). Observational evidence from supernovae for an accelerating universe and a cosmological constant, *Astron. J.*, *116*, 1009–1038, arXiv:astro-ph/9805201.

[19] **Perlmutter, S.** *et al.* (1999). Measurements of Ω and *Lambda* from 42 High-Redshift Supernovae, *The Astrophysical Journal*, *517*(2), 565–586.

[20] **Carroll, S.M.** (2004). *Spacetime and Geometry: An Introduction to General Relativity*, Addison Wesley.

[21] **Zheng, J.**, **Zhao, G.B.**, **Li, J.**, **Wang, Y.**, **Chuang, C.H.**, **Kitaura, F.S. and Rodriguez-Torres, S.** (2019). The clustering of galaxies in the completed SDSS-III Baryon Oscillation Spectroscopic Survey: a tomographic measurement of structure growth and expansion rate from anisotropic galaxy clustering in Fourier space, *Mon. Not. Roy. Astron. Soc.*, *484*(1), 442–450, arXiv:1806.01920.

[22] **Copeland, E.J.**, **Sami, M. and Tsujikawa, S.** (2006). Dynamics of dark energy, *Int. J. Mod. Phys. D*, *15*, 1753–1936, arXiv:hep-th/0603057.

[23] **Kolb, E. and Turner, M.** (1994). *The Early Universe*, Avalon Publishing.

[24] **Fixsen, D.J.** (2009). The Temperature of the Cosmic Microwave Background, *The Astrophysical Journal*, *707*(2), 916–920, arXiv:0911.1955.

[25] **Fukugita, M.**, **Hogan, C.J. and Peebles, P.J.E.** (1998). The Cosmic Baryon Budget, *The Astrophysical Journal*, *503*(2), 518–530, arXiv:astro-ph/9712020.

[26] **Shull, J.M.**, **Smith, B.D. and Danforth, C.W.** (2012). The Baryon Census in a Multiphase Intergalactic Medium: 30% of the Baryons May Still be Missing, *The Astrophysical Journal*, *759*(1), 23, arXiv:1112.2706.

[27] **Cooke, R.J.**, **Pettini, M. and Steidel, C.C.** (2018). One Percent Determination of the Primordial Deuterium Abundance, *Astrophys. J.*, *855*(2), 102, arXiv:1710.11129.

[28] **Abbott, T.M.C.** *et al.* (2019). Dark Energy Survey Year 1 Results: Constraints on Extended Cosmological Models from Galaxy Clustering and Weak Lensing, *Phys. Rev. D*, *99*(12), 123505, arXiv:astro-ph/1810.02499.

[29] **Mantz, A.B.** *et al.* (2014). Cosmology and astrophysics from relaxed galaxy clusters – II. Cosmological constraints, *Mon. Not. Roy. Astron. Soc.*, *440*(3), 2077–2098, arXiv:astro-ph/1402.6212.

[30] **Piattella, O.F.** (2018). Lecture Notes in Cosmology, arXiv:1803.00070.

[31] **Bernstein, J.** (1988). *Kinetic Theory in the Expanding Universe*, Cambridge Monographs on Mathematical Physics, Cambridge University Press, Cambridge, U.K.

[32] **Starobinsky, A.A.** (1982). Dynamics of Phase Transition in the New Inflationary Universe Scenario and Generation of Perturbations, *Phys. Lett. B*, *117*, 175–178.

[33] **Albrecht, A. and Steinhardt, P.J.** (1982). Cosmology for Grand Unified Theories with Radiatively Induced Symmetry Breaking, *Phys. Rev. Lett.*, *48*, 1220–1223.

[34] **Liddle, A.R.**, **Parsons, P. and Barrow, J.D.** (1994). Formalizing the slow roll approximation in inflation, *Phys. Rev. D*, *50*, 7222–7232, `arXiv:astro-ph/9408015`.

[35] **Liddle, A.R.** (1999). An Introduction to cosmological inflation, *ICTP Summer School in High-Energy Physics and Cosmology*, pp.260–295, `arXiv:astro-ph/9901124`.

[36] **Linde, A.** (2005). Particle physics and inflationary cosmology, `arXiv:hep-th/0503203`.

[37] **Hu, W. and Dodelson, S.** (2002). Cosmic Microwave Background Anisotropies, *Annual Review of Astronomy and Astrophysics*, *40*(1), 171–216.

[38] **Bridle, S.L.**, **Lewis, A.M.**, **Weller, J. and Efstathiou, G.** (2003). Reconstructing the primordial power spectrum, *Mon. Not. Roy. Astron. Soc.*, *342*, L72, `arXiv:astro-ph/0302306`.

[39] **Byrnes, C.T. and Cole, P.S.** (2021). Lecture notes on inflation and primordial black holes, `arXiv:astro-ph/2112.05716`.

[40] **Futamase, T. and Maeda, K.i.** (1989). Chaotic inflationary scenario of the Universe with a nonminimally coupled "inflaton" field, *Phys. Rev. D*, *39*, 399–404.

[41] **Faraoni, V.** (1996). Nonminimal coupling of the scalar field and inflation, *Phys. Rev. D*, *53*, 6813–6821, `arXiv:astro-ph/9602111`.

[42] **Faraoni, V.** (2004). *Cosmology in Scalar–Tensor Gravity*, Springer.

[43] **Inagaki, T.**, **Nakanishi, R. and Odintsov, S.D.** (2014). Inflationary parameters in renormalization group improved ϕ^4 theory, *Astrophys. Space Sci.*, *354*(2), 2108, `arXiv:gr-qc/1408.1270`.

[44] **Torres, D.F.** (1997). Slow roll inflation in nonminimally coupled theories: Hyperextended gravity approach, *Phys. Lett. A*, *225*, 13–17, `arXiv:gr-qc/9610021`.

[45] **Morris, J.R.** (2001). Generalized slow roll conditions and the possibility of intermediate scale inflation in scalar tensor theory, *Class. Quant. Grav.*, *18*, 2977–2988, `arXiv:gr-qc/0106022`.

[46] **Granda, L.N. and Jimenez, D.F.** (2019). Slow-Roll Inflation with Exponential Potential in Scalar-Tensor Models, *Eur. Phys. J. C*, *79*(9), 772, arXiv:hep-th/1907.06806.

[47] **Akın, K.**, **Arapoğlu, A.S. and Yükselci, A.E.** (2020). Formalizing slow-roll inflation in scalar–tensor theories of gravitation, *Physics of the Dark Universe*, *30*, arXiv:2007.10850.

APPENDICES

APPENDIX A: Variation of Einstein–Hilbert Action
APPENDIX B: Variation of Scalar–Tensor Theories of Gravitation

APPENDIX A

Variation of Einstein–Hilbert Action

Einstein–Hilbert action including the cosmological constant is given by

$$S = \int \mathrm{d}^4x\sqrt{-g}\left[\frac{1}{2\kappa^2}(R-2\Lambda)+\mathscr{L}_M\right] \tag{A.1}$$

where $\kappa^2 = \dfrac{8\pi G}{c^4}$.

Variation with respect to the inverse of the metric

$$\begin{aligned}\delta S &= \int \mathrm{d}^4x\left\{\frac{1}{2\kappa^2}\left[\frac{\delta(\sqrt{-g}R)}{\delta g^{\mu\nu}}-2\frac{\delta(\sqrt{-g}\Lambda)}{\delta g^{\mu\nu}}\right]+\frac{\delta(\sqrt{-g}\mathscr{L}_M)}{\delta g^{\mu\nu}}\right\}\delta g^{\mu\nu}\\ &= \int \mathrm{d}^4x\sqrt{-g}\left\{\frac{1}{2\kappa^2}\left(\frac{\delta R}{\delta g^{\mu\nu}}+\frac{R}{\sqrt{-g}}\frac{\delta\sqrt{-g}}{\delta g^{\mu\nu}}-2\frac{\Lambda}{\sqrt{-g}}\frac{\delta\sqrt{-g}}{\delta g^{\mu\nu}}\right)+\frac{1}{\sqrt{-g}}\frac{\delta(\sqrt{-g}\mathscr{L}_M)}{\delta g^{\mu\nu}}\right\}\delta g^{\mu\nu}\end{aligned}$$

In order action to vanish, integrand of the above equation must also vanish. Thus,

$$\frac{1}{\kappa^2}\frac{\delta R}{\delta g^{\mu\nu}}+\frac{1}{\kappa^2}\frac{R}{\sqrt{-g}}\frac{\delta\sqrt{-g}}{\delta g^{\mu\nu}}-\frac{2\Lambda}{\kappa^2\sqrt{-g}}\frac{\delta\sqrt{-g}}{\delta g^{\mu\nu}}=\frac{-2}{\sqrt{-g}}\frac{\delta(\sqrt{-g}\mathscr{L}_M)}{\delta g^{\mu\nu}} \tag{A.2}$$

Energy-momentum defined as the RHS of the equation

$$T_{\mu\nu}\equiv\frac{-2}{\sqrt{-g}}\frac{\delta(\sqrt{-g}\mathscr{L}_M)}{\delta g^{\mu\nu}}=-2\frac{\mathscr{L}_M}{\delta g^{\mu\nu}}+g_{\mu\nu}\mathscr{L}_M \tag{A.3}$$

Thus, Eq. (A.2) becomes

$$\frac{\delta R}{\delta g^{\mu\nu}}+\frac{R}{\sqrt{-g}}\frac{\delta\sqrt{-g}}{\delta g^{\mu\nu}}-\frac{2\Lambda}{\sqrt{-g}}\frac{\delta\sqrt{-g}}{\delta g^{\mu\nu}}=\frac{8\pi G}{c^4}T_{\mu\nu} \tag{A.4}$$

In order to proceed, we need the variations of Ricci scalar $\left(\frac{\delta R}{\delta g_{\mu\nu}}\right)$ and determinant of the metric $\left(\frac{\delta\sqrt{-g}}{\delta g_{\mu\nu}}\right)$. We will derive these necessary elements and come back to Eq. (A.4).

Variation of the metric determinant

Employing Jacobi rule,

$$\delta g\equiv\delta(\det g)=gg^{\mu\nu}\delta g_{\mu\nu} \tag{A.5}$$

where $g^{\mu\nu}\delta g_{\mu\nu}$ can be expressed as

$$\begin{aligned}g^{\mu\nu}\delta g_{\mu\nu} &= g^{\mu\nu}\delta(g_{\mu\rho}\,g_{\nu\sigma}\,g^{\rho\sigma})\\ &= g^{\mu\nu}(\delta g_{\mu\rho}\underbrace{g_{\nu\sigma}\,g^{\rho\sigma}}_{\delta^{\rho}{}_{\nu}}+\delta g_{\nu\sigma}\underbrace{g_{\mu\rho}\,g^{\rho\sigma}}_{\delta^{\sigma}{}_{\mu}}+g_{\mu\rho}g_{\nu\sigma}\,\delta g^{\rho\sigma})\end{aligned} \tag{A.6}$$

Thus,

$$\begin{aligned} g^{\mu\nu}\delta g_{\mu\nu} &= g^{\mu\nu}\delta^{\rho}{}_{\nu}\,\delta g_{\mu\rho} + g^{\mu\nu}\delta^{\sigma}{}_{\mu}\,\delta g_{\nu\sigma} + g^{\mu\nu}\,g_{\mu\rho}\,g_{\nu\sigma}\,\delta g^{\rho\sigma} \\ &= g^{\mu\rho}\,\delta g_{\mu\rho} + g^{\sigma\nu}\,\delta g_{\sigma\nu} + g^{\mu\nu}\,g_{\mu\rho}\,g_{\nu\sigma}\,\delta g^{\rho\sigma} \end{aligned} \tag{A.7}$$

and by simply relabeling dummy indices, 3rd term of Eq. (A.7) can be written as

$$\begin{aligned} g^{\mu\nu}\,g_{\mu\rho}\,g_{\nu\sigma}\,\delta g^{\rho\sigma} &= g^{\mu\nu}\delta g_{\mu\nu} - g^{\mu\nu}\delta g_{\mu\nu} - g^{\mu\nu}\delta g_{\mu\nu} \\ &= -g^{\mu\nu}\delta g_{\mu\nu} \end{aligned} \tag{A.8}$$

Therefore, Eq. (A.5) becomes

$$\begin{aligned} \delta g &= -g g^{\mu\nu}\,g_{\mu\rho}\,g_{\nu\sigma}\,\delta g^{\rho\sigma} \\ &= -g\delta^{\nu}{}_{\rho}\,g_{\nu\sigma}\,\delta g^{\rho\sigma} \\ &\boxed{\delta g = -g g_{\rho\sigma}\,\delta g^{\rho\sigma}} \end{aligned} \tag{A.9}$$

Using the above expression, $\delta\sqrt{-g}$ can be obtained as

$$\begin{aligned} \delta\sqrt{-g} &= -\frac{1}{2\sqrt{-g}}\delta g \\ &= \frac{1}{2}\frac{g}{\sqrt{-g}}g_{\mu\nu}\,\delta g^{\mu\nu} \\ &\boxed{\delta\sqrt{-g} = -\frac{1}{2}\sqrt{-g}g_{\mu\nu}\,\delta g^{\mu\nu}}. \end{aligned} \tag{A.10}$$

Variation of Ricci Scalar

We shall start with calculating variation of Riemann tensor in order to obtain variation of Ricci scalar δR.

Remember Riemann tensor is given by

$$R^{\rho}{}_{\sigma\mu\nu} = \partial_{\mu}\Gamma^{\rho}{}_{\nu\sigma} - \partial_{\nu}\Gamma^{\rho}{}_{\mu\sigma} + \Gamma^{\rho}{}_{\mu\lambda}\Gamma^{\lambda}{}_{\nu\sigma} - \Gamma^{\rho}{}_{\nu\lambda}\Gamma^{\lambda}{}_{\mu\sigma}, \tag{A.11}$$

taking the variation

$$\begin{aligned} \delta R^{\rho}{}_{\sigma\mu\nu} = \delta(\partial_{\mu}\Gamma^{\rho}{}_{\nu\sigma}) - \delta(\partial_{\nu}\Gamma^{\rho}{}_{\mu\sigma}) + \delta\Gamma^{\rho}{}_{\mu\lambda}\Gamma^{\lambda}{}_{\nu\sigma} + \Gamma^{\rho}{}_{\mu\lambda}\delta\Gamma^{\lambda}{}_{\nu\sigma} \\ - \delta\Gamma^{\rho}{}_{\nu\lambda}\Gamma^{\lambda}{}_{\mu\sigma} - \Gamma^{\rho}{}_{\nu\lambda}\delta\Gamma^{\lambda}{}_{\mu\sigma} \end{aligned} \tag{A.12}$$

We stated that metric connection itself does not transform like a tensor, however the variation of the two connection transforms tensorially. Thus, due to tensorial transformation, a covariant derivative should be associated with the variation [20].

Covariant Differentiation
Covariant (0,1) Field:

$$\nabla_\mu \phi_\nu = \partial_\mu \phi_\nu - \Gamma^\rho{}_{\mu\nu}\phi_\rho \tag{A.13}$$

Contravariant (1,0) Field:

$$\nabla_\mu \phi^\nu = \partial_\mu \phi^\nu + \Gamma^\nu{}_{\mu\rho}\phi^\rho \tag{A.14}$$

Mixed (1,1) Field:

$$\nabla_\mu \phi^\rho{}_\nu = \partial_\mu \phi^\rho{}_\nu - \Gamma^\alpha{}_{\mu\nu}\phi^\rho{}_\alpha + \Gamma^\rho{}_{\beta\mu}\phi^\beta{}_\nu \tag{A.15}$$

Employing (A.15) for the (1,2) $\delta\Gamma^\rho{}_{\mu\nu}$:

$$\nabla_\mu(\delta\Gamma^\rho{}_{\nu\sigma}) = \partial_\mu(\delta\Gamma^\rho{}_{\nu\sigma}) + \Gamma^\rho{}_{\alpha\mu}\delta\Gamma^\alpha{}_{\nu\sigma} - \Gamma^\beta{}_{\mu\nu}\delta\Gamma^\rho{}_{\beta\sigma} - \Gamma^\gamma{}_{\mu\sigma}\delta\Gamma^\rho{}_{\mu\gamma} \tag{A.16}$$

and,

$$\nabla_\nu(\delta\Gamma^\rho{}_{\mu\sigma}) = \partial_\nu(\delta\Gamma^\rho{}_{\mu\sigma}) + \Gamma^\rho{}_{\delta\nu}\delta\Gamma^\delta{}_{\mu\sigma} - \Gamma^\rho{}_{\nu\mu}\delta\Gamma^\rho{}_{\rho\sigma} - \Gamma^\phi{}_{\nu\sigma}\delta\Gamma^\rho{}_{\phi\mu} \tag{A.17}$$

Substracting Eq. (A.17) from Eq. (A.16) yields

$$\begin{aligned}\nabla_\mu(\delta\Gamma^\rho{}_{\nu\sigma}) - \nabla_\nu(\delta\Gamma^\rho{}_{\mu\sigma}) = \partial_\mu(\delta\Gamma^\rho{}_{\nu\sigma}) - \partial_\nu(\delta\Gamma^\rho{}_{\mu\sigma}) + \Gamma^\phi{}_{\nu\sigma}\delta\Gamma^\rho{}_{\phi\mu} + \Gamma^\rho{}_{\alpha\mu}\delta\Gamma^\alpha{}_{\nu\sigma} \\ -\Gamma^\gamma{}_{\mu\sigma}\delta\Gamma^\rho{}_{\mu\gamma} - \Gamma^\rho{}_{\delta\nu}\delta\Gamma^\delta{}_{\mu\sigma} - \Gamma^\beta{}_{\mu\nu}\delta\Gamma^\rho{}_{\beta\sigma} + \Gamma^\rho{}_{\nu\mu}\delta\Gamma^\rho{}_{\rho\sigma}\end{aligned} \tag{A.18}$$

Therefore,

$$\delta R^\rho{}_{\sigma\mu\nu} = \nabla_\mu(\delta\Gamma^\rho{}_{\nu\sigma}) - \nabla_\nu(\delta\Gamma^\rho{}_{\mu\sigma}) \tag{A.19}$$

using the contraction of Riemann tensor and Eq. (A.19)

$$\delta R^\mu{}_{\sigma\mu\nu} \equiv \delta R_{\sigma\nu} = \nabla_\mu(\delta\Gamma^\mu{}_{\nu\sigma}) - \nabla_\nu(\delta\Gamma^\mu{}_{\mu\sigma}) \tag{A.20}$$

The above expression is also called Palatini identity. Another contraction reads

$$\begin{aligned}\delta R^\nu{}_\nu &= \delta(g^{\sigma\nu}R_{\sigma\nu}) = \delta g^{\sigma\nu}R_{\sigma\nu} + g^{\sigma\nu}\delta R_{\sigma\nu} \\ &= \delta g^{\sigma\nu}R_{\sigma\nu} + g^{\sigma\nu}\left[\nabla_\mu(\delta\Gamma^\mu{}_{\nu\sigma}) - \nabla_\nu(\delta\Gamma^\mu{}_{\mu\sigma})\right]\end{aligned} \tag{A.21}$$

By using the product rule, covariant derivatives in above equation may be rewritten as

$$\begin{aligned}\nabla_\mu(g^{\sigma\nu}\delta\Gamma^\mu{}_{\nu\sigma}) &= \nabla_\mu(g^{\sigma\nu})\delta\Gamma^\mu{}_{\nu\sigma} + g^{\sigma\nu}\nabla_\mu(\delta\Gamma^\mu{}_{\nu\sigma}) \\ &= g^{\sigma\nu}\nabla_\mu(\delta\Gamma^\mu{}_{\nu\sigma})\end{aligned} \tag{A.22}$$

and similarly,

$$\begin{aligned}\nabla_\nu(g^{\sigma\nu}\delta\Gamma^\mu{}_{\mu\sigma}) &= \nabla_\nu(g^{\sigma\nu})\delta\Gamma^\mu{}_{\mu\sigma} + g^{\sigma\nu}\nabla_\nu(\delta\Gamma^\mu{}_{\mu\sigma}) \\ &= g^{\sigma\nu}\nabla_\nu(\delta\Gamma^\mu{}_{\mu\sigma}).\end{aligned} \tag{A.23}$$

Thus, in terms of total derivatives δR becomes

$$\begin{aligned}\delta R &= \delta g^{\sigma\nu} R_{\sigma\nu} + \nabla_\mu (g^{\sigma\nu} \delta\Gamma^\mu{}_{\nu\sigma}) - \nabla_\nu (g^{\sigma\nu} \delta\Gamma^\mu{}_{\mu\sigma}) \\ &= \delta g^{\sigma\nu} R_{\sigma\nu} + \nabla_\mu (g^{\sigma\nu} \delta\Gamma^\mu{}_{\nu\sigma} - g^{\sigma\mu} \delta\Gamma^\nu{}_{\nu\sigma})\end{aligned} \tag{A.24}$$

The second and third terms of Eq. (A.24) form a total derivative, and they do not contribute the variation by Stokes' theorem. δR is obtained as

$$\begin{aligned}\delta R &= \delta g^{\mu\nu} R_{\mu\nu} \\ \Rightarrow \frac{\delta R}{\delta g^{\mu\nu}} &= R_{\mu\nu}\end{aligned} \tag{A.25}$$

Plugging explicit expressions for the variations of Ricci scalar, Ricci tensor, and the determinant of the metric that we found in this section into Eq. (A.4) yields

$$\boxed{G_{\mu\nu} \equiv R_{\mu\nu} - \frac{1}{2} R g_{\mu\nu} + \Lambda g_{\mu\nu} = \frac{8\pi G}{c^4} T_{\mu\nu}} \tag{A.26}$$

APPENDIX B

Variation of Scalar – Tensor Theory Action

The action for a theory with non-minimally coupled scalar field to gravity is given by

$$S = \int \mathrm{d}^4x\sqrt{-g}\left\{F(\phi)R - \frac{1}{2}g^{\mu\nu}\left(\partial_\mu\phi\right)\left(\partial_\nu\phi\right) - V(\phi)\right\} \tag{B.1}$$

In order to perform variation, we shall directly use some of the results from Appendix A. The variation of the metric determinant with respect to the inverse metric is

$$\delta\sqrt{-g} = -\frac{1}{2}\sqrt{-g}\,g_{\mu\nu}\,\delta g^{\mu\nu}, \tag{B.2}$$

and the variation of Ricci Scalar with respect to the inverse metric is

$$\delta R = R_{\mu\nu}\,\delta g^{\mu\nu} - \nabla_\mu\,\nabla_\nu\,\delta g^{\mu\nu} + g_{\mu\nu}\Box\delta g^{\mu\nu} \tag{B.3}$$

where $\Box \equiv g^{\mu\nu}\nabla_\mu\nabla_\nu$. Therefore, variation of total action is

$$\begin{aligned}\delta S = &\int \mathrm{d}^4x\,\delta\sqrt{-g}\left\{F(\phi)R - \frac{1}{2}\left(\partial\phi\right)^2 - V(\phi)\right\}\\ &+\int \mathrm{d}^4x\sqrt{-g}\left\{F(\phi)\delta R - \frac{1}{2}\left(\partial\phi\right)^2\right\}\end{aligned} \tag{B.4}$$

Let us evaluate two lines of Eq. (B.4) separately.

$$\delta S_{\mathrm{I}} = -\frac{1}{2}\int \mathrm{d}^4x\sqrt{-g}g_{\mu\nu}\left\{F(\phi)R - \frac{1}{2}\left(\partial\phi\right)^2 - V(\phi)\right\}\delta g^{\mu\nu} \tag{B.5}$$

and

$$\delta S_{\mathrm{II}} = \int \mathrm{d}^4x\sqrt{-g}\left\{F(\phi)R_{\mu\nu} - \nabla_\mu\nabla_\nu F(\phi) + g_{\mu\nu}\Box F(\phi) - \frac{1}{2}\left(\partial_\mu\phi\right)\left(\partial_\nu\phi\right)\right\}\delta g^{\mu\nu} \tag{B.6}$$

Total action must vanish under such variations, i.e. $\delta S_{\mathrm{I}} + \delta S_{\mathrm{II}} = 0$. Thus,

$$\begin{aligned}&-\frac{1}{2}\sqrt{-g}g_{\mu\nu}\left\{F(\phi)R - \frac{1}{2}\left(\partial\phi\right)^2 - V(\phi)\right\}\\ &+\sqrt{-g}\left\{F(\phi)R_{\mu\nu} - \nabla_\mu\nabla_\nu F(\phi) + g_{\mu\nu}\Box F(\phi) - \frac{1}{2}\left(\partial_\mu\phi\right)\left(\partial_\nu\phi\right)\right\} = 0\end{aligned} \tag{B.7}$$

Multiplying both sides by $2/\sqrt{-g}$ yields,

$$\begin{aligned}-g_{\mu\nu}\left[F(\phi)R - \frac{1}{2}\left(\partial\phi\right)^2 - V(\phi)\right] + 2F(\phi)R_{\mu\nu} - 2\nabla_\mu\nabla_\nu F(\phi)\\ +2g_{\mu\nu}\Box F(\phi) - \left(\partial_\mu\phi\right)\left(\partial_\nu\phi\right) = 0\end{aligned} \tag{B.8}$$

Dividing both sides by $2F(\phi)$, field equations become

$$R_{\mu\nu}-\frac{1}{2}Rg_{\mu\nu}=\frac{1}{2F}\left\{-\frac{1}{2}g_{\mu\nu}\left(\partial\phi\right)^2-g_{\mu\nu}V(\phi)+2\nabla_\mu\nabla_\nu F(\phi)-2g_{\mu\nu}\Box F(\phi)+\left(\partial_\mu\phi\right)\left(\partial_\nu\phi\right)\right\}. \tag{B.9}$$

Now, metric can be employed explicity. For the flat FRW background, components of Ricci tensor are

$$R_{00}=-3\frac{\ddot{a}}{a},\quad R_{ii}=\frac{g_{ii}}{a^2}\left(a\ddot{a}+2\dot{a}^2\right) \tag{B.10}$$

and Ricci scalar is

$$R=6\left(\frac{\ddot{a}}{a}+\frac{\dot{a}^2}{a^2}\right)=6(\dot{H}+2H^2). \tag{B.11}$$

The other required components are

$$\begin{aligned}\nabla_\mu\nabla_\nu F(\phi)&\xrightarrow{00}\ddot{F}=\ddot{\phi}F'+\dot{\phi}^2F''\\ \nabla_\mu\nabla_\nu F(\phi)&\xrightarrow{ii}-g_{ii}\frac{\dot{a}}{a}\dot{F}=-\dot{a}a\dot{\phi}F'\\ \Box F(\phi)&=-3H\dot{F}-\ddot{F}=-3H\dot{\phi}F'-\ddot{\phi}F'-\dot{\phi}^2F''\end{aligned} \tag{B.12}$$

overdot and prime corresponds to derivative with respect to cosmic time and scalar field, respectively. Friedmann equations can be found as

$$\begin{aligned}6H^2F&=\frac{1}{2}\dot{\phi}^2-6H\dot{\phi}F'+V(\phi)\\ 2(2\dot{H}+3H^2)F&=-\frac{1}{2}\dot{\phi}^2+V(\phi)-4H\dot{\phi}-2\ddot{\phi}F'-2\dot{\phi}^2F''.\end{aligned} \tag{B.13}$$

Second equation can simply be expressed

$$4\dot{H}F=-\dot{\phi}^2+2H\dot{\phi}F'-2\ddot{\phi}F'-2\dot{\phi}^2F'' \tag{B.14}$$

In order to vary action with respect to the field, one can use Euler–Lagrange in curved space which is given by

$$\frac{\partial\mathscr{L}}{\partial\phi}-\nabla_\mu\left[\frac{\partial\mathscr{L}}{\partial\left(\partial_\mu\phi\right)}\right]=0 \tag{B.15}$$

Starting with the first term,

$$\frac{\partial\mathscr{L}}{\partial\phi}=\frac{\partial F}{\partial\phi}R-\frac{\partial V}{\partial\phi} \tag{B.16}$$

and the second term is

$$\begin{aligned}\nabla_\mu\left[\frac{\partial\mathscr{L}}{\partial\left(\partial_\mu\phi\right)}\right]&=\nabla_\mu\left\{-\frac{1}{2}g^{\mu\nu}\left[\nabla_\nu+\nabla_\mu\phi\delta^\mu{}_\nu\right]\right\}\\ &=\nabla_\mu\left\{-\frac{1}{2}g^{\mu\nu}\left[2\nabla_\nu\phi\right]\right\}\\ &=-g^{\mu\nu}\nabla_\mu\nabla_\nu\phi=-\Box\phi\end{aligned} \tag{B.17}$$

Thus, equation of motion becomes,

$$\frac{\partial F}{\partial \phi}R + \Box\phi - \frac{\partial V}{\partial \phi} = 0. \tag{B.18}$$

In flat FRW background,

$$\ddot{\phi} + 3H\dot{\phi} - 6F'(\dot{H} + 2H^2) + \frac{\partial V}{\partial \phi} = 0 \tag{B.19}$$

CURRICULUM VITAE

Name Surname : Kemal Akın

- **B.Sc.** **:** 2018, Istanbul Technical University, Faculty of Science and Letters, Department of Physics Engineering

PROFESSIONAL EXPERIENCE AND REWARDS:

- 2019-2021 Research Assistant at Department of Forensic Sciences, Uskudar University
- 2014-2016 Astronomy Instructor at Usturlab Atölyeleri.

PUBLICATIONS, PRESENTATIONS AND PATENTS ON THE THESIS:

- **Akın K., Arapoğlu, A. S., Yükselci A. E.** Formalizing slow–roll inflation in scalar–tensor theories of gravitation. *Physics of the Dark Universe*, 30, 2020

OTHER PUBLICATIONS, PRESENTATIONS AND PATENTS:

- Inflationary Cosmology in Scalar–Tensor Theories of Gravitation, *18. Fizik Haftası*, Istanbul (2021)
- Cosmology: Fundamental Observations and Cosmic Dynamics, *14. Fizik Haftası*, Istanbul Technical University, Istanbul (2016)
- Document Preparation with LaTeX, *12. Fizik Haftası*, Bogazici University, Istanbul (2015)